ISSN 0917-1185

ANNUAL REPORT OF NATIONAL INSTITUTE FOR FUSION SCIENCE

April 2021 – March 2022

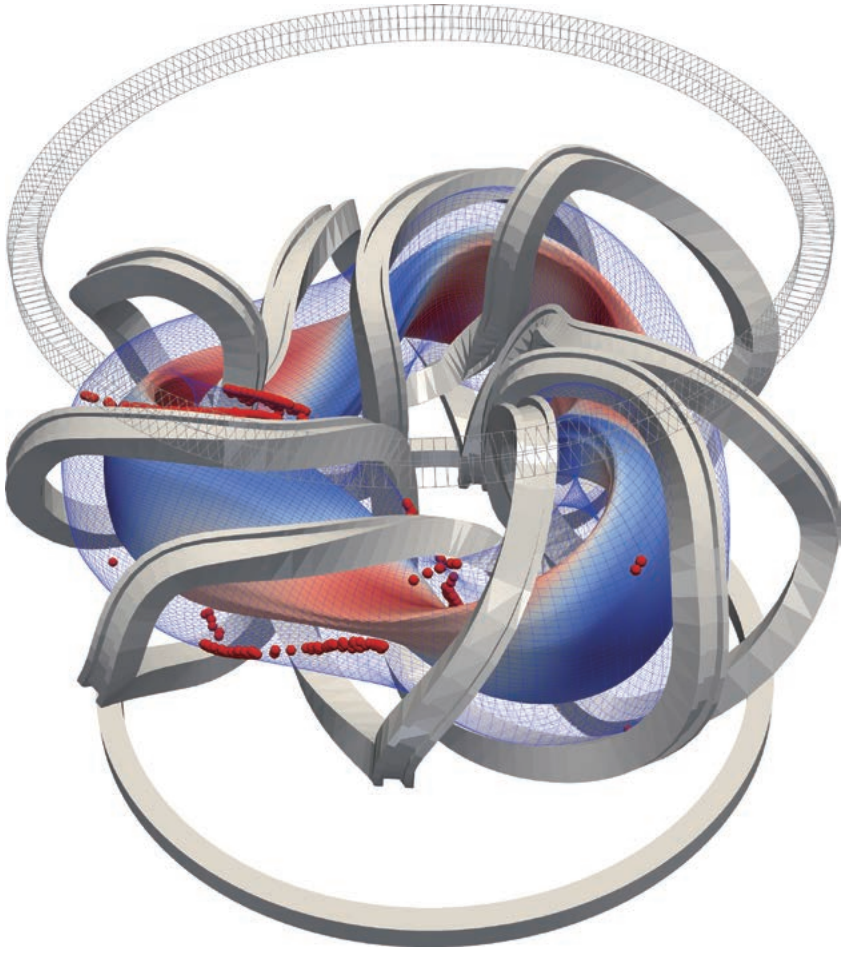

NATIONAL INSTITUTE FOR FUSION SCIENCE
TOKI CITY, JAPAN

Front Cover Caption:
Magnetic field configuration with continuous helical coils obtained by the optimization code, OPTHECS

Printer: Arakawa Printing Co., Ltd.
2-16-38 Chiyoa, Naka-ku, Nagoya-shi 460-0012, JAPAN
Phone: +81-52-262-1006, Facsimile: +81-52-262-2296

Printed in Japan, ISSN 0917-1185

ANNUAL REPORT OF NATIONAL INSTITUTE FOR FUSION SCIENCE

April 2021 – March 2022

December 2022

Inter-University Research Institute Corporation
National Institutes of Natural Sciences

NATIONAL INSTITUTE FOR FUSION SCIENCE

Address : Oroshi-cho, Toki-shi, Gifu-ken 509-5292, JAPAN
Phone : +81-572-58-2222
Facsimile : +81-572-58-2601
Homepage on internet : URL = http://www.nifs.ac.jp/

Contents

National Institute for Fusion Science
April 2021 – March 2022

Towards a new era of fusion science

Fusion science is a comprehensive area encompassing various disciplines with extremely high potential. Not only the immense merit of fusion energy, but also the possibilities of new discoveries give us the motivation to climb a high mountain - the history of overcoming every challenge has brought academic depth and breadth to fusion science. While the physics of fusion reactions is already well known, we have yet to understand how a "system", called high-temperature plasma, can maintain a stable condition. It is a macroscopic system producing an internal energy by which autonomous dynamics sustains. The aim of fusion science is to elucidate t he mechanism of such a spontaneous process; the fundamental principle must be common to the dynamics of the universe, society, or life. Recognizing the problem in a wide context, we pave the way in a zone of fundamental studies. On the way to fusion, the ultimate energy source, we will encounter many crossroads leading to future science and technology.

As we know, there are three different states of matter, i.e., solid, liquid, and gas. Even if the same molecules constitute matter, its "state" varies as the temperature is changed. At a high temperature, all matter becomes a gas, in which molecules are disconnected and distribute sparsely, moving freely. When the temperature is raised further, molecules are broken into ions (positively charged heavy particles) and electrons (negatively charged light particles) by disconnecting the electrical bonding of ions and electrons; we call such a high temperature state "plasma". While plasma is not common on Earth, it is the most typical state of matter in the universe. Our sun is a huge mass of plasma, consisting mainly of hydrogen. inside it fusion reactions produce enormous energy. A star is a naturally made sustainable system of high temperature plasma, energized by fusion reactions.

Although the fusion energy is often likened to a "sun on Earth", we need to think of a system that is completely different from stars. The challenge of fusion science is, indeed, to build a sustainable fusion system, based on a thoroughly new mechanism that we cannot find an example of in nature. A star confines plasma by gravity, but it is a very weak force, only effective against huge masses such as celestial bodies. We have to invoke a much stronger force to create a compact confinement system; magnetic force is the recourse. However, magnetic force acts like "vortex" and its role in creating macroscopic structures is an interesting subject of contemporary physics and mathematics. We also need a much higher temperature than the center of the sun. In a typical star like our sun (the main sequence star), the reaction of synthesizing a helium atom from a hydrogen atom proceeds slowly. This reaction (a so-called p-p chain reaction) is too slow for producing sufficient fusion power in a compact system. We need to apply a faster reaction (a so-called resonant fusion reaction); the easiest is the deuterium-tritium fusion reaction, which produces helium and neutrons, but occurs at temperatures of around 100 million degrees Celsius. On the other hand, several meters away from the plasma, we have to place super-conducting magnets to generate the magnetic field, which are operated at ultra-low temperature. Therefore, fusion on Earth requires an extreme technology, dealing with ultra-high temperatures and ultra-low temperatures, separated only by several meters.

The road to fusion power is purgatory, which is much harder than the prediction made at the beginning (the mid-20th century). However, it is not necessarily unfortunate that we encounter unexpected challenges. As many great researchers say that discovery is born from failure, unknown truths exist outside the range that one can predict. Fusion energy is a steep peak for development researchers to climb, but it is also a treasure trove for academic researchers. The task of the academic researcher is to generate new knowledge from the input of difficult problems.

All members of the National Institute for Fusion Science (NIFS) are working on the construction of a lighthouse that illuminates the direction of fusion science in choppy academic waters ahead. NIFS is a broad avenue for many researchers, through which the scope of "fusion science" will extend in the world of science. We hope that many people will pay attention to our endeavor and participate in these activities.

YOSHIDA Zensho
Director General of National Institute for Fusion Science

1. Large Helical Device (LHD) Project

Research on confining high-temperature plasmas with magnetic fields is being conducted around the world with the aim of realizing nuclear fusion power generation. At the Large Helical Device (LHD) of the National Institute for Fusion Science, a "deuterium plasma experiment" has been conducted since 2017 to generate plasma, using deuterium. In FY2020, we succeeded in generating plasma with both electron and ion temperatures reaching 100 million degrees. With this success, the LHD research has entered a new stage. In FY2021, we conducted experiments on mixed hydrogen isotope plasmas of "deuterium" and "hydrogen" to simulate the mixed hydrogen isotope plasmas of "deuterium" and "tritium" that will be used in future fusion power generation. This experiment has produced results that will form the basis of future fusion research, such as the world's first observation of mixed hydrogen isotopes. We also focused on the physics of multi-ions, including helium, which will be the ash of future nuclear fusion reactions in fusion power plants.

The realization of fusion power generation requires the stable maintenance of such a high-temperature plasma for a long period of time, and there are many issues to be solved to maintain this stability. Plasma confined by a magnetic field must be kept at a high temperature of more than 100 million degrees Celsius in the center where the fusion reaction takes place, while the plasma in the periphery must be kept as cool as possible, to reduce the heat load on the walls of the device that confines the plasma. This temperature gradient is extremely steep, 100 million degrees in about one meter. This causes turbulence, with various sizes of vortices stirring the plasma, resulting in a low center temperature. In addition, when the plasma pressure gradient becomes steep, the plasma becomes unstable, and a part of it which is may be lost (this phenomenon is called instability). Therefore, it is necessary to understand turbulence and instability and to establish methods to control them in order to maintain plasma stability.

Physics experiments on plasma turbulence and instability have provided important insights into the development of control methods for turbulence and instability in future fusion plasmas. Turbulence and sudden instabilities are considered to be deeply related not only to fusion plasmas but also to various phenomena occurring in space and on the earth. We are planning to promote such interdisciplinary research in LHD. Spectroscopy is a powerful tool to investigate the turbulence and instability in high-temperature plasma since it is also widely used in the other scientific field of space and solar plasma physics in. Therefore, the development of the spectroscopy technique should have a strong academic impact on improving the observation technique.

We have four topical groups to proceed with the interdisciplinary research in LHD.
1) multi-ion plasma, 2) turbulence, 3) spectroscopy, 4) instability.
In FY2021, we had 115 principle proponents of the LHD experiment, including NIFS staff, domestic collaborators, and overseas (international) collaborators. Proponents outside NIFS exceeded 50% of the total, as seen in Fig.1.

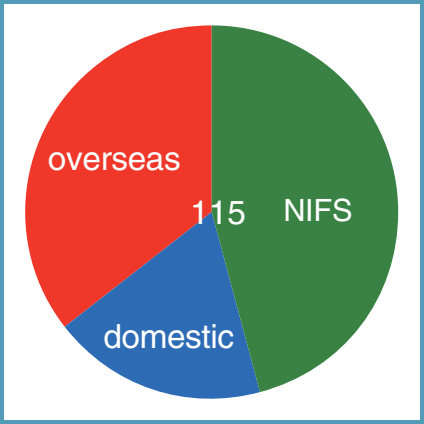

Fig. 1 Fraction of the number of overseas, domestic, and NIFS researchers proponents.

Significant progress in scientific research has been made in experiments on turbulence/transport, magnetic islands, energetic particles, spectroscopy, and machine learning based on international and domestic collaborations. LHD experiments show the importance of

1) Role of turbulence spreading
2) Core-edge-divertor coupling (non-local transport)
3) Non-diffusive transport (especially heat transport)
4) Interaction between magnetic islands (MHD) and transport

Please visit https://www-lhd.nifs.ac.jp/pub/Science_en.html

Based on the LHD experiment in 2021, we released the results when scientific papers were published in high-impact journals such as Nature Physics or Physical Review Letters.
Please visit the NIFS home page at https://www.nifs.ac.jp/en/news/index_list.html.

(K. Ida)

Multi-ion

Highlight

Progress in the research in multi-ion plasmas

A deuterium (D) - tritium (T) fusion reaction will produce helium (He, Z = 2) as a by-product. Therefore, in a possible D-T fusion reactor, we must control the plasma efficiently and effectively, consisting as it does of multi-ions, such as hydrogen isotopes and impurities (impurities other than He would come from the plasma-facing components). One of the critical issues in D-T fusion plasma is to control the radial profile of each hydrogen isotope and impurities in that mixed plasma, so that it achieves sustained nuclear fusion burning. High confinements of hydrogen isotopes and high pumping efficiency of He must be performed simultaneously. To gain the insight needed to achieve such a conflicting capability, we have strategically promoted the research on multi-ion plasmas from the FY2021 experiment campaign of the Large Helical Device (LHD). In the study on multi-ions, we identified the confinement study of thermalized and high-energy He by using an He-beam as a high priority. For such studies, one of the perpendicular NBIs (NBI#5) was modified to allow the injection of the He beam. We successfully measured the spatiotemporal behaviors of fast and thermalized He ions, introduced by the He-beam in the LHD plasma, with charge exchange spectroscopy (CXS, FICXS) diagnostics. Figure 1 shows an example of a waveform summary of the LHD plasma with He-beam injection. Due to the He-beam injection, we observed an increment of charge exchange He II line intensity. And we also observed the increments of line-averaged electron density and central ion temperature due to the He-beam injection. However, we found that the following points make the study of beam-derived He transport difficult and problematic: the He gas inflow from the NBI#5 device and the He recycled from the plasma-facing components (divertor). We are working on solving these problems by devising new experimental methods and further modifications and improvements to the experimental apparatus.

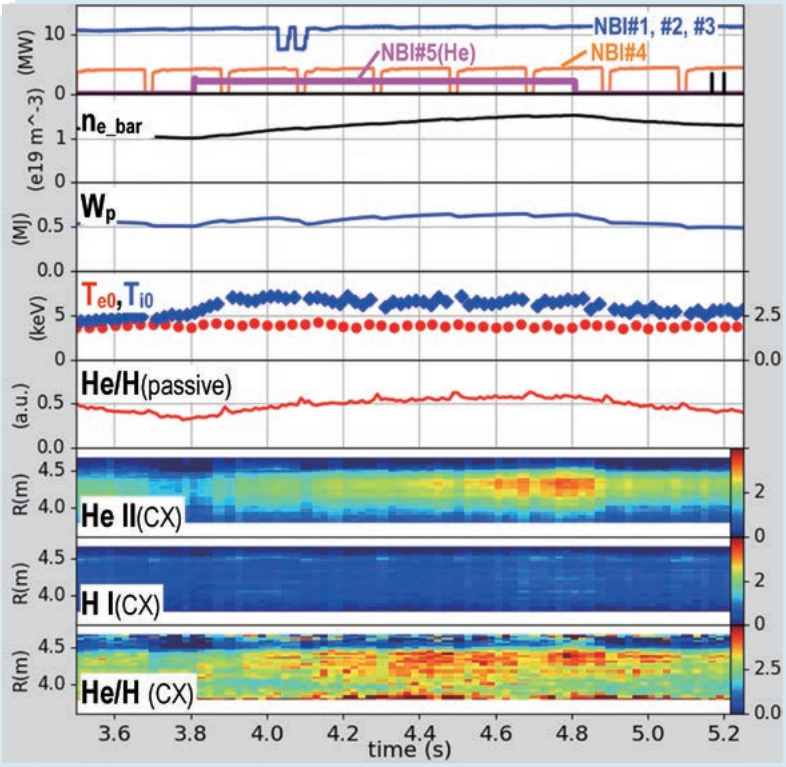

Fig. 1 Example of waveform summary of the LHD plasma with He-beam injection. Here the He-beam was injected from t = 3.8 s until t = 4.8 s. As can be seen in the third frame from the bottom, charge exchange He II line intensity was increased during the He-beam injection, mainly around R = 4.3 m. Also, the line-averaged electron density (the second frame from the top) and central ion temperature (the fourth frame from the top) were increased due the He-beam injection.

(N. Tamura)

Good core plasma performance realized in deuterium plasmas compatible with heat load mitigation at the plasma facing components

In fusion reactors it is necessary to generate and maintain as high a temperature as possible in the core confinement plasma to accelerate a fusion reaction, while heat flux from the confined plasma can damage or melt the plasma facing wall. The solution to this problem is to make the plasma at the edge as cold as possible, to reduce the heat load on the wall. In many cases, however, the energy of the confined plasma is also reduced simultaneously.

In the Large Helical Device (LHD), we have been working with the aim of solving this problem. One way to do this was to create a magnetic field structure called a "magnetic island" in the peripheral region, as shown in Fig. 2 (a), and to separate the cold edge plasma from the hot plasma in the confinement region [1, 2, 3]. It has been shown that when the magnetic island is formed, plasma energy is converted to radiation in the magnetic island and the plasma in the island becomes colder. Consequently the heat load on the device wall is dispersed in a wide area, reducing the peak heat load.

On the other hand, since future fusion reactors will use deuterium and tritium plasmas to generate electricity, it is necessary to investigate how the plasma changes, depending on the hydrogen isotopes. In this experiment, we have compared the operation of deuterium and hydrogen plasmas using the magnetic island described above. As a result, it was observed in the deuterium plasmas, that the energy density (pressure = temperature × density) of the confined plasma increased even when the plasma temperature in the peripheral region decreased, as shown in Fig. 2 (a). When this phenomenon occurs, the plasma fluctuation is reduced, and the temperature and density profiles of the plasma at the boundary between the magnetic island and the confined plasma become steeper, leading to a good confinement of plasma. This phenomenon is more pronounced in the deuterium plasmas than in the hydrogen plasmas, as shown in Fig. 2 (b), where the deuterium plasmas show higher radiated power, compatible with good core plasma confinement [4]. The results indicate that deuterium plasmas can achieve higher performance of confined plasmas than hydrogen ones, while reducing the peak heat load on the plasma facing wall.

The results show that future deuterium and tritium plasmas may be able to reduce the heat load on the device wall, while maintaining higher plasma performance.

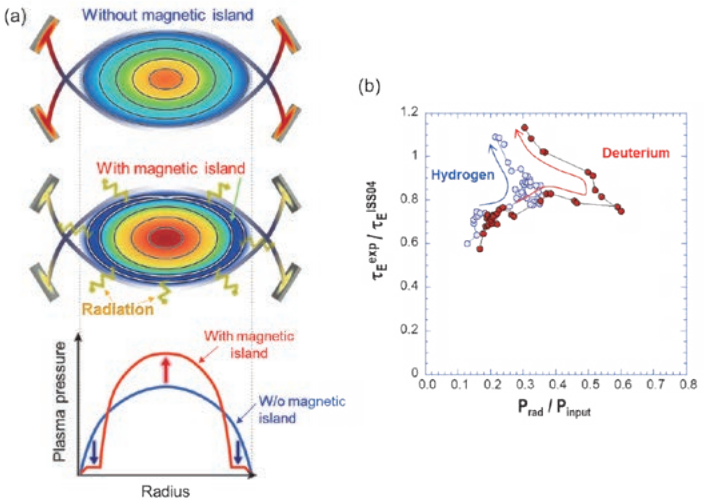

Fig. 2 (a) The plasma cross section in the Large Helical Device (LHD) without (top) and with (middle) a magnetic island. (bottom) The plasma pressure profile without and with a magnetic island. With one, the plasma energy is converted to radiation in the island and the plasma becomes colder there(middle figure). As a result, the heat load on the device wall is dispersed and the peak heat load decreases. At the same time a steep temperature and density gradient is created in the edge region, which increases plasma energy in the confined region (bottom figure). (b) Energy confinement scaling factor as a function of the radiated power with the edge magnetic island. The red and blue symbols show the deuterium and the hydrogen plasmas, respectively. The arrows in the figure indicate time sequence of the discharges.

(M. Kobayashi)

[1] S.N. Pandya *et al.*, Nucl. Fusion **56**, 046002 (2016).
[2] M. Kobayashi *et al.*, Nucl. Fusion **59**, 096009 (2019).
[3] T. Oishi *et al.*, Plasma Fus. Res. **17**, 2402022 (2022).
[4] M. Kobayashi *et al.*, Nucl. Fusion **62**, 056006 (2022).

Control of plasma particles by powerful vacuum pumping [5]

Fusion power generation is achieved by injecting hydrogen fuel into a high-temperature plasma of over 100 million degrees Celsius, where the injected hydrogen becomes high-temperature ions and undergoes a nuclear fusion reaction. The ionized hydrogen (fuel particles) is ejected out of the plasma, some bouncing off the plasma facing walls and back into the plasma, and some being ejected out of the vessel by a vacuum pump. The research team has experimented with the use of powerful cryogenic vacuum pumps in a system called a divertor, to reduce the amount of hydrogen returning to the plasma in experiments in the Large Helical Device (LHD).

In the divertor system, hydrogen fuel is drawn in to compress the hydrogen fuel. The experiment team systematically investigated the relationship between the cage of magnetic field lines that confine the plasma (magnetic field configuration) and the compression of neutral particles in the divertor. As a result, they found that the hydrogen fuel can be highly compressed in the divertor if the position of the center of the plasma (magnetic axis) is inward-shifted.

Next, plasma discharges were performed using a cryogenic vacuum pump inside the divertor in the magnetic configuration, with the inward-shifted magnetic axis. As a result, the density of the plasma was increasing without the cryogenic vacuum pump in the divertor, and eventually collapsed due to its uncontrollable density. On the other hand, the plasma density can be maintained at a constant level with the cryogenic vacuum pump in the divertor and successfully controlled. In addition, plasma heat transport analysis (another major achievement of this research was the creation of a heat transport analysis program) showed that energy confinement was better at the plasma core region when a cryogenic vacuum pump in the divertor was used. This established an easy and stable method for controlling hydrogen fuel. We expect that further progress will be made in our research toward maintaining steady-state fusion plasmas.

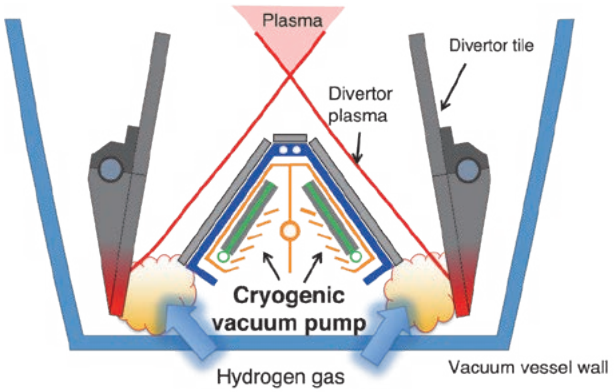

Fig. 3 At the periphery of the plasma confined by the magnetic field in the Large Helical Device (LHD), the plasma is drawn into a region called the divertor, where it becomes neutral gas. A cryogenic vacuum pump is installed inside the divertor to exhaust the neutral gas.

[5] G. Motojima *et al.*, Phys. Scr. **97**, 035601 (2022).

(G. Motojima)

Realization of stable heat load reduction on the wall, using two-species impurity gas injection [6, 7]

Stable and effective heat load reduction on the divertor was realized using neon (Ne) and krypton (Kr) injection, compared with single-species injection in the LHD. In fusion reactors, a fusion reaction occurs by confining high-temperature plasma exceeding 100 million Celsius degrees. Due to the flow of plasma from its high temperature core to a place called the "divertor" in the wall of the device, it is necessary to suppress the local heat load of the divertor. Therefore, an operational method called "divertor detachment" is being investigated, in which impurities are injected around the edge plasma and the heat load is dispersed as radiation. In the LHD, we conducted experiments on the divertor detachment.

In the divertor detachment experiments, one-species of impurity is usually injected. In the case of only seeding Ne, divertor detachment occurred; however, it could only be maintained for about 0.2 seconds, as shown in Fig. 4 (a) → (b) → (c). On the other hand, the LHD research group conducted the experiment using the injection of two species of impurities (Ne and Kr) to explore a more advanced operational method. As a result, we succeeded in stably maintaining the divertor detachment for about one second, as shown in Fig. 4 (a) → (d) → (e).

It was found that in the two-species injection, the radiation of Kr increased by Ne injection. Due to the phenomenon, the divertor heat load could be effectively reduced by the increase of plasma radiation with a smaller amount of impurities. Moreover, accumulation of the injected impurities toward the core plasma was suppressed. We also found that there are optimal conditions for the phenomenon regarding electron temperature and density around the edge plasma.

Since fusion reactors need to operate stably, it is necessary to maintain a stable divertor detachment. In addition, if the injected impurities for the divertor detachment are accumulated toward the core plasma, the fusion output power will decrease; therefore the influence of the impurities must be limited to the edge plasma. This result has provided important insights that will lead to the establishment of operational methods for divertor detachment.

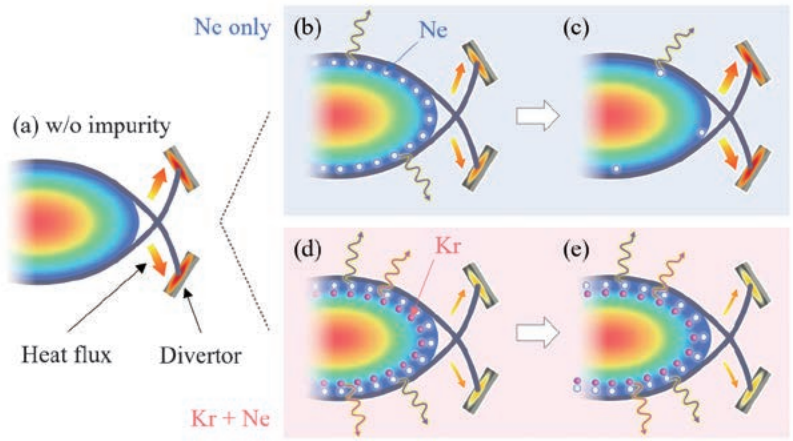

Fig. 4 (a) LHD plasma before impurity seeding. In the seeding of only Ne, (b) divertor heat load decreased with radiation enhancement just after the seeding; however, (c) divertor heat load increased again ~ 0.2 s after the seeding with a decrease of radiation. On the other hand, in the Kr+Ne seeding, (d, e) reduction of divertor heat load with radiation enhancement was maintained for ~ 1 s.

[6] K. Mukai *et al.*, Plasma Fusion Res. **15**, 1402051 (2020).
[7] K. Mukai *et al.*, Nucl. Fusion **61**, 126018 (2021).

(K. Mukai)

TG2: Turbulence topical group

Highlight

Turbulence suppression by boron powder injection

We have discovered that sprinkling boron powder injection into the plasma reduces impurities from the walls and at the same time suppresses plasma turbulence. In order to realize fusion power generation, it is necessary to maintain stable high-temperature plasma. However, impurities generated from the walls of the vessel confining the plasma and turbulence generated in the plasma cause its temperature to drop. One way to prevent impurities entering the plasma is to form a boron film on the wall surface. In international cooperation with the Princeton Plasma Physics Laboratory (PPPL) in the United States, we have installed an impurity powder dropper (IPD) to inject boron and other powders onto plasma in LHD.

When boron powder is injected during plasma discharges from the IPD, it is found that a boron film is formed on the wall surface in real time, reducing impurities from the wall surface, suppressing heat loss from the plasma, and maintaining a stable high temperature state. In other plasma experimental devices, the temperature increase due to powder dispersal has been observed in a very short time, but LHD was able to maintain a stable state for a very long time. Why can such an advantageous plasma state be maintained? We measured plasma turbulence intensity and calculated computer simulation analysis. As a result, we found that the injection of boron powder suppresses the turbulence in the plasma. Figure 1(a) shows clear turbulence suppression in almost the whole radius. It might be caused by the effect of increasing flow shear. This achievement will greatly contribute to the establishment of a method for stably maintaining high-temperature plasma.

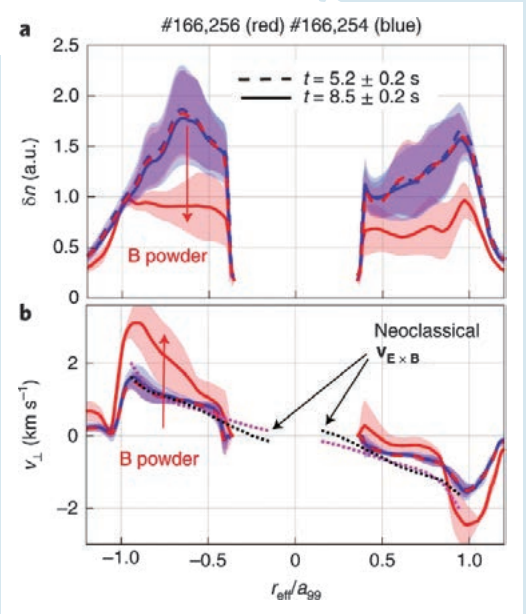

Fig. 1 Radial profiles of turbulent fluctuation amplitude δn (**a**) and the perpendicular velocity $v_\perp$ (**b**) for a powder injection shot (#166,256, red) and its reference (#166,254, blue), at $t = 5.2$ s (before injection, dashed lines) and $t = 8.5$ s (during injection, solid lines). The radial profiles are averaged over a time window of 0.4 s, to avoid instantaneous variations caused by the pulsed diagnostic neutral beam. The shaded area accounts for the standard deviation in time. In b, neoclassical estimates of $\mathbf{E} \times \mathbf{B}$ velocity for #166,256 before (black) and during (magenta) powder injection are shown with dotted lines.

[1] F. Nespoli *et al.*, "Observation of a reduced-turbulence regime with boron powder injection in a stellarator", Nature Physics **18**, 350–356 (2022).

(F. Nespoli and S. Masuzaki)

Plasma turbulence spreading by magnetic fluctuation reduces heat load on a fusion device wall

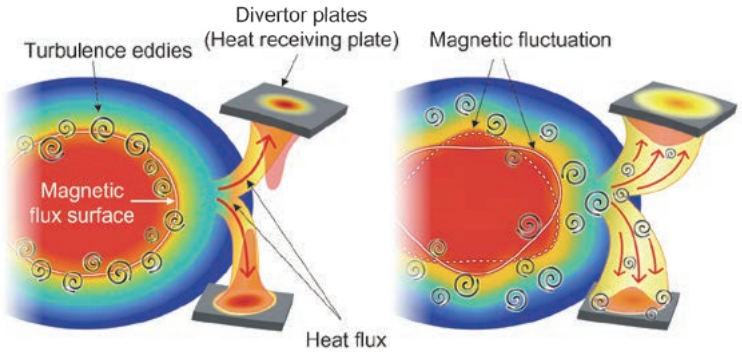

Fig. 1 Picture of turbulence spreading caused by magnetic fluctuation. Left: Turbulence generated in the plasma stays in the same place. A heat load is localized at the divertor plates and the peak value is high. Right: Magnetic field fluctuation occurs and turbulence propagates in the plasma. The heat flux to the divertor plate widens and the peak heat load decreases.

To achieve a nuclear fusion reactor, control of turbulence and the divertor heat load is mandatory. To understand and control the turbulence, it is necessary to clarify how turbulence is generated in the plasma, and how it propagates. However, the propagation of turbulence is not yet fully understood. In addition, to reduce the heat load on the divertor plates, impurity seeding has been studied to disperse the plasma energy to a wider area by radiation from the impurity ions. This method, however, has problems such as cooling of the confined plasma by impurity influx.

In LHD we have conducted experiments with RMP application, where a high temperature and steep density gradients develop at the edge region, simultaneously with their flat profile, adjacent to the gradient region. It has been observed that turbulence was generated in the region with the largest gradient and remained in the same place without propagating. At this time, the heat flowing out of the plasma was concentrated in a narrow area, and the divertor plate was subjected to an extremely large local load.

On the other hand, it has been found that when a magnetic fluctuation was excited around the steep gradient region, the turbulence propagated outward in the plasma. It was also found that the heat flux from the plasma to the divertor plates was scattered over a wide area by this turbulence. As a result, the peak divertor heat load decreased by a factor of about four, compared to a case without the magnetic field fluctuation. It was also confirmed that the center of the plasma remained at a high temperature and density state. Thus, with excitation of a magnetic fluctuation, it was discovered that the heat load could be reduced by propagating turbulence while maintaining a high central temperature and density in the plasma [1].

This result demonstrates a completely new method for controlling turbulence generated in plasmas and the heat load on the divertor plates.

[1] M. Kobayashi *et. al.*, "Turbulence spreading into an edge stochastic magnetic layer induced by magnetic fluctuation and its impact on divertor heat load", Phys. Rev. Lett. **128**, 125001 (2022). DOI: 10.1103/PhysRevLett.128.125001

(M. Kobayashi, K. Tanaka, K. Ida, Y. Hayashi, Y. Takemura and T. Kinoshita)

Direct observation of the non-locality of non-diffusive counter-gradient electron thermal transport during the formation of hollow electron-temperature profiles in the Large Helical Device

Thermal transport is usually considered in a diffusion model where the heat flux is driven by a temperature gradient. In the Large Helical Device (LHD), an external heating method called electron cyclotron heating (ECH) is used, which can heat a narrow plasma region. Normally the plasma center is heated to produce a high-temperature plasma and a peaked electron temperature (T_e) profile. However, in this study [1] we observed for the first

time that heating away from the plasma center produces a hollow T_e profile; in a quasi-steady state where the T_e profile does not change, it is possible to describe the non-diffusive outward heat flux in terms of heat convection. Such a model can reproduce the T_e profile of the LHD plasma.

Next, we experimentally investigated the response of the T_e profile to a plasma with a hollow T_e profile when additional ECH was added to the center of the T_e profile, as shown in Fig. 1. In other words, the transient response of how the heat pulse propagates outward from the center was investigated from the time evolution of the T_e profile. The results showed that the heat pulse propagated transiently against the T_e gradient. Also, with core heating, the T_e profile changed from a hollow profile to a peaked one over time, but there was a period when it just flattened out (the T_e gradient became zero). Even then, net heat flowed outward; direct experimental investigation of the relationship between the T_e gradient and the driven heat flux showed that the diffusion model could not explain the heat transport in this case.

We then stopped the core heating and examined the relationship between the T_e gradient and driven heat flux when the T_e profile returned from the peak profile to the hollow one. Figure 2 shows that the trajectory was different from that during core heating. This phenomenon is called transport hysteresis. We found that the transport at a given location was not determined by the T_e gradient or T_e at that location. This hysteresis was confirmed repeated by turning the core heating on and off; the non-local nature of the non-diffusive heat transport associated with heat convection was experimentally revealed as T_e moved back and forth between peak, flat, and hollow profile states. This finding is a new insight into transport phenomena in fusion plasmas.

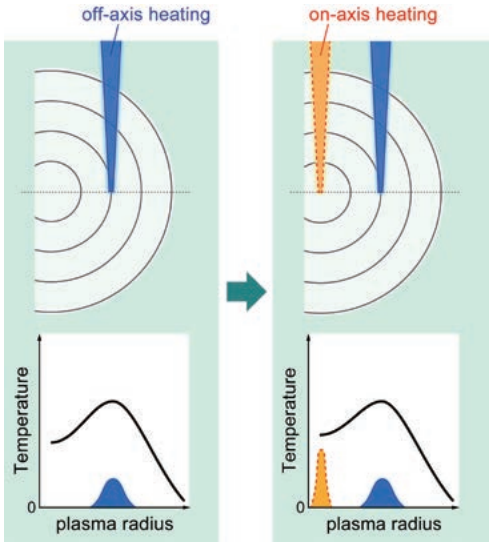

Fig. 1 Schematic diagram of a radial T_e profile during the modulated on-axis ECH, superimposed on the steady-state off-axis ECH.

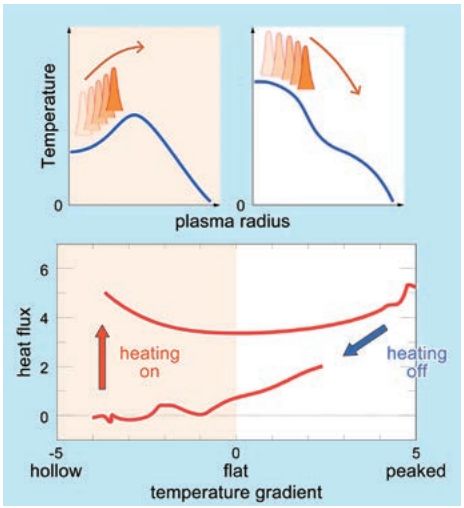

Fig. 2 Diagram of the flux-gradient relation when the non-locality of non-diffusive counter-gradient transport is present under the heat pulse, with the on-axis ECH propagating outward.

[1] T. I. Tsujimura *et al.*, Phys. Plasmas **29**, 032504 (2022).

(T. Tsujimura)

Impact of Magnetic Field Configuration on Heat Transport in Stellarators and Heliotrons

Optimization of magnetic configuration is one of the most important issues in stellarator/heliotron research. Neoclassical and anomalous transport, which are thought to be driven by turbulence, should be minimized in order to increase the confinement time. The optimization criteria can be obtained from comparison studies between LHD and W7-X, which currently represent the largest stellarator/heliotron. LHD is characterized by strong magnetic shear ($d\iota/d\rho$) and large effective helical ripple (ε_{eff}), while W7-X is characterized by weak $d\iota/d\rho$ and small ε_{eff}. These dissimilarities result in different characteristics of neoclassical and anomalous transports.

The plasma volume is almost 30 m^3 in both devices. Thus, comparison with the same heating power can clarify the difference of transport without any normalization. Figure 1 shows the comparison of density and temperature profiles of LHD and W7-X under identical experimental conditions. The magnetic configuration employed is an inward shifted configuration for LHD, where the magnetic axis position (R_{ax}) is 3.6 m at 2.75 T, and the standard configuration for W7-X is at 2.5 T. Heating is 2 MW electron cyclotron resonant heating (ECRH) and power deposition is localized in the central region in both devices. The averaged density is around 1.5×10^{19} m^{-3}. Hollowed electron density (n_e) profiles in LHD and the peaked n_e profile in W7-X are one of the striking differences between the two. The central electron temperature (T_e) is higher in W7-X, while the T_e is higher in LHD at the outer mid-radius. The ion temperature (T_i) is higher in LHD in the entire region, while the T_i gradient is steeper in W7-X. Power balance analyses were carried out. The profiles of experimentally obtained ion thermal conductivities (χ_i^{EXP}) are shown in Fig. 2 (a) for W7-X and (b) for LHD, together with neoclassical ion thermal conductivities (χ_i^{NC}). As shown in Fig. 2 (a) and (b), χ_i^{EXP} are almost comparable in the outer mid radius, while χ_i^{NC} are clearly lower in W7-X. This is attributed to the neoclassical optimization of W7-X configuration. The anomalous contribution of ion thermal conductivity can be defined as $\chi_i^{ANO} = \chi_i^{EXP} - \chi_i^{NC}$. As shown in Fig. 2 (c), the resultant χ_i^{ANO} is much lower in LHD. This is in strong contrast to much lower χ_i^{NC} in W7-X. Theoretical validations using gyrokinetic simulations were performed using GKV for LHD and GENE for W7-X, including both kinetic ion and electron effects. Simulated ion thermal conductivities (χ_i^{Sim}) are shown in Fig. 2 (c). Excellent agreements were obtained both for LHD and W7-X, indicating that the anomalous process of ion transport is driven by ion temperature gradient turbulence. The gyrokinetic simulations suggest that the lower χ_i^{ANO} in LHD is due to stronger zonal flow generation. The obtained results indicate that turbulence reduction and neoclassical transport do not necessarily coincide. Further investigations are necessary to find which magnetic parameter or which combination of it is important, in order to reduce neoclassical and anomalous transport simultaneously.

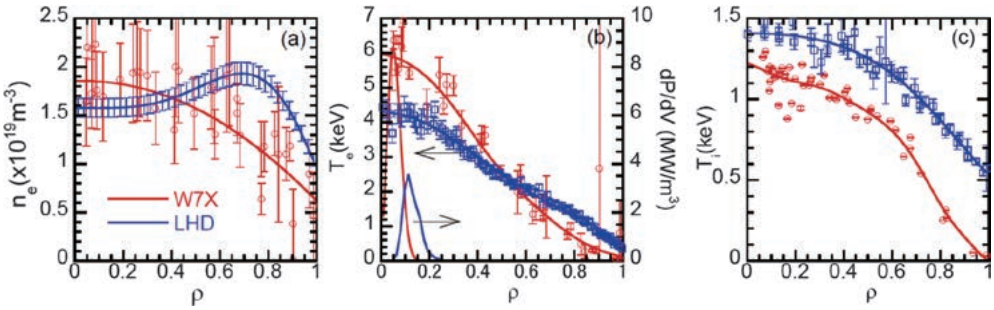

Fig. 1 Comparison of profile (a) n_e, (b) T_e and (c) T_i. ECRH power deposition profiles are shown in (b). LHD is the inward shifted configuration (R_{ax} = 3.6 m) at 2.75 T, W7-X is the standard configuration at 2.5 T.

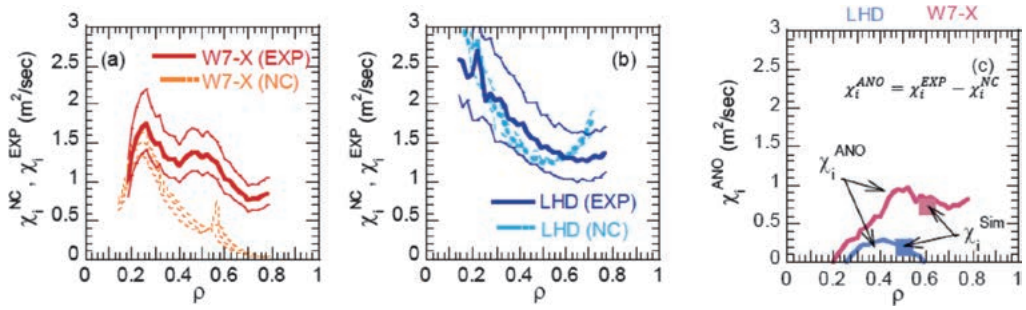

Fig. 2 Spatial profile of χ_i^{EXP}, χ_i^{NC} and χ_i^{ANO}. Plain and dashed line in (a) and (b) indicate χ_i^{EXP} and χ_i^{NC} respectively. In (a) and (b), upper and lower boundaries of estimation uncertainty are shown by thin lines. In (c), plain lines indicate χ_i^{ANO}, symbols indicate χ_i^{Sim}.

[1] F. Warmer *et al.*, Phys. Rev. Lett. **127**, 225001 (2021).

(F. Warmer and K.Tanaka)

Plasma Spectroscopy

Highlight

Assessment of W density in LHD core plasmas using visible forbidden lines of highly charged W ions [1]

Tungsten (W) densities in core plasmas of the Large Helical Device (LHD) have been successfully assessed with measurements of optically forbidden magnetic-dipole (M1) lines in the near-ultraviolet region emitted by W^{26+} and W^{27+} in ground states (Fig. 1). The ground states of W^{26+} and W^{27+} have 4f valence electrons outside the palladium iso-electronic core (Fig. 2); the electron configurations are different from the ground state of any element in the periodic table. In a strong Coulomb field of tungsten nucleus, energy levels of the 4f valence orbitals are split by interaction with the electron spin. The observed emission lines in the near-ultraviolet region were due to M1 transitions between those levels.

We constructed a collisional-radiative model for the M1 lines of highly charged tungsten ions in plasmas, to evaluate tungsten ion densities from the M1 line intensities. Based on the W^{26+} and W^{27+} densities, the spatial distribution of total tungsten density and its time evolution (Fig. 3) were assessed.

The present work showed the potential usefulness of visible forbidden lines for tungsten measurements in fusion plasmas.

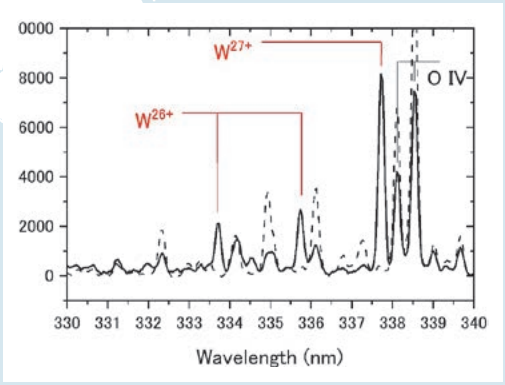

Fig. 1 Near-ultraviolet M1 lines of W^{26+} and W^{27+} (red bars) observed at the LHD. The solid line shows a spectrum observed with tungsten, and the dashed, a spectrum without tungsten.

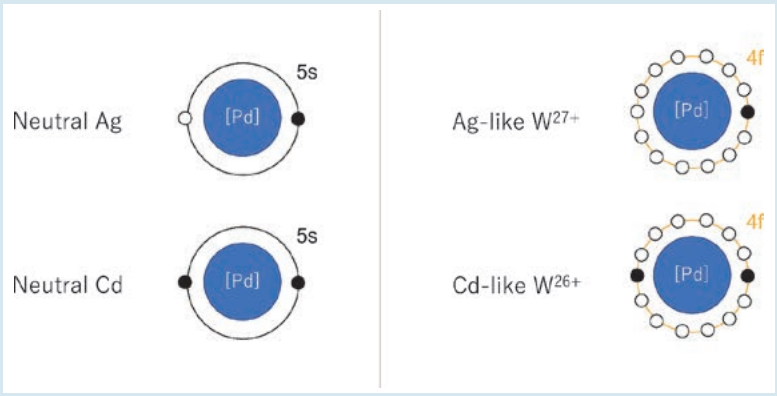

Fig. 2 Ground state electronic configurations of neutral silver (Ag, Z=47), cadmium (Cd, Z=48), silver-like W^{27+}, and cadmium-like W^{26+}. W^{27+} and W^{26+} have 4f valence electrons and a palladium iso-electronic core: $[Pd]=1s^2 2s^2 2p^6 3s^2 3p^6 3d^{10} 4s^2 4p^6 4d^{10}$.

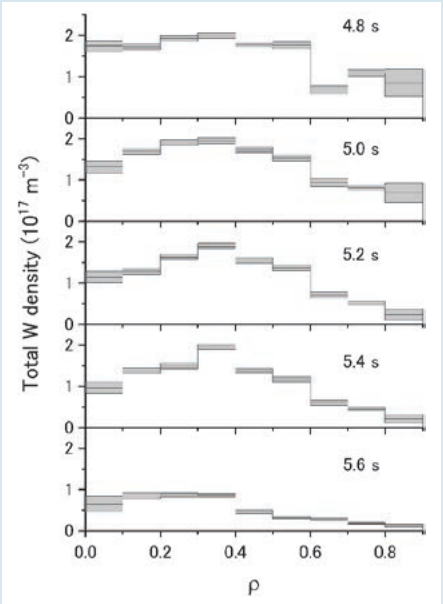

Fig. 3 Radial profiles of the total W density in the core at 4.8 – 5.6 s after W pellet injection at 4.0 s. ρ stands for a normalized minor radius measured from the center of a poloidal cross-section of the LHD. Gray zones represent uncertainty (1σ).

(D. Kato)

Simultaneous Observation of Tungsten Spectra of W^0 to W^{46+} Ions in Visible, VUV and EUV Wavelength Ranges in the Large Helical Device [2]

Spectroscopic studies for emissions released from tungsten ions have been conducted for a contribution to a tungsten transport study in tungsten divertor fusion devices and for expansion of the experimental database of tungsten line emissions (Fig. 4). Tungsten ions are distributed in the LHD plasma by injecting a pellet consisting of a small piece of tungsten metal wire enclosed by a carbon tube. Line emissions from W^0, W^{5+}, W^{6+}, W^{24+}–W^{28+}, W^{37+}, W^{38+}, and W^{41+}–W^{46+} are observed simultaneously in visible (3200–3550 Å), vacuum ultraviolet (250–1050 Å), and extreme ultraviolet (5–300 Å) wavelength ranges, and the wavelengths are summarized. Temporal evolutions of line emissions from these charge states are compared for comprehensive understanding of tungsten impurity behavior in a single discharge. The charge distribution of tungsten ions strongly depends on the electron temperature (Fig. 5). Measurements of emissions from W^{10+} to W^{20+} are still insufficient, which is addressed as a future task.

(T. Oishi)

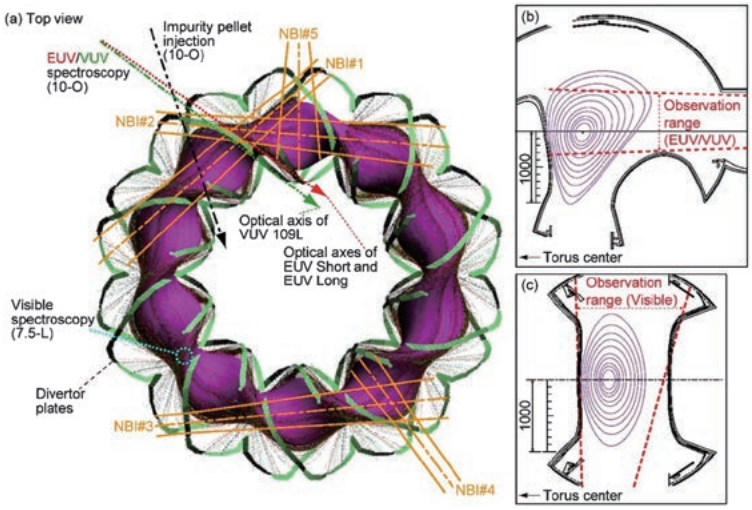

Fig. 4 (a) Top view of shape of plasma in LHD device together with schematic drawings of neutral beam injection (NBI) for heating, spectroscopic diagnostics, and impurity pellet injection. Cross- sections of magnetic surfaces where optical axes of (b) VUV/EUV and (c) visible spectroscopy systems are located, together with viewing angle of each system.

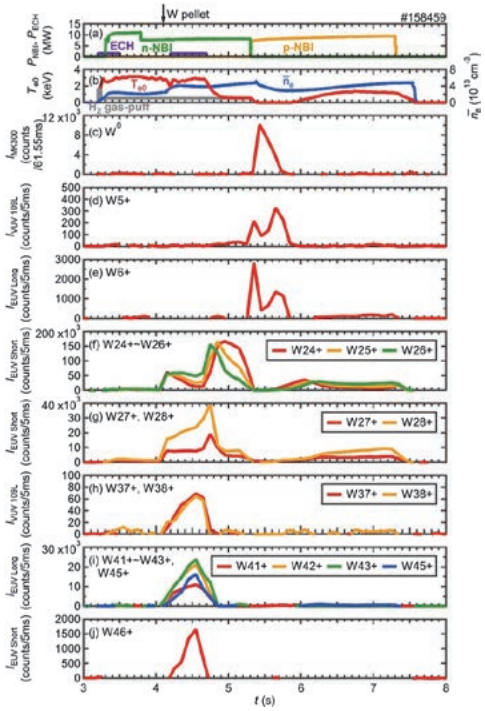

Fig. 5 Temporal evolution of (a) heating power of ECH, n-NBI, and p-NBI, (b) central electron temperature and line-averaged electron density, and W^0–W^{46+} intensities integrated over wave- length ranges of (c) 3426.2–3427.9 Å for W^0, (d) 637.8–641.2 Å for W^{5+}, (e) 261.0–261.5 Å for W^{6+}, (f) 32.15–32.30 Å for W^{24+}, 30.73–31.69 Å for W^{25+}, 29.29–30.40 Å for W^{26+}, (g) 28.58–28.69 Å for W^{27+}, 27.35–27.78 Å for W^{28+}, (h) 645.3–647.1 Å for W^{37+}, 558.6–560.3 Å for W^{38+}, (i) 131.0–131.3 Å for W^{41+}, 129.2–129.5 Å for W^{42+}, 126.1–126.5 Å for W^{43+}, 126.9–127.3 Å for W^{45+}, and (j) 7.89–7.95 Å for W^{46+}.

Spectra of Ga-like to Cu-like praseodymium and neodymium ions observed in the Large Helical Device [3]

Fifteen elements with atomic numbers of 57–71, called lanthanides, have a similar nature to each other. Regarding the emission spectra from highly charged lanthanide ions, available experimental data are still insufficient for some of the elements. The Large Helical Device (LHD) can be exploited for producing spectral data of highly charged heavy ions because high-temperature and high-emissivity plasmas can be stably generated, and impurity injection systems and advanced diagnostic systems are available.

In this study, we focus on extreme ultraviolet (EUV) emission spectra of highly charged praseodymium (Pr) and neodymium (Nd) ions, introduced into optically thin high-temperature plasmas produced in LHD. Discrete spectral lines emitted mainly from highly charged ions having 4s or 4p outermost electrons were observed in plasmas with electron temperatures of 0.8–1.8 keV (Fig. 6). Based on the recently published list of lines of neodymium ions in an electron beam ion trap (EBIT) experiment, most of the isolated lines of Ga-like to Cu-like praseodymium ions were identified as well from the similarity of the spectral features of the two elements. Some of them have been identified experimentally for the first time in LHD.

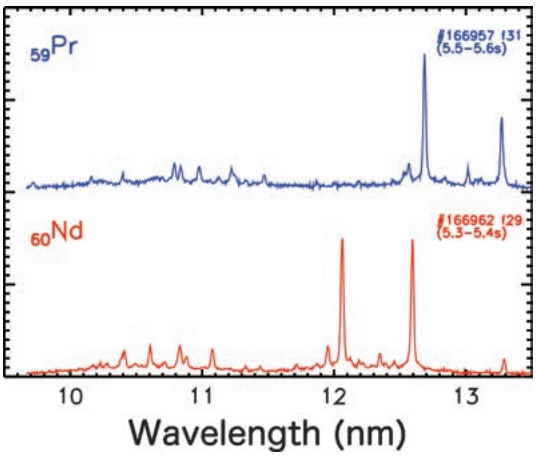

Fig. 6 Emission spectra of praseodymium (Pr) and neodymium (Nd) ions in the wavelength range of 10–13 nm, observed in high-temperature plasmas produced in the Large Helical Device (LHD). It is clearly seen that there are similar spectral structure shifts to shorter wavelengths in Nd (Atomic number: 60), in comparison with Pr (Atomic number: 59).

(C. Suzuki)

Z-dependent crossing of excited-state energy levels in highly charged galliumlike lanthanide atomic ions [4]

Extreme ultraviolet (EUV) optical transitions of lanthanide highly charged ions have been studied. The [Ni]$4s^2 4p$ – [Ni]$4s^2 4d$ and [Ni]$4s^2 4p$ – [Ni]$4s 4p^2$ transition lines of galliumlike lanthanide elements have been spectroscopically measured in Large Helical Device (LHD) plasma and electron-beam ion trap (EBIT) plasma. Figure 7 gives the typical line spectra measured in LHD. The wavelengths for europium ions agree within 0.03% between the LHD and EBIT measurements. The precise spectroscopic data not only give useful knowledge for diagnostics of fusion plasma but also challenging subjects for atomic and molecular physics research. Due to the enhancement of spin-orbit interactions along with the increase of atomic number Z in $4p$ atomic orbitals, energy splitting between $4p_-$(or $4p_{1/2}$) and $4p_+$(or $4p_{3/2}$) orbitals increases significantly from lanthanum to lutetium, causing the crossing of Z-dependent wavelength curves. Figure 8 gives the Z-dependent level-crossing features. The relativistic effects are stronger in lower orbital angular momentum orbitals such as $4p$, because they stick to

the area of the atomic center; the effect of spin-orbit interaction is larger in the electron configurations with lower orbital angular momentum orbitals. The spectral line positions and strengths are theoretically calculated by means of the multi-configuration Dirac-Fock method. The mixing of the [Ni]4$s^2$4d_- and [Ni]4s4p_+^2 configurations leads to an avoided crossing in the apparent wavelength curves. The configuration mixing makes both the [Ni]4$s^2$4p_- – [Ni]4$s^2$4d_- and originally optically forbidden [Ni]4$s^2$4p_- – [Ni]4s4p_+^2 lines well visible in the EUV spectra near the level crossing point. The levels are found to cross between Z = 62 and 63.

(F. Koike)

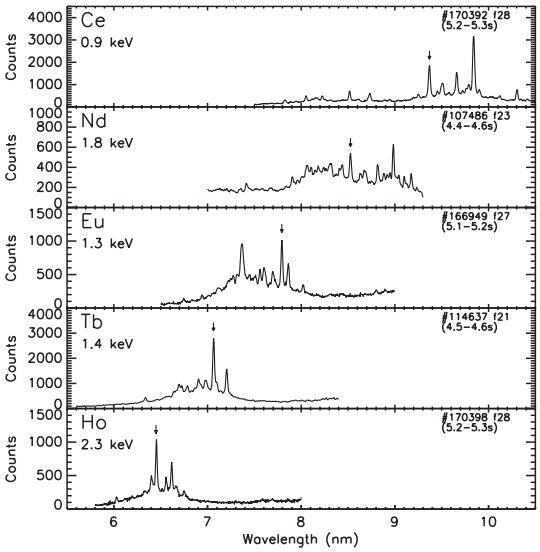

Fig. 7 Discrete EUV emission spectra of highly charged Ce, Nd, Eu, Tb, and Ho ions in LHD. The vertical arrows indicate the lines due to the transition [[Ni]4$s^2$4p_-]$_{1/2}$ – [[Ni]4$s^2$4d_-]$_{3/2}$ of Ga-like ions. The central electron temperature associated with each spectrum is shown in each panel.

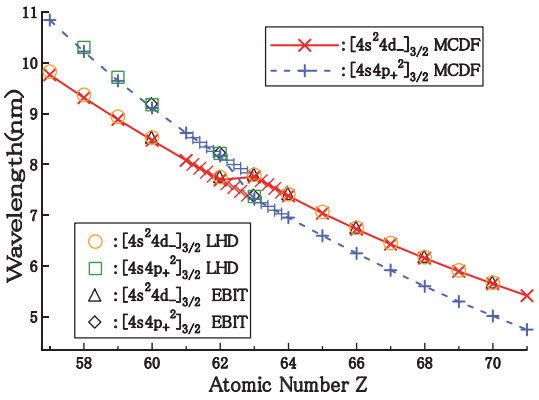

Fig. 8 Wavelength for the transitions of Ga-like ions of lanthanide elements with Z = 57–71 (La to Lu). Solid (red) line and symbol x, present MCDF calculation; open (orange) circle, LHD experiment; open (black) triangle, EBIT experiment for the [[Ni]4$s^2$4p_-]$_{1/2}$ – [[Ni]4$s^2$4d_-]$_{3/2}$ transition. Broken (blue) line and symbol +, present MCDF calculation; open (green) square, LHD experiment; open (black) diamond, EBIT experiment for the [[Ni]4$s^2$4p_-]$_{1/2}$ – [[Ni]4s4p_+^2]$_{3/2}$ transition.

[1] D. Kato *et al.*, Nuclear Fusion **61**, 116008 (2021).
[2] T. Oishi *et al.*, Atoms **9**, 69 (2021).
[3] C. Suzuki *et al.*, Atoms **9**, 46 (2021).
[4] F. Koike *et al.*, Phys. Rev. A **105**, 032802 (2022).

Annual Report of Instability TG

Highlight

Observation of self-sustained divertor oscillation driven by magnetic island dynamics in LHD

In magnetically confined plasmas, a magnetic island, an isolated magnetic field structure embedded in nested tori, occasionally forms. In the Large Helical Device (LHD), the magnetic island can be externally induced by perturbation coils installed outside the device, in order to study interaction between plasma and the magnetic island. One of the outcomes in forming the magnetic island is that plasma radiation is distinguishably enhanced at a specific point of the magnetic island (the so-called X-point) and the plasma heat load onto the plasma-facing materials is significantly mitigated, maintaining core plasma performance. This operation regime, the so-called detached state, is beneficial for fusion reactor development. The background physics of this operation regime is studied in detail.

In LHD, oscillations in the magnetic island width at a constant frequency (several tens of Hertz) were discovered. This oscillation was driven by a continuous power input, and was called self-sustained oscillation. The oscillations were also found in the divertor heat load and radiation losses therefore, were considered to be sequential detachment transitions and back-transitions. In order to analyze the background physics, a model used in biology, the so-called predator-prey model, was used. The model was composed by nonlinearly coupling two equations: one for the magnetic island dynamics (modified Rutherford equation) and the other for the bootstrap current (an empirical model). According to the model, the following interpretation was made possible. Once the magnetic island extends, the X-point radiation is enhanced and eventually a detachment transition occurs. In the detached phase, high X-point collisionarity impedes the X-point remnant bootstrap current, and then the magnetic island starts to shrink. The plasma returns to the attached phase and the X-point collinearity decays. As a result, the X-point remnant bootstrap current recovers and the magnetic island again starts to grow. Schematic of this interpretation is overviewed in Figure 1. By numerically examining the system equation, it was found that the model can qualitatively explain the observation [1].

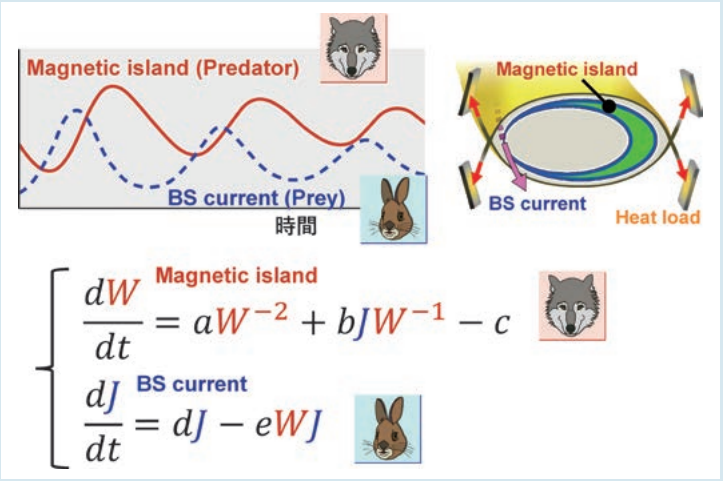

Fig. 1 Schematic of predator-prey model in divertor oscillation: (Left top) competition between magnetic island and bootstrap (BS) current, (Right top) illustration of geometry, and (Bottom) equations describing two variables (*a*-*e* are constants).

[1] T. Kobayashi *et al.*, Phys. Rev. Lett. **128**, 085001 (2022).

(T. Kobayashi)

First observation of characteristic fine structure of MHD fluctuations with decreasing frequency

In magnetic confinement plasmas, rapid growth of MHD fluctuations after a decrease in frequency of these fluctuations is one of key problems. In order to clarify the frequency decreasing mechanism in the LHD, fine local electron temperature profiles were measured by using the Thomson scattering system with a high-repetition-rate Nd:YAG laser.

Figure (a) shows the schematic view of electron temperature profiles in the first stage of the slowing-down phase, a flattening (red line) or tilting (blue line) structure in temperature profiles was repeatedly observed with the time. If a magnetic island is formed, in the region called the O point of the magnetic island, the temperature profile is flattened, but at the X point, the effect on the temperature profile is small. Therefore, the above result suggests that the magnetic island rotates with plasma.

On the other hand, in the last stage of the slowing-down phase as shown in Figure (b), it was found for the first time that some of the region constantly flattens (yellow hatched area). This result suggests a possibility that there is a non-rotating magnetic field formed the non-rotating island, and the interaction between it and a perturbed current due to instability leads to the j × B braking torque [1].

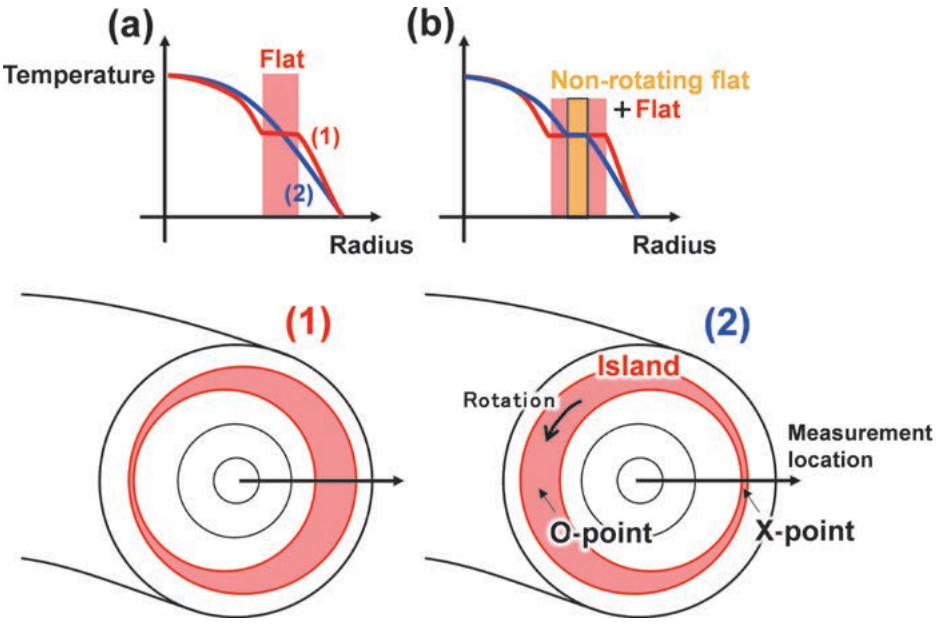

[1] Y. Takemura *et al.*, Plasma Fusion Res. **16**, 1402091 (2021).

(Y. Takemura)

Analysis of NB Fast-Ion Loss Mechanisms in MHD Quiescent LHD Plasmas

The beam-ion loss mechanism in the Large Heical Device (LHD) has been analyzed quantitatively by using neutron measurement and integrated simulation. It had been expected that "neo-classical transport" was dominant as the beam ion loss mechanism in LHD, the same as in large size tokamaks. In this paper, it was clarified that neo-classical simulation not can reproduce the experimental results in LHD, contrary to tokamak cases. In figure 1, the x axis indicates the neutron decay time, assuming no fast-ion loss and the y axis indicates the measured (blank) and simualted (filled) neutron decay time. The decay of neutrons generated by a DD fusion reaction comes from the two components. One is fast-ion slowing down, the other is the fast-ion loss. In fig. 1, these two components are separated by simulation. If fast ions are confined perfectly, data should be distributed along the y = x line. and data should be distributed along the line. If fast ions are lost with the time constant, data should be distributed on the fitting curve. As shown in fig. 1, the neo-classical simulation results are distributed along a line contrary to the experimental results. This result indicates that the other mechanism is as dominant as the beam ion loss mechanism in LHD. According to our preliminary analysis, the most plausible candidate for the dominant fast-ion loss mechanism is charge exchange (CX) loss. An accurate quantitative estimation of the CX loss is difficult because neutral particle density, which is crucial for the estimation of CX reactivity in the plasma core region, not can be measured. Detailed discussion about the CX loss estimation is to be found in future work.

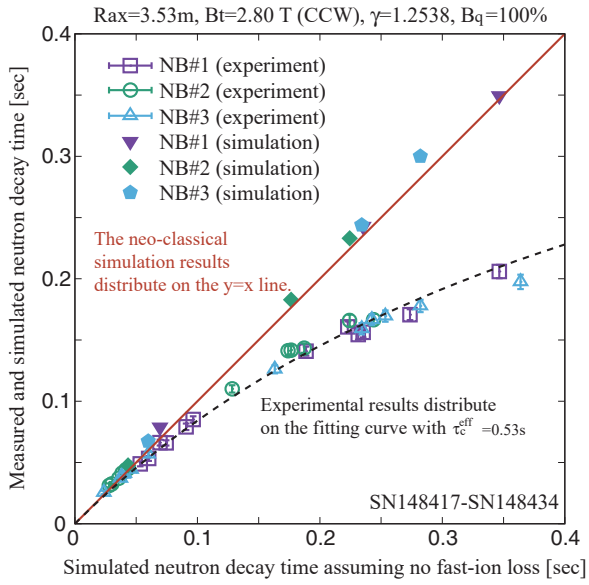

Fig. 1 Comparison between the experimental results and the neo-classical simulation results.

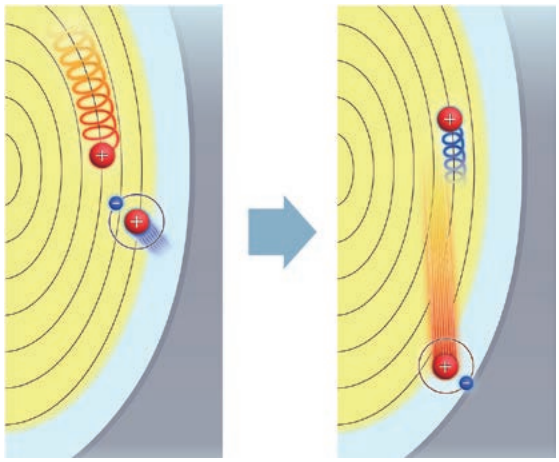

Fig. 2 A conceptional image of the CX loss. A fast-ion losses its charge due to CX loss and then the neutralized fast-ion is lost from the magnetic field.

(H. Nuga)

Measuring the spatial distribution of energetic particles in a deuterium plasma

In this study, we focused on how the neutral beam injection (NBI) direction and the magnetic field strength affect the spatial distribution of energetic particles by utilizing neutron emission profile diagnostics, recorded by a vertical neutron camera [1].

The vertical neutron camera was utilized to measure neutron emission profiles in LHD deuterium plasmas with tangential NBI under various magnetic field conditions. The peak of the line-integrated neutron profile shifts outward in the co-injection case and inward in the counter-injection case. The shift becomes more significant when the magnetic field decreases in strength.

We compared the observed neutron emission profile in the experiment and it was calculated by a guiding center orbit following simulation DELTA5D [2]. The shapes of the neutron emission profile, calculated for high and medium field strength conditions, were in good agreement with those obtained experimentally, and the numerical simulations were validated for LHD [3].

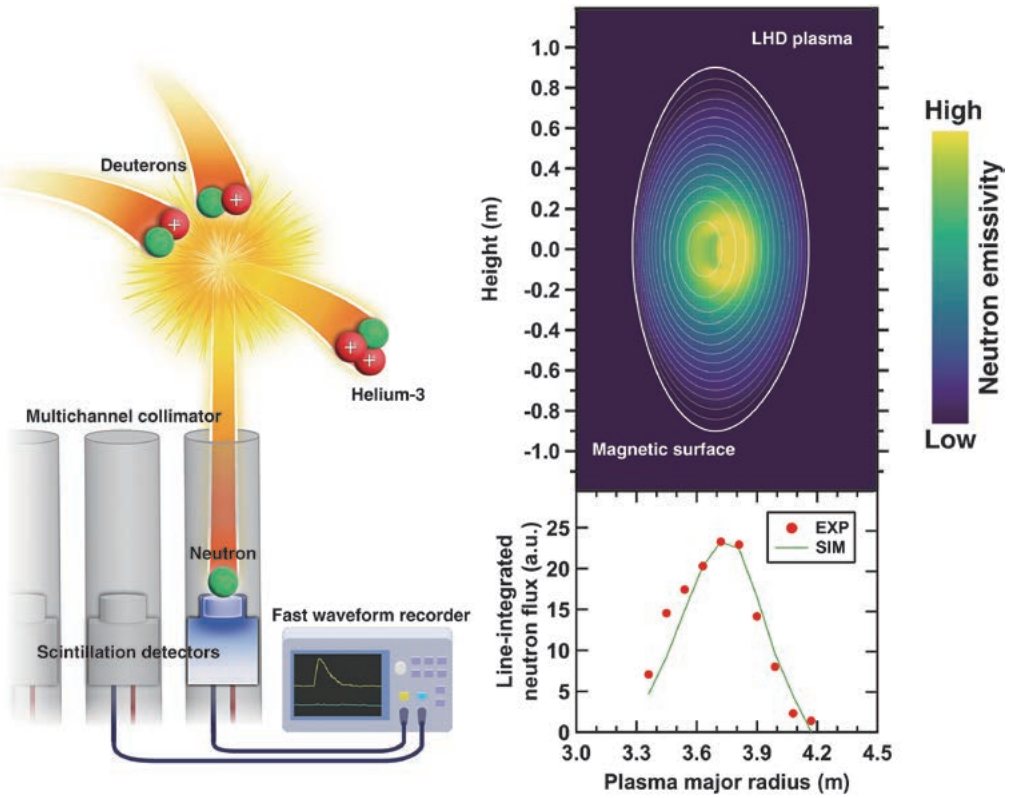

[1] K. Ogawa *et al.*, Rev. Sci. Instrum. **89**, 113509 (2018).
[2] D. A. Spong, Phys. of Plasmas **18**, 056109 (2011).
[3] K. Ogawa *et al.*, Plasma Phys. Control. Fusion **63**, 065010 (2021).

(K. Ogawa)

Research and Development Collaboration Program for LHD-Project

An RF induced transport model for the study of RF wave sustained plasmas

An RF transport model is constructed to understand the energy, momentum and particle confinement properties of lower hybrid wave sustained plasmas. Using the model, major properties of RF wave sustained TST-2 spherical tokamak plasmas are reproduced. The reproduction indicates that electrons are accelerated by the RF wave, and simultaneously transported toward a limiter and are lost.

Plasma current generation and sustainment by an RF wave are important issues for spherical tokamak research. In most of the experiments so far, the obtained plasma density and the plasma current are relatively low. In such a case, RF induced transport of high energy electrons can be the dominant process determining the energy, momentum (i.e., current) and particle confinement of electrons. In the constructed model, the velocity evolution of an electron is obtained through the equation $\Delta V_{\parallel} = \Delta \widetilde{V}_{\parallel} - \nu_{\parallel} V_{\parallel} \Delta t - \frac{eE}{m} \Delta t$, where the terms in the RHS represent a random velocity change due to the RF wave, collisional slowing down and acceleration by electric field, respectively. The orbit of an electron can be calculated from the velocity, and the electron is lost when the orbit touches one of the limiters. The electron velocity distribution function (EVDF) is obtained by following many electrons, and the plasma current, the deposited RF power, energy and particle confinement times are calculated from the EVDF. Some model parameters are adjusted to reproduce the measured plasma current, electron density and RF wave power. The model results suggest that a major fraction of the deposited RF power, which generates fast electrons, is lost by the electrons hitting a limiter, while a minor fraction is used to heat bulk electrons and ions. From the energy distribution of the lost electrons, we can calculate the hard X-ray generation and the energy spectrum of measured hard X-rays. Figure 1 shows the calculated and the experimental hard X-ray spectra, and qualitative agreements between the experimental and the model results are shown.

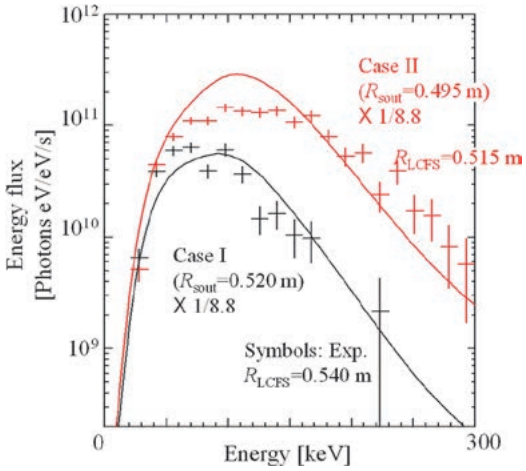

Fig. 1 Calculated (solid curve) and experimental (plus symbols) energy spectra. The calculated spectra are obtained by using the energy distribution of lost electrons in the model. They are multiplied by a factor of 1/8.8 in the plot to reproduce the experimental spectra. Two cases with different plasma sizes are shown by black and red. [1]

[1] A. Ejiri *et al.*, "A Fast Electron Transport Model for Lower Hybrid Wave Sustained Plasmas", Plasma and Fusion Research **17**, 1402037 (2022).

(A. Ejiri)

Spatially resolved measurements of SOL electron temperature and density using near-infrared Zeeman spectroscopy

In fusion-related toroidal plasmas, emission spectroscopy is used for plasma control and machine protection by measuring impurity generation and transport, confinement mode transition, the hydrogen isotope ratio, neutral density, and so forth. These diagnostics have however, a drawback that they can measure only the viewing-chord-integrated spectrum. To obtain a spatially resolved spectrum, additional methods such as computer-aided

tomography, with more than two directional observations, using multiple viewing chords or active emission spectroscopy, for detecting a neutral beam or laser-induced emission from the intersection between the beam and the viewing chord are required. The application of these methods will however, become difficult in future fusion reactors owing to a limitation in the available port area. It is thus desirable to develop an alternative method that is implementable by using a single diagnostic port.

A method that can satisfy this requirement is Stokes spectropolarimetry, which is widely used in the fields of astrophysics and ellipsometry. It determines the polarization state of an emission line spectrum by measuring the Stokes parameters I, Q, U, and V of this spectrum. Particularly for plasma spectroscopy, Stokes spectropolarimetry can be used as a method to spatially invert the viewing-chord-integrated spectrum, on the basis of the correspondence between the given magnetic field profile along the viewing chord, and the Zeeman effect appearing on the spectrum. Its application to fusion-related toroidal plasmas is however, limited, owing to low spatial resolution as a result of the difficulty in distinguishing between the Zeeman and Doppler effects. To resolve this issue, we increased the relative magnitude of the Zeeman effect by observing a near-infrared emission line on the basis of the greater wavelength dependence of the Zeeman effect than of the Doppler one.

The measurement was applied to the HeI 2^3S-2^3P emission line from a helium-puffed deuterium plasma produced in Heliotron J (Fig. 1(a)). Owing to the enhancement of the Zeeman effect relative to the Doppler one, the former was conspicuously observed at a magnetic field strength smaller than those used in other devices. By utilizing the Zeeman effect, we were able to reproduce the chord-integrated spectrum by a simulation with empirically optimizing recycling conditions of atoms at the first walls (Fig. 1(b)). In a future study, we intend to spatially resolve multiple near-infrared HeI emission line spectra and evaluate the spatially resolved SOL electron temperature and density using collisional-radiative model analysis.

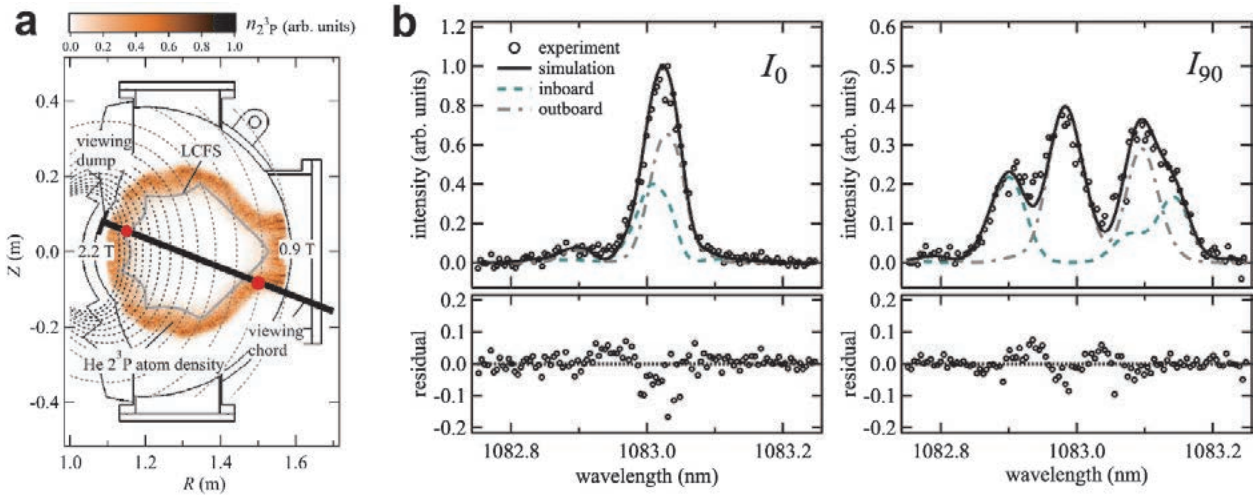

Fig. 1 (a) #10.5 poloidal plane of Heliotron J with a viewing chord. The magnetic field strength of 0.9–2.2 T is shown by dashed lines. The relative 2^3P excited helium atom density obtained by simulation is shown by the color map and the emission locations and relative intensities determined using the two-point emission model adopted in early studies of spatial inversion are plotted with red circles. (b) Orthogonal linear polarization spectra, I_0 and I_{90}, which are nearly parallel and perpendicular to the magnetic field, respectively, of a chord-integrated HeI 2^3S-2^3P emission line spectrum averaged over 10 discharges (#80303–312). The lines show the fitted spectra obtained by a simulation with optimizing recycling conditions of atoms at the first walls. Figures are cited from T. Chatani, T. Shikama *et al.*, *Sci. Rep.* **12**, 15567 (2022); doi:10.1038/s41598-022-19747-8.

(T. Shikama)

2. Fusion Engineering Research Project

The Fusion Engineering Research Project (FERP) started in FY2010 at the National Institute for Fusion Science (NIFS). Along with the conceptual design studies for the helical fusion reactor FFHR, the FERP has been developing technologies for key components, such as the superconducting magnet, blanket, and divertor (Fig. 1). The research also focuses on materials used for blankets and divertors, the interaction between the plasma and the first wall including atomic processes, handling of tritium, plasma control, heating, and diagnostics. The FERP is composed of 13 tasks and 44 sub-tasks with domestic and international collaborations. There is also a cooperation with the Large Helical Device Project and the Numerical Simulation Reactor Research Project. The FERP is also assisting the ongoing discussion on forming new "Units" for the restructuring of NIFS.

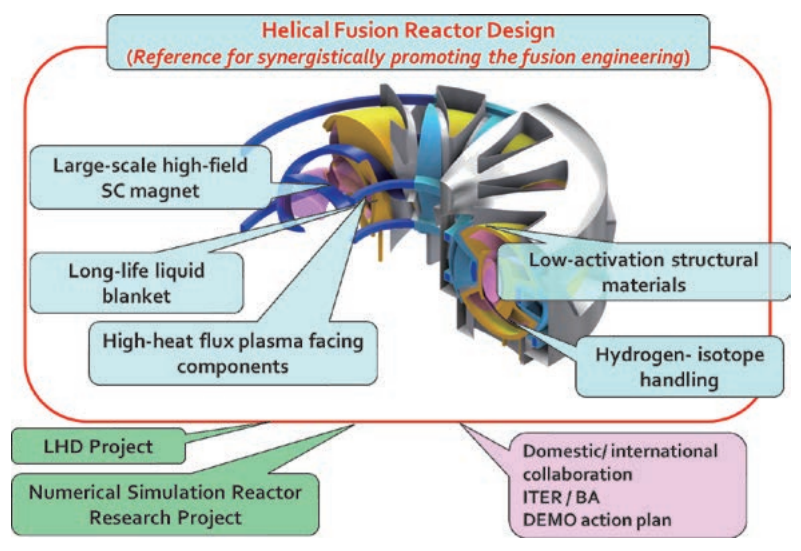

Fig. 1 Research targets of the Fusion Engineering Research Project with collaborations.

(I. Murakami)

Design Studies on Helical Fusion Reactor

In FY2020, a new design called FFHR-b3 was proposed and the step-by-step development strategy for the helical fusion power plant FFHR-d1 was updated. The construction and operation of three intermediate devices are assumed in the updated strategy: FFHR-a1 (non-nuclear system for the examination of improved magnetic configuration and advanced engineering concepts), FFHR-b3 (100 MWe class power plant that can operate for more than five years and twice the size of LHD), FFHR-c1 (500 MWe class power plant that can operate with a self-ignition condition). Because FFHR-b3 requires better plasma performance (MHD stability and energy confinement) with a large coil-to-plasma distance, configuration optimization beyond the variation of the helical coil shape based on the conventional winding law is required, such as shown in Fig. 2 for the operation window. The optimization study using the helical coil optimization code OPTHECS is being conducted in cooperation with the Numerical Simulation Reactor Research Project and a new configuration that has plasma performance equivalent to LHD with a 10% larger coil-to-plasma distance has been identified. The search for further optimized configuration is ongoing.

The design of a cartridge-type blanket for the helical reactor has been updated. The new design CARDISTRY-B3 adopts a slit wall fabricated by alternately stacking solid metal plates and porous ones made of metal or ceramic, as shown in Fig. 3. This slit wall can form a 3D curved surface along the plasma without 3D machining and realize a liquid metal wall including the divertor section by exuding liquid metal through the porous plates. Since the free surface of the liquid metal is exposed to the plasma, the vapor pressure of the working liquid metal should be low enough. Because the liquid metal also works as a coolant and

a tritium breeder for the blanket, it should have various functions including a high tritium breeding ratio, low density, low viscosity, a low melting temperature, high heat removal performance, a small amount of radioactive waste generation, low corrosion, a low MHD pressure drop, low toxicity, low chemical activity, and abundant resources. To satisfy these requirements, functional liquid metal (FLM), which is ternary or quadruple alloys including Li, Sn, Pb (or Bi), and Er has been studied.

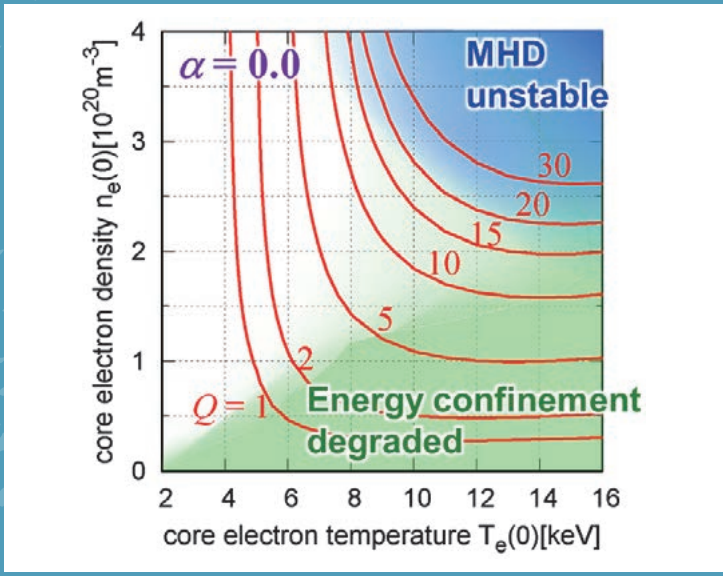

Fig. 2 Operation window for the FFHR-b3 helical fusion reactor on the core electron temperature and density.

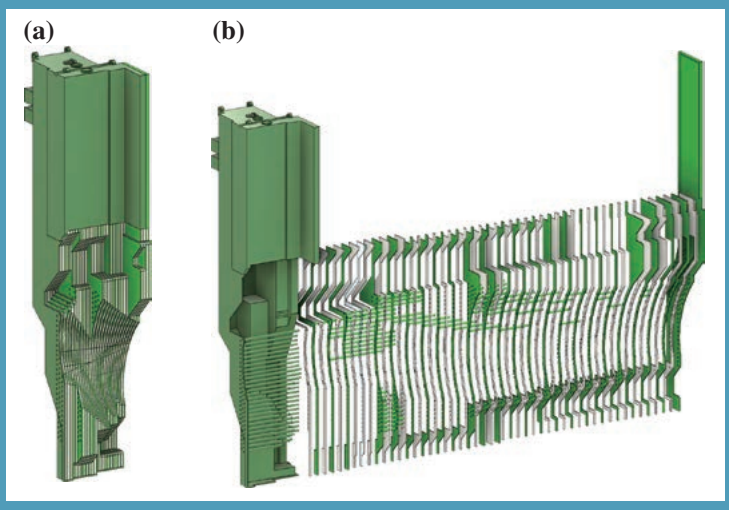

Fig. 3 (a) 3D diagram and (b) its exploded view of a breeding blanket module of CARDISTRY-B3.

(T. Goto and J. Miyazawa)

Research and Development on Blanket

In the FLiNaK/LiPb twin loop system Oroshhi-2, a tritium recovery test from circulating LiPb using a vacuum sieve tray (VST) was continued actively in FY2021. The details of the successful results are described in the following section. In the LiPb loop, a new test section was installed for analysis of impurity concentrations in LiPb circulated in the loop for more than 1000 hours (Fig. 4). LiPb circulated in the loop was introduced into a 1/2-inch diameter tube and rapidly cooled by water to avoid segregation of impurities. After solidification, the tube was taken out of the test section and concentration analysis of impurity elements was performed by inductively coupled plasma mass spectrometry (ICP-MS). Concentrations of Fe, Cr, Ni, etc. were successfully obtained and detailed analyses of the results are being conducted at present. The study will also examine the performance of the cold trap system of Oroshhi-2 which purifies the LiPb circulating in the loop. Regarding the operation of Oroshhi-2, the Department of Engineering and Technical Services has conducted the installation of a remote-control system to enhance the secure and flexible operation of the system.

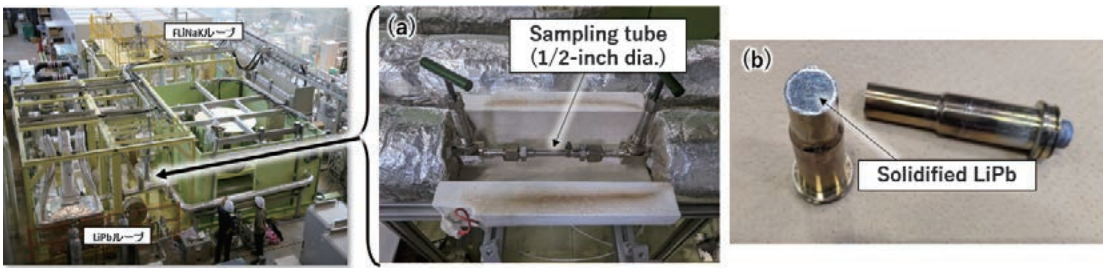

Fig. 4 Photos of (a) new test section for a sampling of LiPb and (b) sampled solidified LiPb.

(T. Tanaka and Y. Hamaji)

Development of advanced structural materials

Low-activation vanadium (V) alloys are promising candidate structural materials for the first wall/blanket applications in advanced fusion reactor systems. One of the recent studies on the V-Cr-Ti system alloys is to further reduce the radioactive characteristic after use in fusion reactors. Effects of titanium (Ti) and chromium (Cr) concentrations on microstructure and tensile properties of high purity vanadium alloys, which contain less than 300 mass ppm interstitial impurities (e.g., carbon, nitrogen, oxygen), have been investigated. It has been found that Ti can be reduced from 4wt% to 1wt% for scavenging and precipitation. On the other hand, Ti reduction results in the strength degradation of the V-Cr-Ti system alloy for both room temperature and high temperatures. Furthermore, it reveals that tensile strength gradually rises with increasing Cr concentration, indicating that a higher level of Cr can compensate for strength degradation by lowering the Ti concentration. Compared to the yield stress of V-4Cr-4Ti alloy, low-Ti and high-Cr candidates are V-6Cr-3Ti, V-8Cr-3Ti, V-10Cr-1Ti, V-12Cr-0.5Ti, and V-12Cr-1Ti alloys. The Ti and Cr concentrations will be further optimized according to irradiation damage resistance and ductile-to-brittle transition temperature investigations in the future.

(J. Shen)

Research and Development on Divertor

Advanced Multi-Step Brazing (AMSB) for fabricating the plasma-facing component has been developed. AMSB is based on the repetitive application of the Advanced Brazing Technique (ABT), which was originally developed for joining tungsten (W) and oxide dispersion strengthened copper alloy (ODS-Cu; GlidCop®). The new AMSB-type divertor heat removal component with a rectangular-shaped cooling flow path channel and V-shaped staggered rib structure was developed. The component was inserted into the divertor strike point of the Large Helical Device (LHD) and exposed to divertor plasmas for 1,180 shots. The high heat removal capability did not show any degradation over the experiment period. After extracting the component, surface analysis was conducted using an optical microscope, a focused ion beam (FIB), and a scanning electron microscope (SEM). Some micro-scale cracks with a ~50 μm width, and remarkable sputtering erosion and redeposition phenomena due to the strong influx of the divertor plasma were simultaneously confirmed on the W armor, even though the heat removal capability deduced by thermocouples did not change from the initial condition.

Reduced activation ferritic/martensitic (RAFM) steel is one of the candidates for the divertor cooling pipe and heat sink of the dome or baffles in fusion reactors. To obtain a reliable joint between W armor and RAFM steel, an appropriate intermediate layer, such as Cu, is required to be inserted between the W armor and RAFM steel to absorb residual stress during a heat treatment procedure of the joint. As a first step, we tried to fabricate a W/Cu/RAFM steel joint using the ABT between W/Cu and Cu/RAFM steel. Fig. 5(a) shows a photograph of the W/Cu/RAFM steel joint sample. The joint structure was successfully made without any macro-scale cracks, which was confirmed by a scanning electron microscope (SEM). Fig. 5(b) and (c) correspond to the cross-sectional SEM images in the vicinity of the joint interfaces for the W/Cu and Cu/RAFM steel joints, respectively. A very fine microstructure without any small-scale defects, such as delamination or voids, can be confirmed for both interfaces. To apply in the reactor environment, a tolerant material against the neutron dose should be used in the intermediate layer instead of Cu. We will continue to improve the W/Cu/RAFM steel joint structure in the next fiscal year.

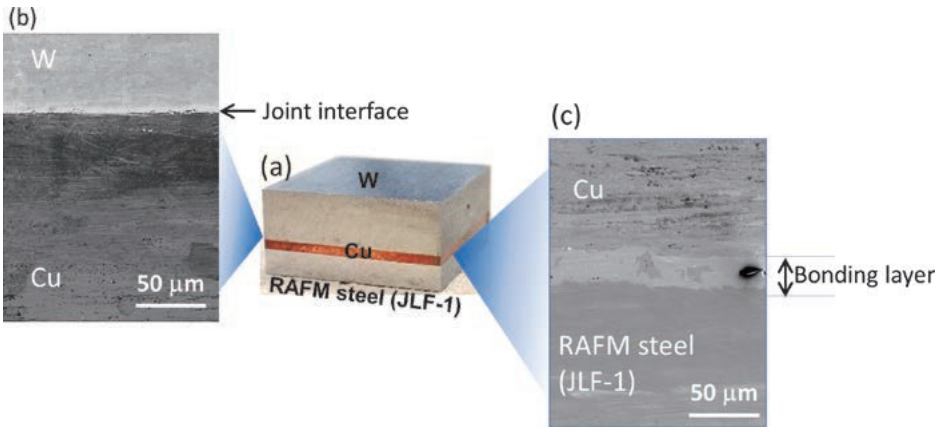

Fig. 5 Photograph of W/Cu/RAFM steel joint sample by ABT (a), and cross-sectional SEM images of the vicinity of the joint interfaces for W/Cu (b) and Cu/RAFM steel joint.

Highlight

Development of oxide dispersion strengthened tungsten (ODS-W) including titanium oxide

For improvement of plasma facing tungsten on a fusion divertor, we have developed a new oxide dispersion strengthened tungsten (ODS-W) including titanium Oxide as strengthening particles (Fig. 6(a)), fabricated by mechanical alloying (MA)-hot isostatic pressing (HIP), which can inhibit the decrease of a mechanical property even after recrystallization occurs. Our past studies have shown that the condition of the MA process affects the mechanical and thermal properties of the products. For the fabrication of DS-W generally, mechanical alloying is known as an essential process, and important in view of the material design on DS alloys. Even though the MA process needs the understanding of criteria parameters for evaluation of the alloyed state, detailed research of the alloying process on DS-W has not been done. In this study, the influence of the MA ball diameter on the ODS-W products by characterizing the evolution of the milled particles during MA was elucidated. Considering the ball diameter, the differences in the lattice constant and microstructure directly indicate the progress rate of mechanical alloying. The effect of the ball size was interpreted as that of collision energy delivered by the MA balls.

Fig. 6(b) shows lattice constants with MA time. The MA powders with 1.6, 3.0- and 5.0-mm balls exhibited a slight rise and fall of the lattice constant from 0-hr MA to 8-hr MA, then started the re-dilatation from 8-hr MA to 16-hr MA. The slight change of lattice constant indicates that MA less than 16 hr is not sufficient for alloying and forming an inhomogeneous microstructure. The lattice constant of the MA powder with a 1.6-mm ball after 16-hr MA time did not reach that of pure tungsten even though MA of 64-hr had finished, inferring that the forced solid-solution state was not caused between the tungsten matrix and the titanium element. On the other hand, lattice constants of MA powders with 5.0- and 3.0-mm balls exceeded that of pure tungsten from 16 hr to 32 hr, implicating the starting of mechanical alloying between tungsten matrix and titanium element. Finally, both MA powders with 3.0- and 5.0-mm balls exhibited dilatations of 0.14% and 0.29% after 64-hr MA. These results reflect that collision energy caused by the MA ball weight affected the acceleration, suggesting the possible beneficial effect of shortening MA time.

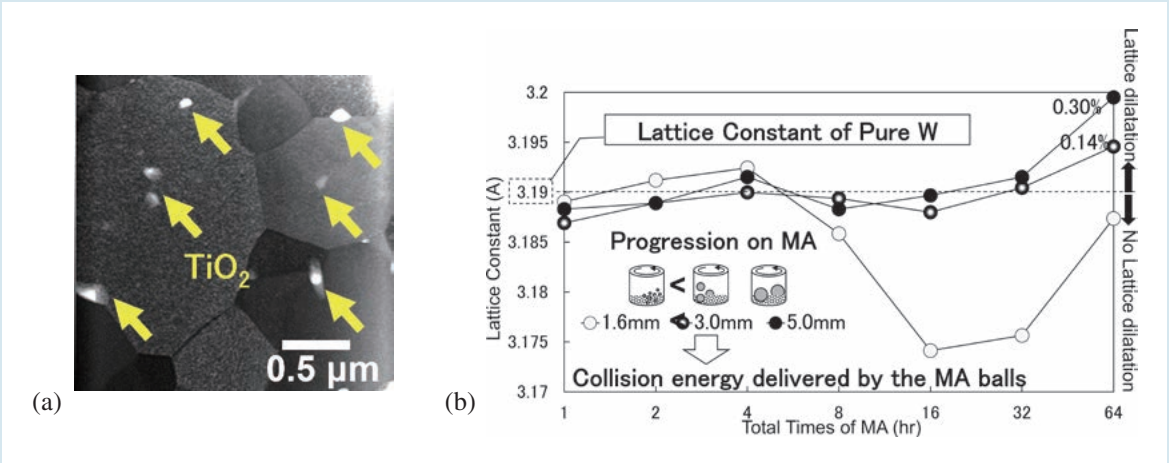

Fig. 6 (a) Microscopic image of oxide dispersion strengthened tungsten (ODS-W) using titanium oxide, (b) variation of lattice dilatation (LD) with MA time

(H. Noto)

For spectroscopic diagnostics on impurity ions in fusion plasmas, we have been acquiring spectroscopy data of highly charged tungsten ions using an electron beam ion trap (called CoBIT). High-resolution spectral measurements are required to resolve many spectral lines to be identified for performing detailed spectral analysis. Recently, we attempted high-order and high-resolution spectroscopy using higher-order light from a diffraction grating for the extreme ultraviolet wavelength region and succeeded in resolving broad lines around 50 Å of highly charged tungsten ions ($W^{26\sim30+}$). (Fig. 7)

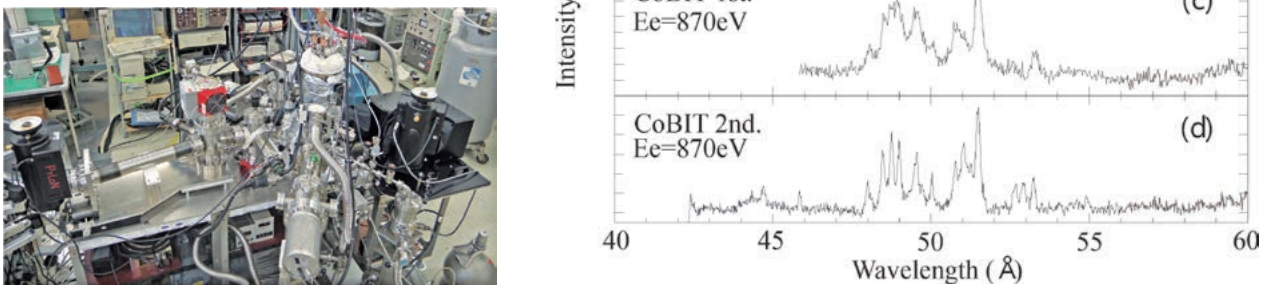

Fig. 7 [Left] Photo of the electron beam ion trap "CoBIT" with installed spectrometers and [right] highly charged tungsten ions spectra: (a) CR-model calculation, (b) typical LHD spectrum, (c) CoBIT spectrum, and (d) second-order spectrum of CoBIT.

(M. Tokitani and H. Sakaue)

Research and Development on Superconducting Magnet

In recent designs of the helical fusion reactor series FFHR, the High-Temperature Superconducting (HTS) magnet is considered and a 100-kA-class HTS conductor has been developed. It is noted that large-current capacity HTS conductors are also being developed in the world to be applied to a variety of designs of fusion reactors. As a prior phase to fusion reactors, applying HTS magnets to the next-generation fusion experimental devices is now being explored. For this purpose, a relatively smaller conductor is required, and presently the target is found at 10–20 kA current in a magnetic field of ~10 Tesla at a temperature of 20 K. Three types of HTS conductors, STARS, FAIR, and WISE (Fig. 8) with different internal structures are being developed with all using REBCO tapes. For these conductor types, 1-3-m long samples have been fabricated and tested in liquid nitrogen (77 K) with no external magnetic field, and the fabrication method has been improved. Then the conductors are tested in a high magnetic field (<8.5 Tesla) and at low temperature (20–50 K) using the large-superconductor testing facility by installing 2-m long conductor samples. A 6-m long, coiled sample was fabricated for the STARS conductor (Fig. 9) and successfully tested at 20 K, 8 T in the large-bore, high-field superconductor testing facility.

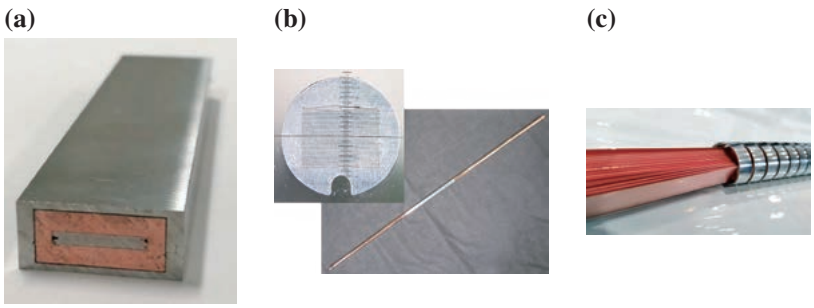

Fig. 8 Schematic drawings of the three types of large-current HTS conductors being developed to apply to the next-generation fusion experimental devices: (a) STARS, (b) FAIR, and (c) WISE conductor.

Fig. 9 A 6-m-long coiled HTS-STARS conductor sample and the research team.

Development of Rapid Heating/Quenching and Transformation (RHQT) processed Nb_3Al multifilamentary tapes has progressed for the new Low-Temperature Superconducting (LTS) magnet option on the DEMO reactor design. We employed a rectangular shape for the improvement of wire flexibility, aiming for the "React and Wind" process. No critical current density (Jc) deterioration was already confirmed, even if a bending strain was applied above 0.6%. Effects of cold flat-rolling on the non-Cu Jc of the RHQT processed Nb_3Al multifilamentary tapes were also investigated. As shown in Fig. 10(a), the non-Cu Jc property was amplified by increasing the accumulated reduction ratio. And non-Cu Jc values corresponded to above twice higher than that of the conventional round-shaped sample before cold flat-rolling. As shown in Fig. 10(b), the non-Cu Jc property of the rectangular tape-shaped sample under an external magnetic field above 18 T was higher compared with that of the round-shaped sample. This Jc improvement under a higher magnetic field would be caused by the increase of pinning centers due to the grain boundary density increment associated with the Nb_3Al grain refinement.

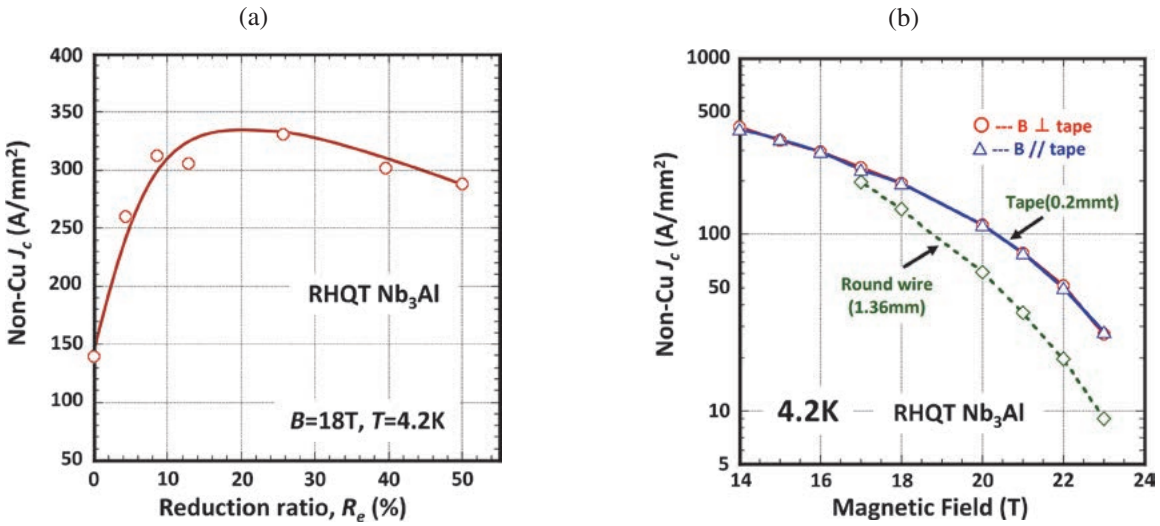

Fig. 10 (a) Non-Cu Jc as a function of the accumulated reduction ratio, (b) Non-Cu Jc of the rectangular tape-shaped sample under an external magnetic field.

(N. Yanagi and Y. Hishinuma)

LHD-Project Research Collaboration

The LHD Project Research Collaboration program has been contributing to enhancing both the scientific and technological foundations of research related to the LHD project as well as to future helical fusion reactors. A feature of this collaboration program is that all research is performed at universities and/or institutions outside NIFS. For fusion engineering, the following eleven subjects were conducted in FY2021:

1. Development of highly ductile tungsten composite systems
2. Fundamental engineering of tritium recovery process for liquid blanket of helical reactor
3. Development of new rapid-heating and quench processed Nb_3Al large-scaled cables for the helical winding due to the react and winding method
4. Evaluation of heat-transfer-enhanced channel under high magnetic field for liquid molten salt blanket development
5. Evaluation of multi hydrogen isotope transfer behavior on plasma driven permeation for plasma facing materials
6. Studies on liquid hydrogen cooled HTC superconducting magnet
7. The analysis of biological effects elicited by organically bound tritium using life science techniques
8. Technological development of FeCrAl-ODS alloys coexisting with liquid metal cooling system of helical fusion reactor
9. Development of REBCO high Tc coated conductor with conductive micro-path
10. Fabrication technology development toward practical use of functional coating for helical reactor liquid blanket
11. Improvement of environmental tritium transfer model based on the observation near tritium released facilities

From the above eleven collaborative research items, subject 2 is briefly described below:

2. Fundamental engineering of tritium recovery process for liquid blanket of helical reactor

NIFS is collaborating with universities to study liquid metal lithium-lead (LiPb) as one of the candidate tritium breeding and cooling materials for fusion blanket systems. LiPb was already short-listed as a candidate material in the 1980s, whereas it was not treated as a primary design target due to the impractical tritium extraction device size. Estimation of a tritium release rate Q for the device was performed based on a static diffusion coefficient of hydrogen isotopes in LiPb. A breakthrough proof of principle (PoP) was performed in 2010 in a laboratory at Kyoto University. The release rate Q was enhanced by two orders of magnitude when LiPb droplets with dissolved tritium were falling in a vacuum (hereafter named vacuum sieve tray (VST)). This discovery, however, was at a laboratory scale with a single column of droplets, and its technology readiness level (TRL) was not high. To ensure that the VST is a viable blanket technique for a practical fusion reactor, the following requirements must be met. One is the stability of the high tritium release rate Q during a practical operation. Another is proof of the same release rate from multiple falling droplets which is mandatory for supplying a quantity of liquid LiPb for a fusion reactor. To enhance the VST TRL level, a scaled-up setup was integrated into Oroshhi-2 (liquid metal test loop at NIFS) as shown in Fig. 11. A couple of campaigns were undertaken. Results showed the

viability of the VST for a practical operation. An epoch-making result was the discovery of a significantly high Q value, which is six orders of magnitude higher than that in the static condition. It is owing to the quick dispersion of tritium in falling LiPb droplets with spherical oscillation. This result affects the tritium inventory analysis of blanket systems, which is one of the major issues of safety and fuel self-sufficiency. The experimental campaign will continue in FY2022.

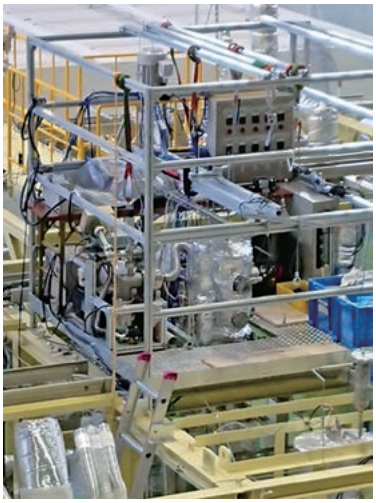

Fig. 11 Overview of the VST experimental setup which was integrated into the Oroshhi-2 facility at NIFS.

(Y. Hamaji, T. Tanaka, J. Yagi (Kyoto Univ.) and F. Okino (Kyoto Univ.))

3. Numerical Simulation Reactor Research Project

Fusion plasmas are complex systems which involve a variety of physical processes interacting with each other across wide ranges of spatiotemporal scales. In the National Institute for Fusion Science (NIFS), we are utilizing the full capability of the supercomputer system, the Plasma Simulator, and propelling domestic and international collaborations in order to conduct the Numerical Simulation Reactor Research Project (NSRP). Missions of the NSRP are i) to systematize understandings of physical mechanisms in fusion plasmas for making fusion science a well-established discipline and ii) to construct the Numerical Helical Test Reactor, which is an integrated system of simulation codes to predict behaviors of fusion plasmas over the whole machine range.

The Plasma Simulator "Raijin (雷神)" (Fig. 1) began operations in July 2020. It consists of 540 computers, each of which is equipped with eight "Vector Engine" processors. The 540 computers are connected to each other by a high-speed interconnecting network. The computational performance is 10.5 petaflops. The capacities of the main memory and the external storage system are 202 terabytes and 32.1 petabytes, respectively.

Presented below in Figs.2 and 3 are examples of successful results from collaborative simulation research in 2021-2022 on gyrokinetic simulation of multi-scale (ion-scale and electron-scale) turbulence and on optimization of magnetic field configuration, based on continuous helical coils by the optimization code, OPTHECS, respectively. Also, highlighted in the following pages are achievements of the NSRP research task groups on energetic-particle physics, peripheral plasma transport, multi-hierarchy physics, and a basis of simulation science.

(H. Sugama)

Fig. 1 The Plasma Simulator, "Raijin (雷神)"

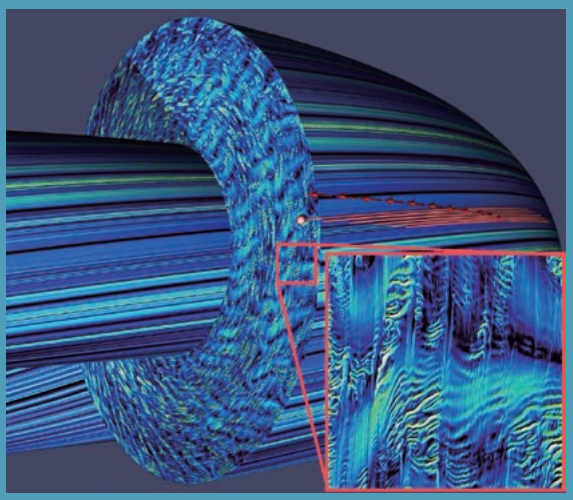

Fig. 2 Perturbed electric field obtained by gyrokinetic simulation of multi-scale (ion-scale and electron-scale) turbulence in a tokamak plasma [presented by Dr. S. Maeyama (Nagoya University)]. Trapped electron motion and magnified perturbation pattern are also shown. Reference: S. Maeyama *et al.*, Nature Communications **13**, 3166 (2022).

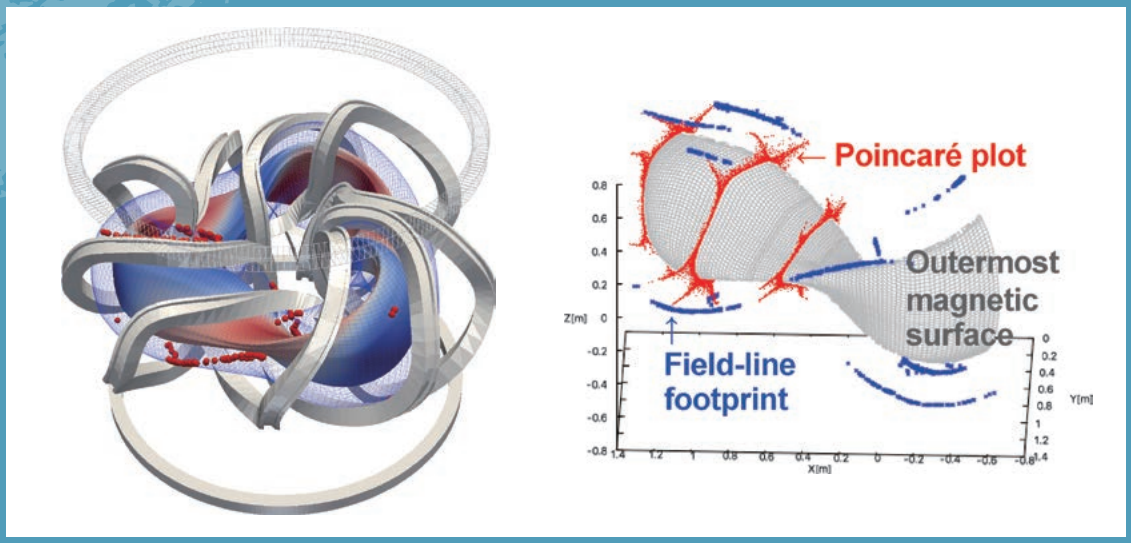

Fig. 3 Optimization of magnetic field configuration based on continuous helical coils by the optimization code, OPTHECS. Low aspect ratio configuration based on quasi-helical symmetry (left) and divertor leg structure created by helical coils (right) [presented by Dr. H. Yamaguchi (NIFS)]. Reference: H. Yamaguchi *et al.*, Nucl. Fusion **61**, 106004 (2021).

Energetic-particle driven instabilities and energetic-particle transport in helical plasmas

Highlight

Simulations of energetic-particle driven instabilities in CFQS

A nonlinear simulation of the energetic-particle (EP) driven instabilities in the Chinese First Quasi-Axisymmetric Stellarator (CFQS) has been conducted for the first time. MEGA, a hybrid simulation code for EPs interacting with a magnetohydrodynamic (MHD) fluid, was used in the present work. Both the m/n = 3/1 energetic particle mode (EPM) and the m/n = 5/2 toroidal Alfvén eigenmode (TAE) were found, where m is the poloidal mode number and n is the toroidal mode number. Four important results were obtained, as follows. First, the instability in the CFQS in three-dimensional form was demonstrated for the first time, as shown in Fig. 1(a). Second, strong toroidal mode coupling was found for the spatial profiles, and it is consistent with the theoretical prediction. Third, the resonant condition caused by the absence of axial symmetry in the CFQS was demonstrated for the first time, as shown in Fig. 1(b) and (c). The general resonant condition is $f_{mode} = Nf_{\varphi} - Lf_{\theta}$, where f_{mode}, f_{φ}, and f_{θ} are mode frequency, particle toroidal transit frequency, and particle poloidal transit frequency, respectively; N and L are arbitrary integers, representing toroidal and poloidal resonance numbers. For the EPM, the dominant and subdominant resonant conditions are $f_{mode} = 3f_{\varphi} - 7f_{\theta}$ and $f_{mode} = f_{\varphi} - f_{\theta}$, respectively. For the TAE, the dominant and subdominant resonant conditions are $f_{mode} = 4f_{\varphi} - 9f_{\theta}$ and $f_{mode} = 2f_{\varphi} - 3f_{\theta}$, respectively. On the one hand, the toroidal resonance numbers (N) are different by two from the toroidal mode numbers (n) for the dominant resonance. This indicates that two-fold rotational symmetry affects the resonance condition. On the other hand, the subdominant resonances satisfy N = n, which is expected for axisymmetric plasmas and most of the toroidal plasmas, including stellarators. Fourth, the nonlinear frequency chirping in the CFQS was demonstrated for the first time. Hole and clump structures were formed in the velocity space of pitch angle and energy, and the particles comprising the hole and clump were kept resonant with the modes during the mode frequency chirping.

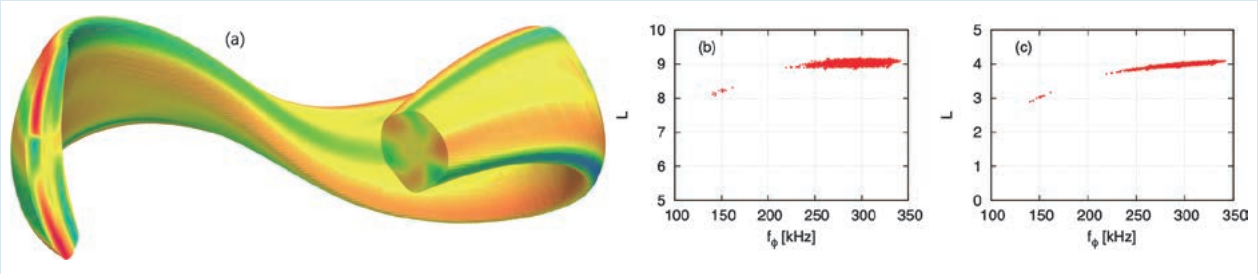

Fig. 1 (a) Radial velocity v_{rad} of the simulated EPM in three-dimensional form. The orange and red represent the velocity from core to edge, while the green and blue represent the velocity from edge to core. (b) The L values of 4096 resonant particles of the TAE for N = 4, where the L = 9 particles represent the dominant resonant condition. (c) The L values of 4096 resonant particles of the TAE for N = 2, where the L = 3 particles represent the subdominant resonant condition.

[1] H. Wang *et al.*, Nucl. Fusion **62**, 106010 (2022).

(H. Wang)

Numerical investigation into the peripheral energetic-particle-driven MHD modes in Heliotron J with free-boundary hybrid simulation

The interaction between EPs and EP-driven MHD instabilities in the Heliotron J, a low-shear helical axis stellarator/heliotron, is investigated with MEGA under a free boundary condition on the last closed flux surface. The m/n = 2/1 EPM and the m/n = 4/2 global Alfvén eigenmode (GAE) in the peripheral plasma region of the Heliotron J are successfully reproduced under the free boundary condition. The free boundary condition affects the EP driving rate of the m/n = 2/1 EPM and the m/n = 4/2 GAE through the changes in the mode spatial profile. Under a fixed boundary condition, the linear growth rate of the EP-driven MHD modes with low mode numbers is underestimated. The interaction between EPs and these experimentally observed modes is kinetically analyzed, as shown in Fig. 2. It is found that the strongest EP-shear Alfvén wave interactions arise from toroidicity-induced resonances in the high-velocity region. These high-velocity EPs have large orbit width, and they can efficiently interact with the peripheral EP-driven mode. Additional toroidally-asymmetric resonances are localized in the low-velocity region; therefore, their effects are weak for the bump-on-tail EP velocity distribution function.

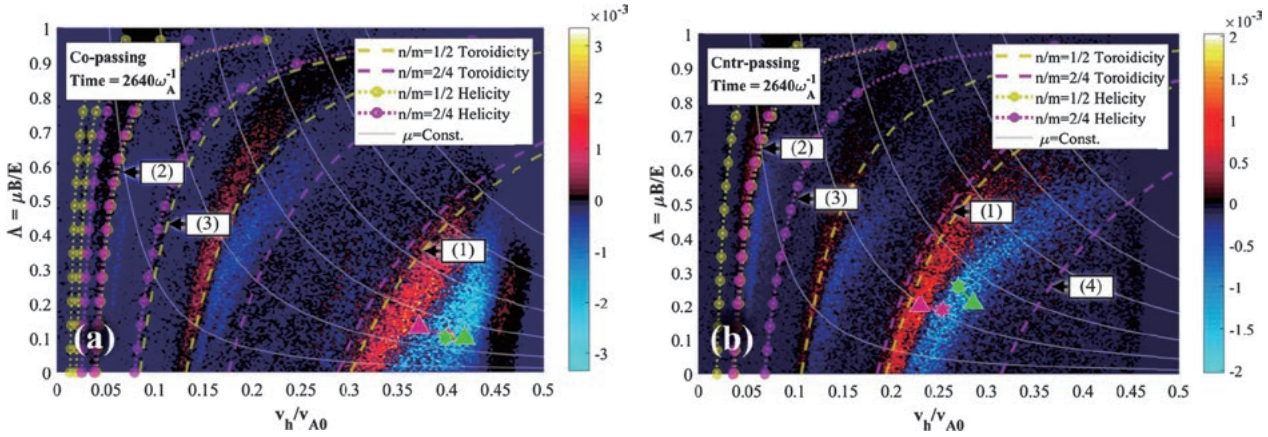

Fig. 2 The EP distribution function variations due to the interaction with EPM and GAE in (v, Λ) phase space, where Λ is the pitch angle. (a) co-passing and (b) counter-passing EPs. The dashed lines and dotted lines with circles represent toroidicity and helicity-induced resonances, respectively. The yellow and purple colors represent the resonant curves for the EPM and GAE, respectively. The purple and green markers indicate the destabilizing and stabilizing resonant EPs with the highest value of |δf|, respectively. The hexagram and triangle indicate the initial and final locations in velocity space of these resonant EPs, respectively.

[2] P. Adulsiriswad *et al.*, Nucl. Fusion **61**, 116065 (2021).

(P. Adulsiriswad)

Simulation study of energetic-particle driven off-axis fishbone instabilities in tokamak plasmas

Hybrid simulations for EPs interacting with MHD fluid were performed to investigate the linear growth and the nonlinear evolution of the off-axis fishbone mode (OFM), destabilized by trapped EPs in tokamak plasmas. The spatial profile of the the OFM is mainly composed of m/n = 2/1 mode inside the q = 2 magnetic flux surface where q is the safety factor, while the m/n = 3/1 mode is predominant outside the q = 2 surface, as shown in Fig. 3(a). The spatial profile of the OFM is a strongly shearing shape on the poloidal plane, suggesting a nonperturbative effect of the interaction with EPs. The frequency of the OFM in the linear growth phase is in good agreement with the precession drift frequency of trapped EPs, and the frequency chirps down in the nonlinear phase. Two types of resonance conditions between trapped EPs and the OFM are found. For the first type of resonance, the precession drift frequency matches the OFM frequency, while for the second type, the sum of the precession drift frequency and the bounce frequency matches the OFM frequency. The resonance frequency, which is defined based on precession drift frequency and bounce frequency of the nonlinear orbit for each resonant particle, is analyzed to understand the frequency chirping. As shown in Fig. 3(b), the resonance frequency of positive δf particles chirps down, which may result in the chirping down of the OFM frequency.

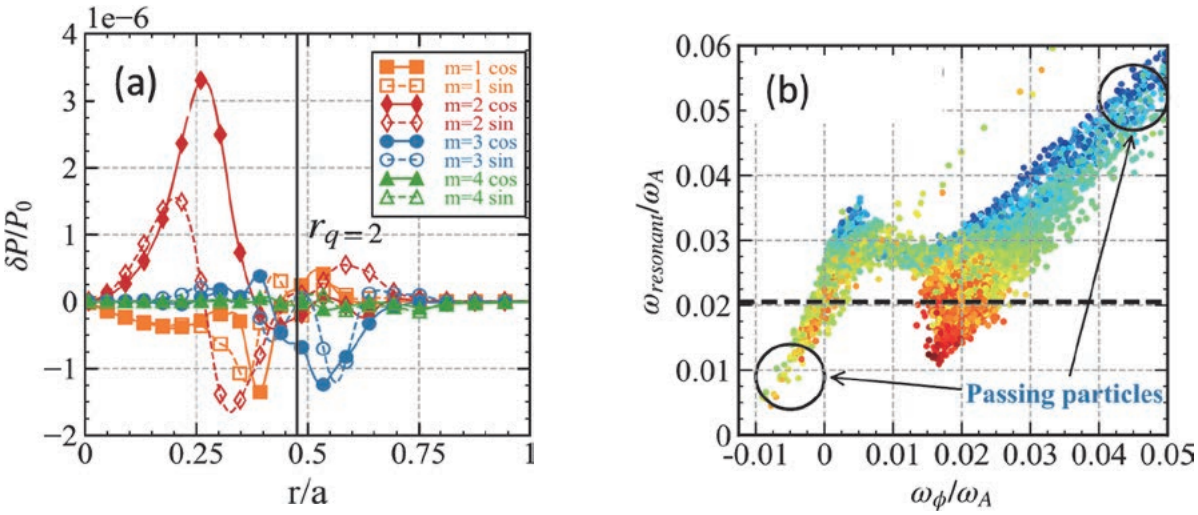

Fig. 3 (a) Radial structures of MHD pressure perturbation at the linear growth phase. The solid (dashed) lines with symbols represent the cosine (sine) parts of Fourier components. The location of the q = 2 magnetic flux surface is denoted by the black solid line. (b) The 8000 particles with the largest |δf| values in (ω_φ, $\omega_{resonant}$) phase space in the nonlinear phase, where ω_φ is particle toroidal orbit frequency and $\omega_{resonant}$ is resonant frequency. Red (blue) color represents positive (negative) δf. The frequency of the OFM is represented by the black dashed line.

[3] H. Li *et al.*, Nucl. Fusion **62**, 026013 (2022).

(H. Li)

New challenges for controlling peripheral plasma transport

Highlight

Divertor configuration control of a quasi-symmetry stellarator by external coils

A new attempt to control the divertor configuration by external coils has been proposed for a stellarator, and its validity has been confirmed by the numerical transport code EMC3-EIRENE. This study has been published [1] and is expected to be one of bases of configuration optimization studies for stellarator devices.

A standard divertor concept has been established for tokamak devices, and many design studies have been performed for many years, while the divertor concept for helical/stellarator devices is not well-established. We installed a set of three external saddle loop coils for each stellarator-symmetry section of a quasi-symmetry stellarator, to control the rotational transform at the edge of the confinement region with closed flux surfaces. The current ratio of the three coils were adjusted to cancel the change of the rotational transform in the core region. We performed a current scan of the external coils, and confirmed the controllability of the confinement region from the connection length distributions shown in Figs. 1(a) and (b); 1) the radial position of the last closed flux surface (LCFS) changes according to the coil current linearly, 2) a positive/negative current increases/decreases the size of the confinement region, and 3) the divertor leg structure outside the LCFS remains and the lengths of the legs change. Steady-state transport calculations were performed for various divertor plate positions, shown in the poloidal cross section in Figs. 1(a) and (b). We use a fixed core electron density and a fixed heating power to see the influence of the divertor configurations on the core electron temperature. The numerical results elucidated the characteristics of divertor configurations; 1) the extension of the leg structure reduces the core temperature because of a smaller core volume and 2) makes the dependence of the divertor plate position on the temperature weaker when the plate is installed outside the LCFS. We concluded that the divertor configuration control for longer divertor legs is effective to reduce the influence of the wall in the core region and to increase the freedom of the divertor plate design.

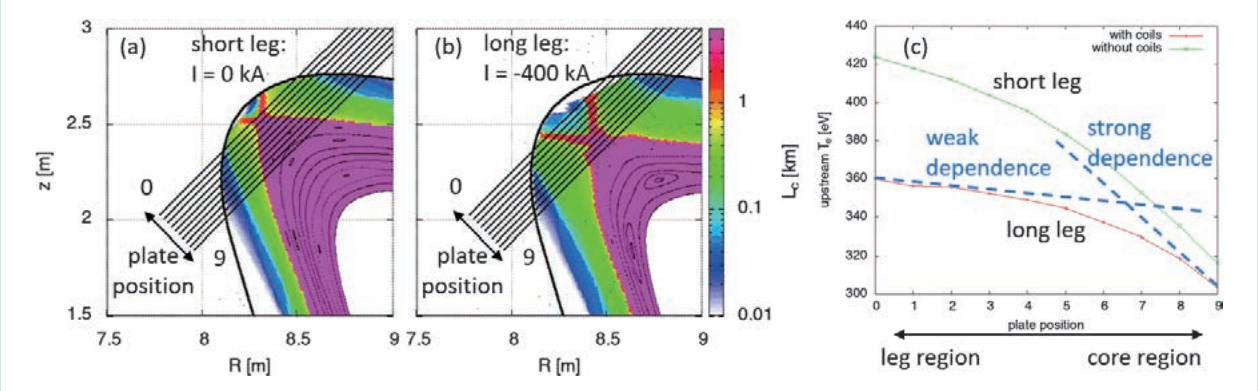

Fig. 1 (a) divertor configuration without coil current and (b) with negative coil current, and (c) dependence of the electron temperature of the core region on the divertor plate position. The two blue dashed lines stand for the gradient of the temperature at the divertor tile positions 0 and 9, in the case of the long leg configuration shown in Fig. 1 (b).

[1] G. Kawamura, M. Nakata, Y. Suzuki, Y. Hayashi, and R. Sakamoto, *"Divertor leg control of a quasi-symmetry stellarator with external coils and its consequences for transport,"* Contrib. Plasma Phys. **62**, e202100196 (2022).

(G. Kawamura)

Particle Simulation of Controlling Particle and Heat Flux by Magnetic Field

An idea for shielding high energy ion and electron fluxes is proposed by applying external magnetic fields [2]. In this work, we model a flowing plasma in a small region by utilizing one spatial dimension and three coordinates for velocities, (the 1D3V) Particle-In-Cell (PIC) code. The plasma which consists of ions and electrons is produced from the source region and absorbed at the conductor wall. The external magnetic field is modified by applying a change of magnetic field in the direction perpendicular to the plasma flow. This magnetic field is localized and switched from strong negative values to strong positive ones at several locations in the simulation region. In figure 2 (a), the magnetic field, B_y, is illustrated. The magnetic fields, B_x, and B_z, are constant and are not changed in this simulation. This magnetic field, B_y, is a small value in comparison with the background magnetic field, B_x, along the simulation domain. We found that this localized reversed magnetic field traps the particles and then reduces the particle and heat fluxes to the wall. Figure 2 (b) shows the comparison of particle and heat fluxes with and without changing the magnetic field. Except for the small region near four "magnetic mirrors", total particle flux is reduced approximately by 76.2% and around 78.9% for the energy flux. Based on the modeling results, external localized-reversed magnetic fields can control the particle and heat fluxes to the wall. These results can be applied for shielding high energy ion and electron fluxes to satellites or spacecraft in space.

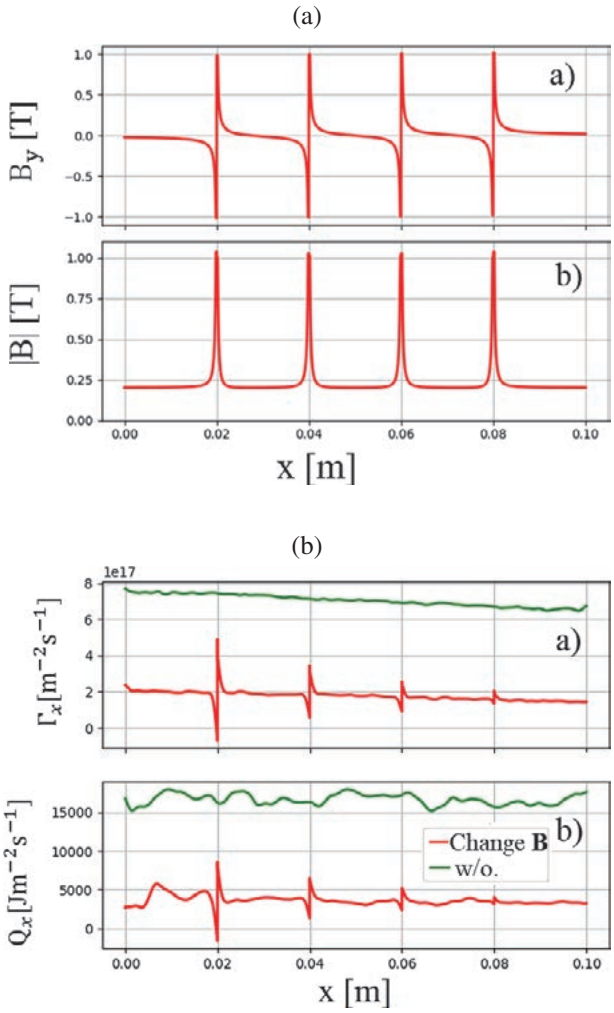

Fig. 2 (a) The analytic function of the magnetic field in y direction and the absolute value of total magnetic field generated by its analytic function in the system. (b) Comparison of one-dimensional total particle flux and energy flux in the case with (red line) and without (green line) changing the magnetic field.

[2] Trang Le, Yasuhiro Suzuki, Hiroki Hasegawa, Toseo Moritaka and Hiroaki Ohtani, *"Particle Simulation of Controlling Particle and Heat Flux by Magnetic Field,"* Plasma Fusion Res. **16**, 1401103 (2021).

(Y. Suzuki, Hiroshima Univ.)

Pseudo-Maxwellian velocity distribution in magnetic reconnection

Highlight

Particle simulations of magnetic reconnection reveal pseudo-Maxwellian velocity distributions, which are almost indistinguishable in shape from a Maxwellian distribution

For realization of fusion on earth, plasma heating to extremely high temperature is required. In a different type of device from LHD, "a spherical tokamak," a heating method via magnetic reconnection is employed. Magnetic reconnection has attracted extensive attention and has been actively studied all round the world. In this study, we investigate magnetic reconnection physics by using our particle simulation code "PASMO." Fig. 1 (a) shows an ion velocity distribution in the downstream region of magnetic reconnection, obtained by the simulation. At first glance, this looks like a Maxwellian velocity distribution, but this is pseudo-Maxwellian, which is almost indistinguishable in shape from a Maxwellian one. Furthermore, we clarify that pseudo-Maxwellian distribution belongs to ring-shaped distribution with a large width [1]. The distribution shape remarkably depends on the width and radius of the ring. When the width is much less than the radius, we can clearly see a ring shape, as displayed in the left case of Fig. 1 (b). As the ring width becomes larger, it is overlapped near the center, and thus the ring's hole is being plugged. If the width is larger than a criterion, the center is transformed from a hole into the peak of a mountain, that is, a pseudo-Maxwellian distribution is formed, as shown in the right case of Fig. 1 (b).

The formation of pseudo-Maxwellian distributions will not be limited to magnetic reconnection. This result means that although a system is not in a thermal equilibrium state, velocity distributions indistinguishable from a Maxwellian one can exist, and has a potential to significantly affect existing knowledge in experiments and observations.

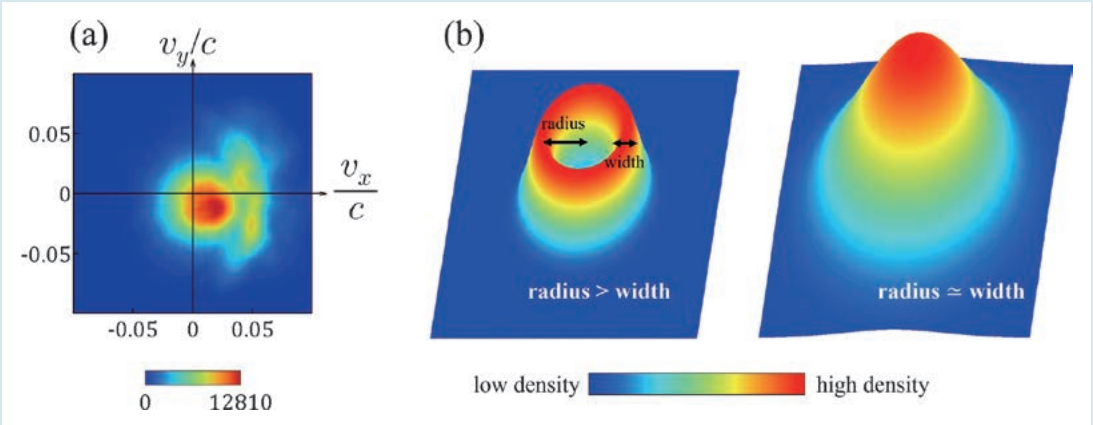

Fig. 1 (a) Pseudo-Maxwellian ion velocity distribution found in a particle simulation, where c is the speed of light. (b)Schematic diagram of velocity distributions (bird's eye view). In the left case, the ring width is much less than the radius, and hence we can clearly see a ring-shaped structure. In the right case, in which the width is nearly equal to the radius, we can see a pseudo-Maxwellian distribution.

[1] S. Usami and R. Horiuchi, Front. Astron. Space Sci. **9**, 846395 (2022).

(S. Usami)

Theoretical Analysis of Cross-field Dynamics on Detached Divertor Plasmas

In order to reduce heat flux into divertor plates, it has been proposed that the plasma is detached from the divertor plates with neutral gases. On the other hand, the correlation between the detachment and cross-field plasma transports has been observed in various magnetic confinement devices. Such a correlation is expected to reduce the maximum heat flux density with an expansion of its width. In this study, we proposed a theoretical model of feedback instability for the mechanism of the correlations. We considered the detached divertor plasma model with both electric currents in the upstream plasma and the detached region. As a result, we found that a feedback instability mode could be induced under a certain condition and that the waves of the unstable mode could transport the plasma across the magnetic field line. We also analyzed the dependences of the feedback instability mode on the total collision frequency and the recombination coefficient in the detached region, as shown in Fig. 2, and that on the density gradient [2,3].

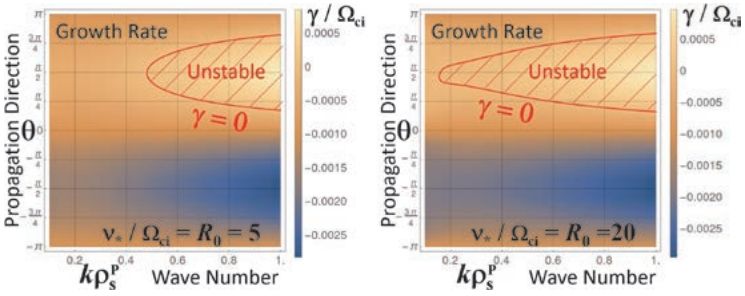

Fig. 2 Dependences of the growth rate of the feedback instability mode on the wave number and the propagation direction with the parameters of a typical fusion torus device. Here the total collision frequency and the recombination coefficient in the detached region for the left panel are lower than those for the right panel.

[2] H. Hasegawa, H. Tanaka, and S. Ishiguro, 28th IAEA Fusion Energy Conference, TH/P4-18 (2021).
[3] H. Hasegawa, H. Tanaka, and S. Ishiguro, Nuclear Fusion **61**, 126005 (2021). (H. Hasegawa)

Isotope effect in multi-ion-species helical plasmas under radial electric fields

Confinement of mixed hydrogen isotope plasmas is necessary for effective fusion reactions in future thermonuclear reactors. We focus on the mass number dependency of ion thermal conductivity, due to the ion temperature gradient mode (Fig. 3) in such multi-ion-species plasmas. The global gyrokinetic code, XGC-S, is employed for quasi-linear estimation of ion thermal conductivity under a global radial electric field in a helical configuration.

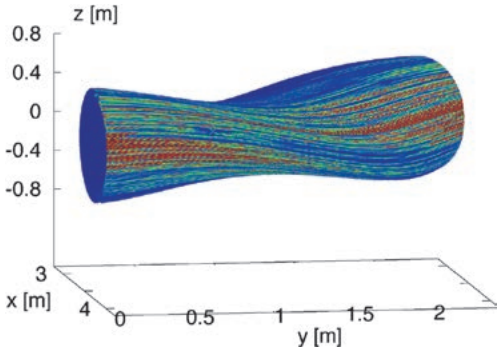

Fig. 3 Potential fluctuations due to ion temperature gradient mode in a helical configuration.

It is found that the heavy hydrogen component effectively enhances the light hydrogen heat flux, which mainly affects the ion thermal conductivity. This effect is evident for light-hydrogen-dominated plasmas with small average mass numbers. As a result, the average mass number dependency becomes more favorable than conventional gyro-Bohm scaling. The radial electric field can affect ion thermal conductivity through mode stabilization and wavelength elongation. In single-ion-species plasmas, these two effects result in the transition from unfavorable gyro-Bohm scaling to favorable mass number dependency. The present simulation study shows that the radial electric field suppresses the ion heat flux, while keeping the favorable mass number dependency in multi-ion-species plasmas. In conclusion, the radial electric field and the heavy hydrogen component potentially realize the favorable mass number dependency, observed in the Large Helical Device and other experimental devices. This result was presented at the 28th IAEA Fusion Energy Conference [4].

[4] T. Moritaka, M. Cole, R. Hager *et al.*, "Isotope effects in ion temperature gradient modes with radial electric field in Large Helical Device", 28th IAEA Fusion Energy Conference, online, May 10–15 (2021). (T. Moritaka)

Visualization analysis of data, and development of simulation methods

Highlight

Visualization of plasma shape in the LHD-type helical fusion reactor, FFHR, by a deep learning technique

A magnetic confinement fusion reactor generates a helical magnetic field to limit plasma in a certain region. To achieve a continuous nuclear reaction, it is important to prevent plasma from having a collision with inner components of the reactor. Therefore, the shape of this region, the plasma shape, is relative to the inner components design of a fusion reactor. To represent the shape of this region, thousands of magnetic field lines are traced in the helical magnetic field and it causes some problems. First, rendering all the lines takes a lot of time. Besides, to check for interferences, it is unnecessary to consider those magnetic field lines buried under other lines. Second, separated lines cannot provide a continuous and clear boundary. Finally, the Larmor radius is hard to represent with lines. Therefore it is suitable to represent plasma shape by a surface. However, due to the helical magnetic field, it lines are twisted and entwined with each other. Regardless of whether the connectivity information of a line has been provided, the relative position information between two lines is extremely complex. Therefore it is difficult to know which lines are contributing to surface generation.

To tackle the challenge, we propose using a deep neural network (DNN) to learn the representation of the plasma shape and to reconstruct a regular scalar field from the magnetic field lines [1]. The intersection points on each poloidal plasma cross-section are used to make annotations, according to the connection length of the magnetic field line to which they belong. Afterward, these labeled points are inputted into a DNN as training material. Therefore the trained DNN can label each point from its new position in the scalar field. Then the scalar field can represent the different parts of the plasma shape by collecting the points with the same label. Since the scalar field has been structured, the magnetic flux intensity at any position of this scalar field is easily obtained. The Larmor radius then can be calculated. The representation of a Larmor radius is embedded in the scalar field. With a scalar field, the marching cubes (MC) method can be used to generate an isosurface for different parts of the plasma shape. The right of Fig. 1 shows a visualization result of a quarter of the plasma shape model. The model accurately reproduces the complicated plasma shape structure. Compared with rendering using line objects, it clearly distinguishes the two areas. Furthermore, because of the surface representation, it enables us to check the interferences directly between the plasma shape model and 3D design data of components in the FFHR, as shown on the right of Fig. 1.

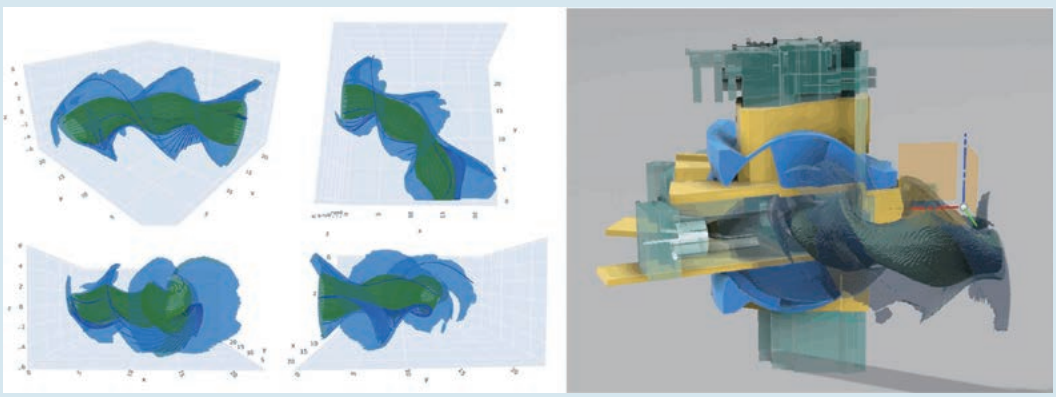

Fig. 1 On the left is a visualization result of a quarter of the plasma shape. The surface represents the edge surface layers and part magnetic field lines inside it, which are in blue, and the LCFS and part magnetic field lines inside it are in green. On the right is rendering result of the plasma shape and the fusion reactor.

(Kunqi Hu, Kyoto University)

Virtual-reality visualization of collision points of energetic tritons and plasma facing wall

The collision points of energetic tritons with a plasma facing wall of LHD are displayed with the divertor plates and vacuum vessel in a virtual-reality (VR) space, to research the distribution of the collision points [2]. The trajectory of the energetic tritons is calculated by the LOBIT code from the triton generation distribution given by the FIT3D-DD code. The trajectory calculation is performed without any collision effects under conditions in which the magnetic field is in a vacuum, the effect of the plasma is not included, and the electric field is negligibly small. Then the intersection points of the tritons and the plasma facing wall are detected. Each intersection point is stored in Cartesian coordinates. A point is visualized as a sphere by the Point-Sprite method in VR space with the rendered CAD data of divertor plates and the vacuum vessel. The points and CAD data are rendered by different visualization software, OpenGL-CAVE and Unity, respectively. The image data generated by the different software are captured and superimposed by a Fusion SDK. It is possible to investigate the distribution of the collision points on the divertor and vacuum vessel with realistic descriptions, shown in Fig. 2. This visualization helps the experiment researchers to determine the position of the material probe which catches the energetic tritons in real LHD experiments.

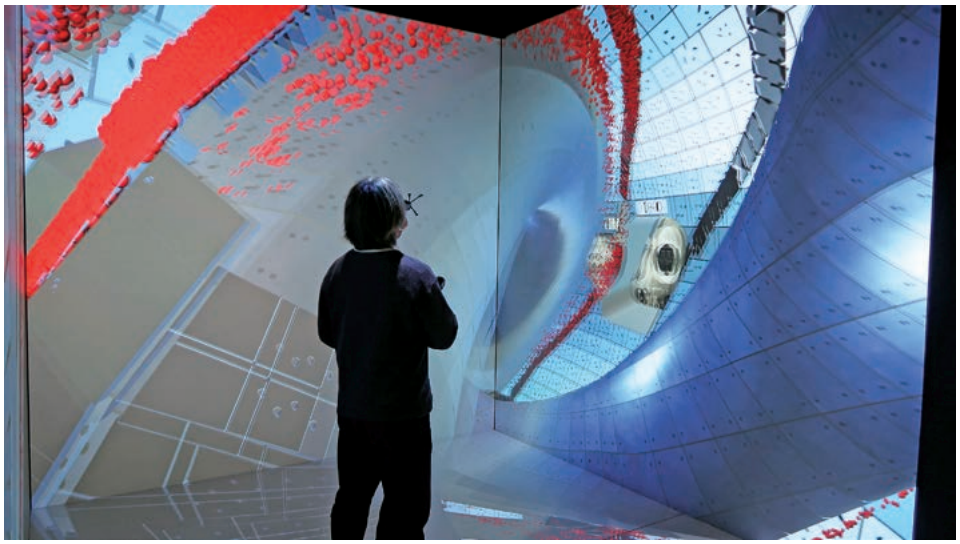

Fig. 2 The collision points of the energetic tritons and the plasma facing wall in LHD are visualized in the vacuum vessel in the VR space.

Development of the edge-based finite element method for investigation of high-temperature superconducting tape.

The permanent magnet method was proposed for measuring critical current density in HTS tape contactlessly and non-destructively. When a permanent magnet approaches and leaves the HTS tape, a shielding current is induced in the tape and the repulsive and attractive forces act on the permanent magnet, respectively. When the HTS tape is exposed to sufficiently large magnetic field, the shielding current becomes equal to the critical current and the repulsive and attractive forces are proportional to the critical current. Our developed numerical code, based on the edge-based finite element method, can evaluate the shielding current in the HTS tape and the force working on the permanent magnet, by solving the Maxwell equation with superconductivity characteristics. Figure 3 shows the dependence of the maximum force acting on the magnet on the number of the HTS tapes. When the magnetic flux density B_0 of the permanent magnet is 0.3T, the maximum force, F_M/F_{single}, is proportional to the number L of tapes for $L < 25$. On the other hand, when $B_0 = 1$T, F_M/F_{single} is proportional to L for $L < 40$. From this result, it is found that the permanent magnet method can measure the critical current density in multiple HTS tapes, and that the method has an upper limit of the number L of HTS tapes, in which the current density can be evaluated.

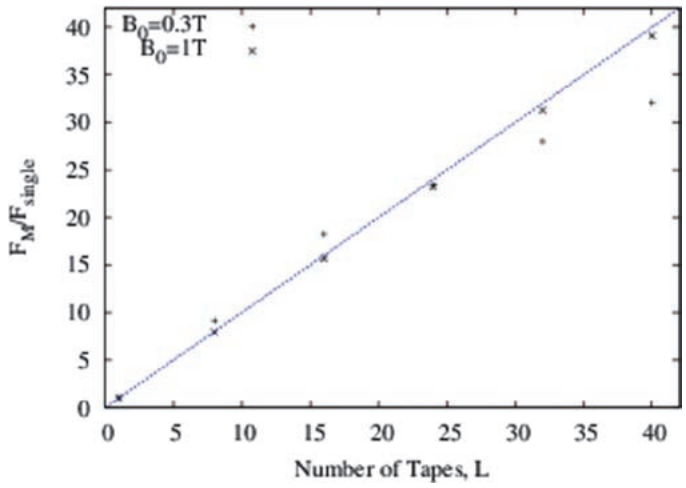

Fig. 3 Dependence of the maximum force, F_M, on the number of HTS tapes. The maximum force is divided by the value of the force, F_{single}, in a single HTS tape ($L = 1$). B_0 is a magnetic flux density of the permanent magnet.

[1] Kunqi Hu *et al.*, J. Visualization **24**, 1141 (2021).
[2] Hiroaki Ohtani *et al.*, J. Visualization **25**, 281 (2022).
[3] Takazumi Yamaguchi *et al.*, Plasma Fusion Res. **17**, 2405035 (2022).

(H. Ohtani)

4. Basic, Applied, and Innovative Research

As an inter-university research institute, NIFS activates collaborations with researchers in universities, as well as conducting worldwide top-level research. It is important to establish an academic research base for various scientific fields related to fusion science and to maintain a powerful scientific community to support the research. Programmatic and financial support to researchers in universities who work on small collaboration projects are important.

For basic plasma science, NIFS operates several experimental devices and offers opportunities to utilize them in a collaboration program for university researchers. A middle-size plasma experimental device the HYPER-I is available for basic plasma research. The compact electron beam ion trap (CoBIT) for spectroscopic study of highly charged ions, atmospheric-pressure plasma jet devices for basic study on plasma applications, and other equipment are all used for collaborations.

(I. Murakami)

Improvement of energy conversion fraction towards electrons in high guide field magnetic reconnection

The macroscopic behavior of magnetic reconnection is drastically affected by a guide magnetic field, which is involved in the spherical tokamak formation process by use of a plasma merging technique. A self-generated in-plane electric field is essential to sustain steady plasma outflow from the reconnection region under the presence of a large guide field. Fig. 1 shows spatiotemporal evolutions of (a) reconnection electric field E_t, (b) current density j_t, (c) in-plane electric field E_z, and (d) parallel electric field $E_{//}$ along the current layer formed on the mid-plane of the UTST plasma merging experiment, with limiter plates equipped on the center stack [1]. It was found that E_z was largely suppressed in the region where magnetic field lines were connected to the conducting limiter plates (shown by the hatched area in Fig. 1 (c)) due to the electric short-circuit effect. This suppression of E_z lead to maintaining large $E_{//}$, as shown in Fig. 1 (d), resulting in electron acceleration along the field lines in the inboard-side downstream region. This result suggests that boundary condition modification could change the energy conversion fraction towards electrons in high guide field magnetic reconnection.

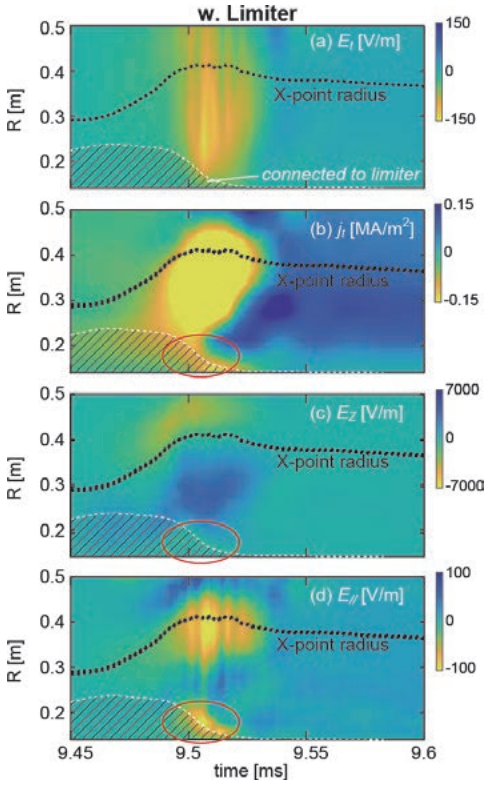

Fig. 1 Time evolutions of radial profiles of (a) toroidal electric field E_t, (b) toroidal current density j_t, (c) axial electric field E_Z, and (d) parallel electric field $E_{//}$ measured on the midplane ($Z = 0$) in the ST merging start-up with limiter plates [1].

(M. Inomoto, Univ. of Tokyo)

Development of a compact negative ion source towards improving beam focusing based on velocity distribution functions

A strict requirement is placed on beam divergence lower than 7 mrad for ITER relevant negative ion beams [2]. A single negative ion beam extracted from a research and development negative ion source at the National Insti-

tute for Fusion Science (NIFS-RNIS) has been observed with multiple velocity distribution functions, as shown in Fig. 2, and their abundance ratio has been quantified with an emittance meter [3]. This experimental result indicates that several production and extraction processes of negative ions, due to a cesium seeded negative ion source, may affect such velocity distributions and the resultant superimposed beam divergence.

In order to investigate the correlation between the production and extraction mechanism of negative ions and their velocity distributions, a compact negative ion source, including beam diagnostics to measure transverse velocity distributions, is being developed at Nihon University.

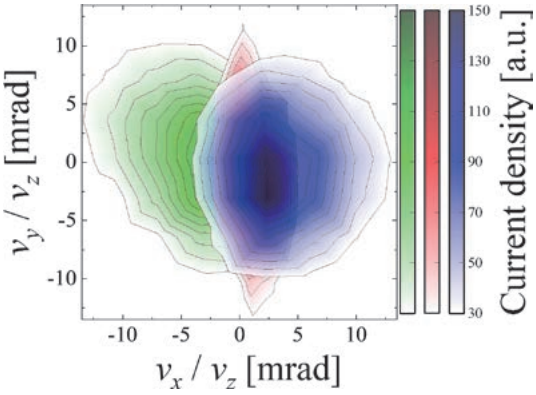

Fig. 2 The velocity distributions for the single negative ion beam produced by the NIFS-RNIS.

(Y. Haba, Nihon Univ.)

Application study of data analysis technology to medical data in nuclear fusion towards a medical-engineering cooperation

Aiming to apply data analysis techniques in the field of nuclear fusion, this study is conducting data analysis of Kawasaki disease. This pediatric disease is unique to children, and the cause of its onset is still unknown. Possible causes of pathogenesis include infections, autoimmune abnormalities, and environmental factors. In 2020, the incidence of Pediatric Infectious Diseases (PIDs) decreased dramatically due to the COVID-19 pandemic. Therefore, this study investigated the impact of the pandemic on the incidence of Kawasaki disease using infection surveillance data collected by Jichi Medical University. Figure 3 shows percentage changes in the weekly numbers of patients with Kawasaki disease (red) and PIDs (others) in 2020, compared with 2017–2019 [4]. The average number of incidences between 2017 and 2019 was used to calculate the percentage change. It was found that the issuance of the emergency declaration led to a rapid decrease in PIDs and a subsequent decrease in the incidence of Kawasaki disease. A decrease of up to 60% was observed, and the results suggest that PIDs are involved in the development of the disease. This research is a good example of medical-engineering collaboration in data analysis and an application of data analysis techniques developed in the nuclear fusion field.

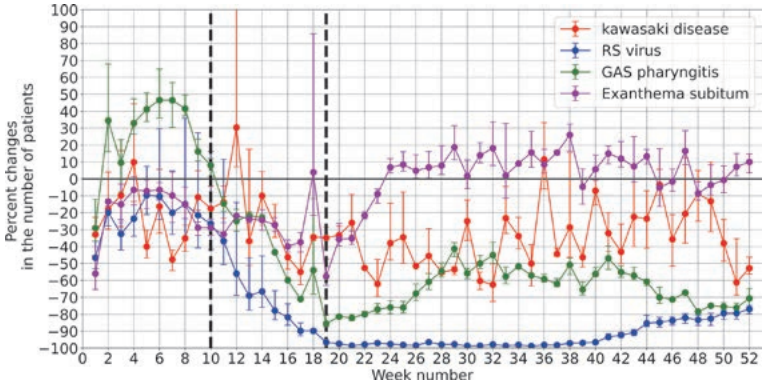

Fig. 3 Percentage changes in the weekly numbers of patients with Kawasaki disease and PIDs in 2020, compared with 2017–2019. The mean and range of weekly percentage changes in the numbers of patients who developed Kawasaki disease and PIDs are compared between 2020 and 2017–2019, shown using error bars in the charts. The school closure period (weeks 10–19) is highlighted using dashed lines. [4]

(Y. Shibata, National Inst. Tech., Gifu)

[1] M. Inomoto *et al.*, Nucl. Fusion **61**, 116069 (2021).
[2] A. Hurlbatt *et al.*, AIP Adv. **11**, 025330 (2021).
[3] Y. Haba *et al.*, AIP Adv. **12**, 035223 (2022).
[4] R. Ae, Y. Shibata *et al.*, J. Pediatrics **239**, 50-8 (2021).

5. Network-Type Collaboration Research

This research is eligible for research conducted by collaborating with facilities owned by the NIFS and multiple universities.

In this fiscal year, the research shown below was done. The titles and brief summaries of the research topics are listed below.

(1) "Development of Plasma Source for Active Control in High Beta Torus Plasmas"

N. Fukumoto (Univ. of Hyogo)

The basic subjects of this collaborative research are the development of plasma sources based on the magnetized coaxial plasma gun (MCPG) method, the theta pinch-Field Reversal Configuration (FRC) method, and the rotating magnetic field (RMF)-FRC method. In this FY, studies were conducted on the development of a new type of MCPG, collisional coalescence generation of FRC, injection of CT into orthogonal magnetic fields, collisionless magnetic pump heating of FRC, the electron acceleration effect during spherical tokamak generation, and aurora simulation by CT injection.

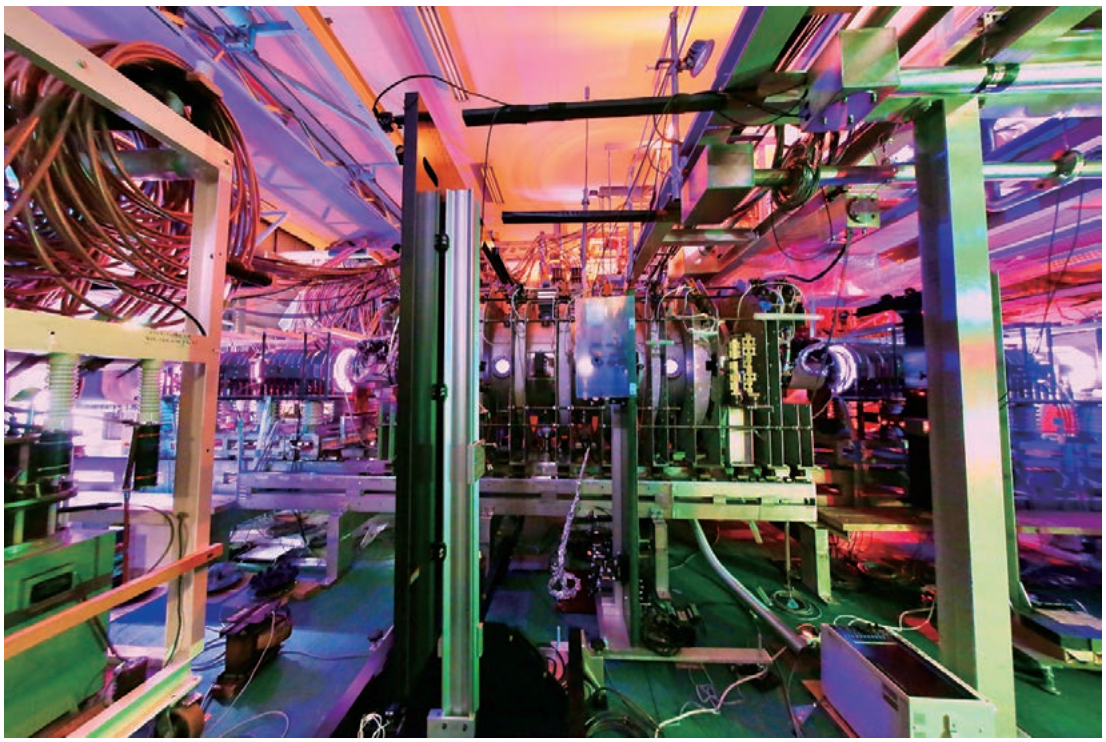

(2) "Study of suppression and avoidance of vertical position shift phenomena in tokamaks using three-dimensional magnetic fields"

T. Fujita (Nagoya Univ.)

In this study, the method of suppressing and avoiding a VDE (Vertical Displacement Effect), which is a problem in tokamak fusion devices during disruption, by using a three-dimensional magnetic field will be studied both experimentally and theoretically. In this FY, studies were conducted on Vertical Position Stabilization by a three-dimensional magnetic field and on the interaction between external RMP and plasma.

(3) "Creation of plasma meta-state science" Y. Sentoku (Osaka Univ.)

This research aims to form a network across the boundaries of magnetized plasma, laser plasma, and plasma applications, to understand dynamically ordered structures, and to gain a new perspective on plasma physics.

(4) "Study on tritium, radon and radium concentrations and dynamics of tritium, radon, and radium in environmental water in Japan" T. Sanada (Hokkaido Univ. of Science)

In this study, a wide-area continuous observation of tritium concentration in environmental water will be carried out by multiple institutions established in this network study, together with NIFS, which has a tritium precision measurement system, at the core. In addition, an analysis of radon (222Rn) and radium (226Ra), which are natural radionuclides, will be conducted to investigate the causes of fluctuation of their concentrations and their usefulness as tracers. Samples to determine tritium concentration in precipitation were collected at Hokkaido University of Science, Hirosaki University, NIFS, Kumamoto University, and the University of the Ryukyus. A measurement method for radium radioactivity concentration in water samples was developed. In addition, groundwater samples were collected from the Hirosaki city area, and radon and radium concentrations in the samples were measured.

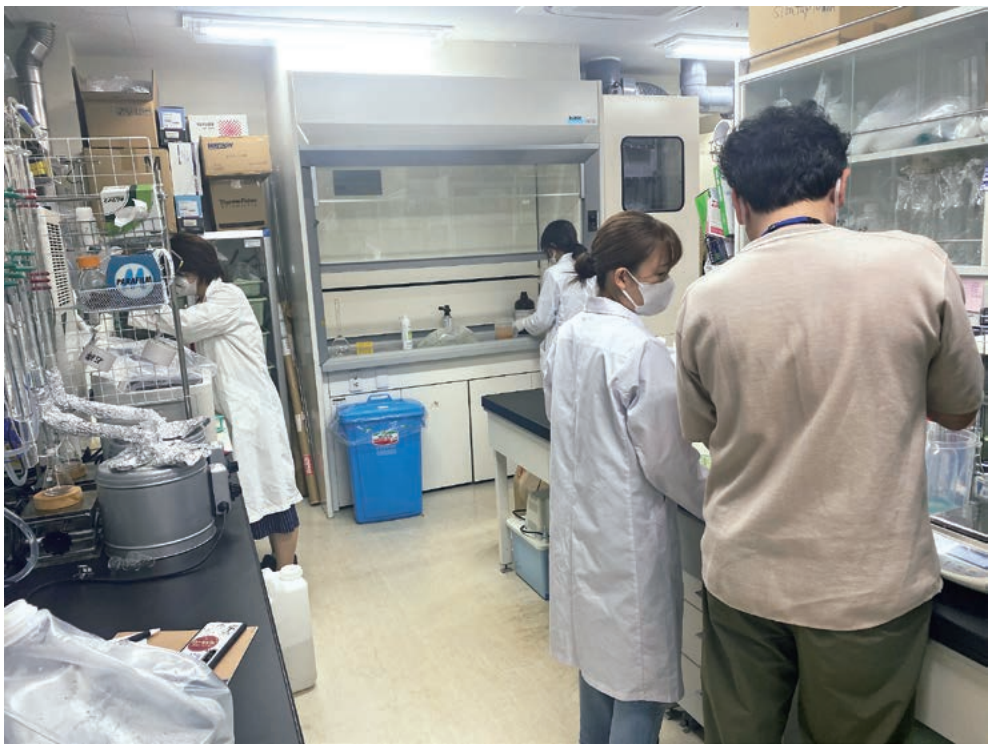

6. Fusion Science Archives (FSA)

The Fusion Science Archives (FSA) was established in 2005 to learn lessons from past fusion science archives which have been preserved and to maintain collections of historical documents and materials that are related to fusion research in Japan. These activities are important from the viewpoint of the historical evaluation of fusion research, its social accountability, and creating references for seeking future directions. Since then, historical materials on fusion research and/or organizations related to fusion research have been collected and preserved at the FSA. They are stored in acid-free folders and boxes. Catalogs of registered items are available to the public through the internet in a hierarchical structure.

The following are some of the collaborative works done this fiscal year.

- **Archival Studies on Collaborations in Heliotron Studies at Kyoto University**

  T. Mizuuchi (Kyoto Univ.) *et al.*

  The activities of this archival study are focused on the materials relating to the development of plasma devices, especially on the development of the series of Heliotron devices originating from Kyoto University. These archives cover not only the hardware but also related researchers, research groups, and their activities which have contributed to the development of the Heliotron concept. In these years, digitizing work of the minutes of research group meetings (PEC, etc.) from the Heliotron-E project has progressed. As of the end of this fiscal year, up to 33 of the 44 volumes of PEC files have been digitized. In addition, we have started to transfer materials recorded on older media such as MO to a new recording medium that can be easily accessed in the current PC environment. As for about 60 volumes of MO data, we have finished transferring the data from MO to HDD. For other materials that have not been sorted, we are trying to categorise and digitize them in turn.

- **Construction of Digital Library of Husimi Kodi Archives**

  H. Iguchi (NIFS, FSA) *et al.*

  Until the end of the last fiscal year, about 900 documents among a total of 4,800 Husimi Kodi documents had been digitized. This year, we started work on those documents in Box 500s, which are mainly related to nuclear development in the early phase in Japan. Kodi Husimi had been a key person in Japanese nuclear development from the early 1950s. After becoming director of the Institute of Plasma Physics, Nagoya University, in 1961, he continued to be involved in policy making. There is a reasonable number of related documents left in the archives, for example, an application form for permission for the construction of the Fukushima Nuclear Power Plant by Tokyo Electric Power Co., Inc (TEPCO). Unfortunately, only a small part of the documents has been digitalized this year, due to the COVID-19 situation. The project should be continued in the daily work of NIFS-FSA.

- **Studies on the history of the establishment of the Institute of Plasma Physics, Nagoya University**

  T. Amemiya (CST Nihon Univ.) *et al.*

  In 1961, the Institute of Plasma Physics (IPP), Nagoya University, was established as the Inter-University Research Institutes of plasma physics and controlled fusion research in Japan. The purpose of this collaborative research is to find new historical interpretations of the IPP, based on the historical documents in NIFS FSA and CST Nihon University. This collaborative research of FY2021 consists of the following subjects: 1) "On the relationship and influence between the Assembly for Nuclear Fusion Reaction (Kakuyugo-Hannou Kondankai) and the Nuclear Fusion Research Group (Kakuyugo-Kondankai)", 2) "On the drafting and background of the plan for the IPP" and 3) "Analysis of historical documents about the establishment of the IPP."

- **Improving name authority data about persons, groups, and organizations related to fusion science in Japan, for fusion science archives**

  H. Gotoh (The Kyoto University Museum) *et al.*

  This study aims to establish a methodology for improving archival name authority data related to fusion science in Japan, which is necessary for identifying names and of proper understanding of various materials. Information about the steering and scientific committee of the Institute of Plasma Physics, Nagoya University, and organizations that committee members belonged to was collected and analyzed (187 committee members and 51 organizations). On February 4, 2022, we held a meeting online and discussed methodologies and desirable output formats. The meeting resulted in the following conclusion: the authority data that we will create in this study needs to be a key data set that can be used to get information from existing authorities' data services and academic data ones, but not necessarily to have a full information set, according to the standard authority data format.

- **Collaborative Activities at NIFS Fusion Science Archives**

  S. Kubo (Chubu Univ.) *et al.*

  One of the topics of this fiscal year is the acceptance of Kazuhisa Mori's personal records and historical materials. Kazuhisa Mori is a younger brother of Shigeru Mori who led Japanese fusion research from its dawn period. He belonged to Hideki Yukawa's laboratory at Kyoto University when the atomic bomb was dropped on Hiroshima. After using up his nine lives, he entered journalism and campaigned for the peaceful usage of atomic power throughout his life, dying in 2010. Reiji Sugano established a voluntary editorial committee, recognizing the importance of archiving Kazuhisa Mori's historical material, and finally completed his reminisces and catalogues of a part of the materials. (Details can be seen and downloaded from https://www2.yukawa.kyoto-u.ac.jp). These important materials that had been kept privately were transferred to FSA through a kind offer from his wife in November 2021.

(I. Murakami, T. Mizuuchi, H. Iguchi, T. Amemiya, H. Gotoh and S. Kubo)

7. SNET Collaborate Research

NIFS is promoting the “Fusion Virtual Laboratory Initiative” to integrate fusion experiments and research environments in Japan using SNET, and is remotely collecting and storing data from plasma experiment devices such as the QUEST at Kyushu University, the GAMMA10 at Tsukuba University, and the TST-2 at the University of Tokyo.

In addition, NIFS is working with the ITER Remote Experimentation Center (REC) on the ITER project, which is an international collaboration, on the demonstration of the remote participation, storage of large amounts of data, and with the National Institute of Informatics (NII) on research related to the transfer of large amounts of data over long distances across national boundaries.

Research Highlights

The TST-2 is a pulse discharge device, and noise is generated around it. To suppress this noise, an isolation amplifier is required. Four types of isolation amplifier modules were tested: the AD215, the ISO122, the ISO124, and the TLP7920. As a result, we concluded that the ISO124 is suitable.

In FY2021, 2228 plasma experiments were conducted using the GAMMA10 device. The data are stored on a Linux server and transferred in the LABCOM data format. A direct transfer system from the GAMMA10 to NIFS by the PXI system is also in use. Last year, 16 channels of Doppler reflectometer data were fully operational in this system and are being used stably for experimental data analysis. This data can be easily retrieved using the LabView program. In addition, the microwave interferometer data previously collected by the CAMAC system is now also collected by the Compact DAC, allowing the data to be checked immediately after the plasma discharge.

The REC is promoting the Fusion Information Science Center (FISC) concept as an infrastructure to promote data-driven modeling for DEMO reactors. In this study, network storage, which plays a central role in the FISC, was investigated. The conceptual design of a storage system that satisfies both of these requirements was developed. As a result, we have concluded that a combination of all-flash storage for short-term storage of relatively small data, long-term and high-speed storage such as Data Warehouse for storing structured data for efficient machine learning and other applications is effective (Fig. 1). Detailed technical design will be conducted according to this framework in the future.

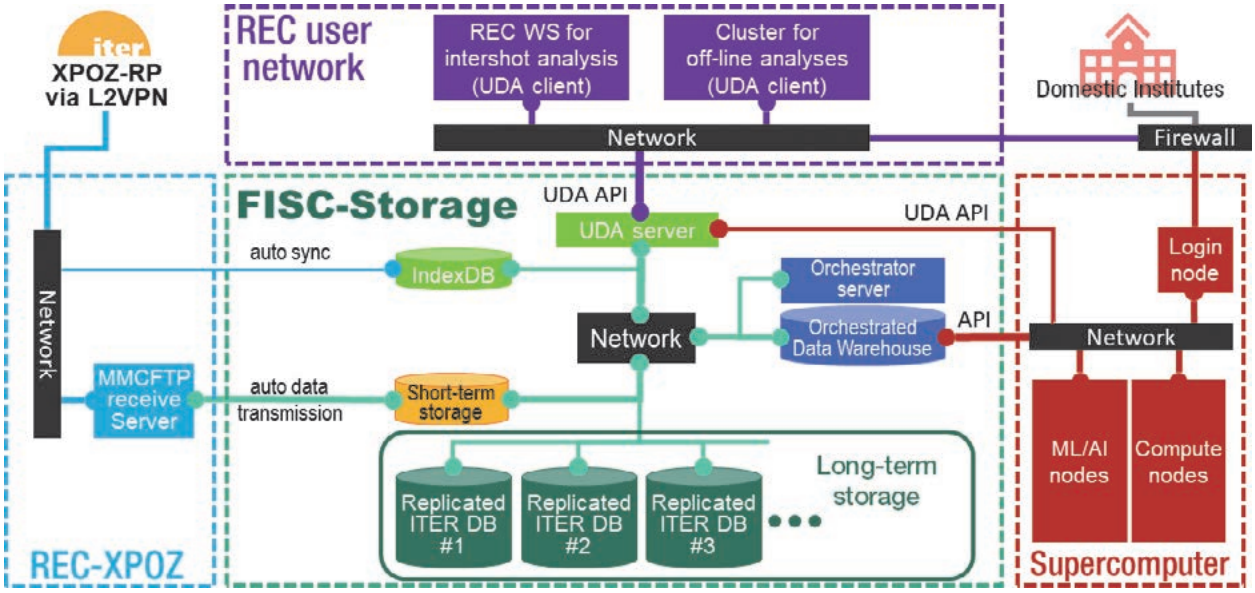

Fig. 1 Conceptual design of FISC storage network

In this term's research, we evaluated the ITER Dashboard, a web-based system for displaying ITER measurement and monitoring information as a live data display system, and conducted research and development to address issues with the file transfer tool MMCFTP that were pointed out in the previous year's joint research.

MMFCTP, a high-speed file transfer tool, divides a group of files to be transferred into several parts, archives them sequentially, sends them one after another, starting with the archived ones, and decompresses them after completion of reception at the receiving end. However, a problem was pointed out that the longer the distance, the greater the time between archive-to-archive transfers. As a solution to this problem, it was decided to use the TCP connection, once established. In addition, we studied and began implementation of a database to enable efficient transfer.

(M. Emoto)

8. Bilateral Collaboration Research

The purpose of the Bilateral Collaboration Research Program (BCRP) is to enforce the activities of nuclear fusion research in the universities by using their middle-size experimental facilities of the specific university research centers as the joint-use facilities for all university researchers in Japan. The current program involves five university research centers as follows:

- Plasma Research Center, University of Tsukuba
- Laboratory of Complex Energy Process, Institute of Advanced Energy, Kyoto University
- Institute of Laser Engineering, Osaka University
- Advanced Fusion Research Center, Research Institute for Applied Mechanics, Kyushu University
- Hydrogen Isotope Research Center, University of Toyama

In the BCRP, each research center can have its own collaboration programs, using its main facility. Researchers at other universities can visit the research center and carry out their own collaboration research there, as if the facility belongs to NIFS. That is, all these activities are supported financially by NIFS for the research subjects in the BCRP. The BCRP subjects are subscribed to from all over Japan every year as one of the four frameworks of the NIFS collaboration program. The collaboration research committee, which is organized under the administrative board of NIFS, examines and selects the subjects.

(S. Sakakibara)

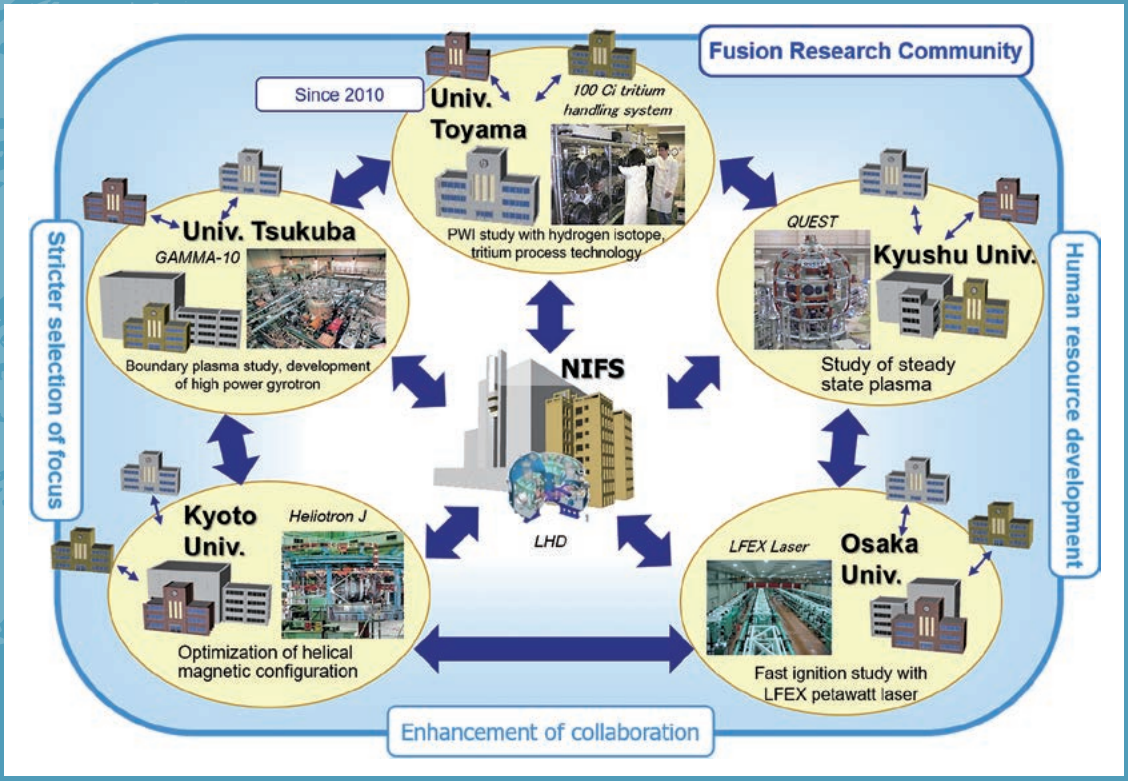
Fusion Research Community
Since 2010
Univ. Toyama
100 Ci tritium handling system
PWI study with hydrogen isotope, tritium process technology
Univ. Tsukuba
GAMMA-10
Boundary plasma study, development of high power gyrotron
QUEST
Kyushu Univ.
Study of steady state plasma
NIFS
LHD
Kyoto Univ.
Heliotron J
Optimization of helical magnetic configuration
LFEX Laser
Osaka Univ.
Fast ignition study with LFEX petawatt laser
Stricter selection of focus
Human resource development
Enhancement of collaboration

University of Tsukuba

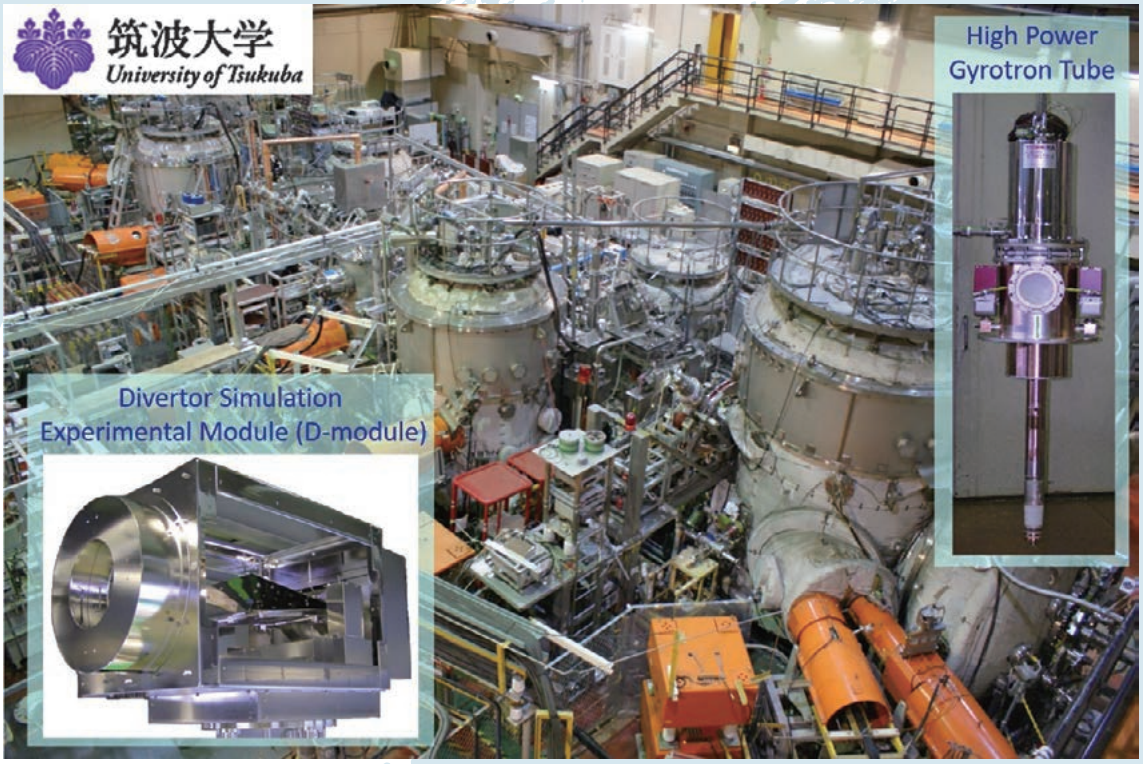

Fig. 1 Bird's eye view of GAMMA 10/PDX.

Highlight

Study of boundary plasmas by making use of open magnetic field configuration and development in high power gyrotrons towards the DEMO project

In the Plasma Research Center, University of Tsukuba, studies of boundary plasma and development of high-power gyrotrons have been performed under a bilateral collaboration research program. The GAMMA 10/PDX (Fig. 1) is the world's largest tandem mirror device with many plasma production/heating devices. A divertor simulation study has been intensively promoted by using a divertor simulation experimental module (D-module), shown at the lower left of Fig. 1. Nitrogen Molecular Assisted/Activated Recombination (N-MAR) processes have been investigated by combination seeding of N_2 and H_2, which leads to a clear decrease of ion flux to the divertor target. In the case of N_2 seeding, the emission intensity ratio of H_α/H_β does not increase, unlike the case of H_2 or Ne seeding, indicating dominant recombination process changes from Hydrogen-MAR (H-MAR) to N-MAR. A test of a new 28/35 GHz dual-frequency gyrotron has been carried out. The new linear plasma device with superconducting coils has been constructed to contribute to the DEMO divertor design.

Remarkable progress has been made on understanding the role of N_2 and H_2 seeding on plasma detachment in divertor simulation experiments, using the end-loss region of GAMMA 10/PDX. These issues have been experimentally studied for different gas species, seeding rate and target angles. We have investigated Nitrogen Molecular Assisted/Activated Recombination (N-MAR) processes during combination seeding of N_2 and H_2, which led to a clear decrease of ion flux to the divertor target. In the case of N_2 seeding, the emission intensity ratio of H_α/H_β does not increase, unlike cases of H_2 or Ne seeding. These indicate dominant recombination process changes from Hydrogen-MAR (H-MAR) to N-MAR. Spatial profiles of N_2 emission observed by a high-speed camera with a band-pass filter show that N_2 emission was initially strong near the corner of the V-shaped target, and then it became weaker with increasing H_2 pressure. This indicates that N_2 was consumed by N-MAR. Concerning target configuration, the V-shaped target experiment at different target angles shows that an area of H-MAR moved upstream in the case of a small angle slot. It is important to measure the plasma density and temperature at the center part of the V-shaped target. We plan detailed measurements by microwave interferometer and Thomson scattering in the region.

As for the advanced diagnostic development, a Ku-band (12-18 GHz) multichannel Doppler reflectometer (DR) and a multi-pass Thomson scattering (TS) system at the end region have progressed. The former system has been developed in the GAMMA 10/PDX tandem mirror to improve the applicability of DR measurement for simultaneous monitoring of turbulent flows at different radial locations. In this fiscal year, the previous single-channel DR circuit was replaced by a multichannel microwave system using a nonlinear transmission line (NLTL) based combgenerator with the heterodyne technique. An initial result of the application to GAMMA 10/PDX central cell plasma was obtained and it showed clear Doppler frequency shifts during an additional ion cyclotron resonance frequency (ICRF) heating and gas-puffing experiment. In order to improve the signal intensity of the Thomson scattering (TS) system in the end region, we have been developing a multi-pass system in the end-TS system. The double-pass TS system was constructed by adding a lens and a reflection mirror for the image transfer optical system, leading to an increase in TS scattering signals. We plan to develop the multi-pass TS system by adding a laser polarization control system.

A new 154/116 GHz dual-frequency gyrotron and 28 GHz gyrotron have been developed for LHD and QUEST, respectively. The Output power of 1.66 MW and 1.34 MW has been achieved at oscillation frequencies of 154.05 GHz and 116.15 GHz, respectively. At the experimental test of a new 28 GHz gyrotron, the output power of 1.24 MW at an oscillation frequency of 28.06 GHz has been achieved. A maximum total efficiency of 53.1% has been obtained with collector potential depression (CPD). Both gyrotrons were also confirmed to be problem-free in also other property tests.

In order to further promote divertor simulation study, a new linear plasma device Pilot GAMMA PDX-SC (Fig. 2) has been constructed. A pair of NbTi superconducting coils with a bore of 0.9m and a pair of Cu coils with one of ~1.5 m were utilized to produce a simple mirror configuration. The maximum magnetic field was 1.5 T and the mirror ratio was 20~30. The superconducting coils, Cu coils and the vacuum vessel have already been constructed and installed. The target plasma parameters are the following: plasma density 10^{19} m^{-3}, electron and ion temperatures several tens of eV and a discharge duration of 10~100 s. A biased limiter and biased segmented plates will be used to suppress MHD instability. Hot cathode plasma discharge with LaB_6 and helicon plasma discharge have been developed as a steady state plasma source. The first plasma is expected in 2022.

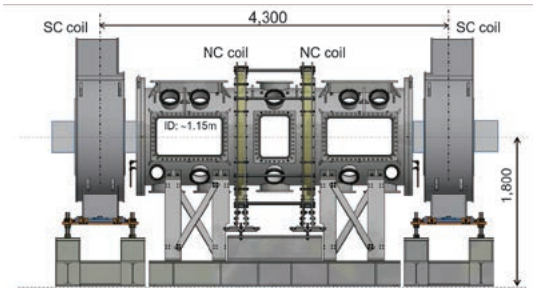

Fig. 2 Schematic view of Pilot GAMMA PDX-SC.

(M. Sakamoto)

Kyoto University

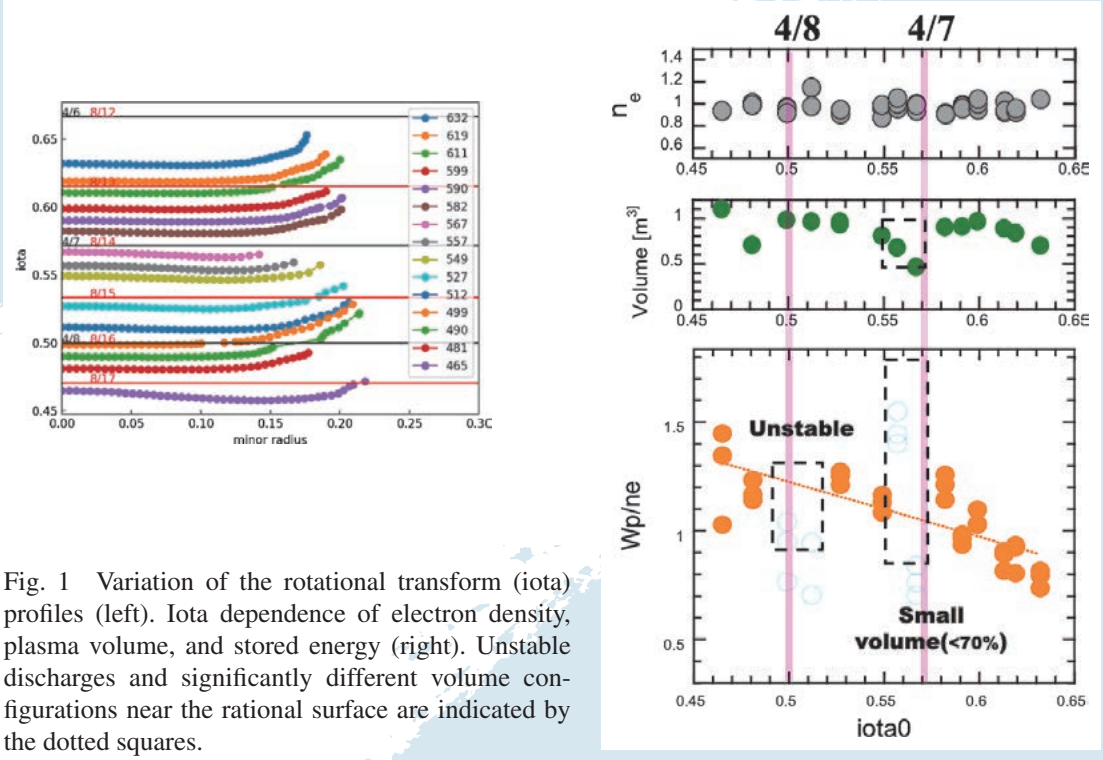

Fig. 1 Variation of the rotational transform (iota) profiles (left). Iota dependence of electron density, plasma volume, and stored energy (right). Unstable discharges and significantly different volume configurations near the rational surface are indicated by the dotted squares.

Highlight

Iota dependence of the confinement properties in Heliotron J

The Heliotron J device features a wide flexibility of configuration control. So far, the effect of the bumpiness component (toroidal mirror ratio) in the magnetic field spectrum on neoclassical transport, MHD, and fast ion confinement has been investigated as a key control knob for configuration optimization. We have recently attempted to extend the parameter spaces characterizing magnetic field configuration and focused on rotational transformation (iota) control experiments this year.

The iota profile can be modified by controlling the current ratio between the toroidal and helical coils in the Heliotron J. In this experiment, the iota profile with low magnetic shear varied widely from 0.46 to 0.63, while keeping a line-averaged density at about 1×10^{19} m^{-3}. The magnetic field strength was adjusted so that the power deposition of the electron cyclotron heating (ECH) was kept at the plasma center.

As shown in Fig. 1, the energy confinement degraded with increasing the rotational transform, as a general tendency. Note that some data was excluded from the analysis because the plasma conditions were not regarded as stable, as indicated by the dotted square. The unstable discharges were observed at the iota near the low-order rational surfaces.

A comparison between the stored energy and the effective helical ripple (ε_{eff}) calculated with the MCviewer code shows an unclear dependence of the stored energy on the helical ripple. This result is different from that of the LHD, where improved neoclassical transport in the lower ε_{eff} configuration accompanies a reduction of turbulence transport through enhanced zonal flow activity. In the Heliotron J case, in contrast, the rotational transform seems to relate more directly to the turbulent suppression. This study is still ongoing, based on a comparison with a numerical study of turbulence transport.

Research Topics from Bilateral Collaboration Program in Heliotron J

The main objectives of the research in the Heliotron J device under this Bilateral Collaboration Program are to experimentally and theoretically investigate the transport and stability of fusion plasmas in an advanced helical field and to improve the plasma performance through advanced helical-field control. Picked up in FY2021 are the following five key topics; (1) plasma structure formation control and plasma transport improvement by magnetic field configuration control, (2) spatial distribution, flow, and current control for confinement improvement, (3) clarification and control of plasma fluctuation structure formation in the core and peripheral regions, (4) characterization and control of energetic-particle-driven MHD instabilities, and (5) optimization of particle fueling and heating scenarios. Nineteen projects, including our baseline one, were adopted. High magnetic field experiments were conducted for about five months, from September to the beginning of February.

Characterization of small-pellet ablation cloud

In recent years, diagnostic systems for the pellet ablation cloud have progressed at the Heliotron J. A low-speed (260 ± 30 m s^{-1}) and small-size (1.1 – 1.2 mm) pellet injection enabled a high-density operation even in the middle-size device. Visible imaging, the emission of which is dominated by the bright Balmer-β line, using a high-speed camera, observed a fluctuation surrounding the ablation cloud that rotated around the magnetic field line. The relative fluctuation level went up to about 15%, suggesting that this phenomenon was induced by the ablation process. For the measurement of the ablation cloud density, fast-imaging spectroscopy for the Balmer-β line at 486.135 nm has been developed. We found that conventional filter spectroscopy, based on the intensity ratio of Balmer-β between band-pass filters having different pass-band widths, was not applicable because the Stark-broadening was too small for our density regime. The newly applied near-infrared Paschen-α line supports this observation at 1875.13 nm, which has a broader Stark-width than Balmer-β for the same density.

Free-boundary simulation of energetic-particle driven modes in Heliotron J

The confinement of fusion-produced energetic particles (EP) is essential for achieving self-sustainable fusion plasmas. However, EP-driven MHD instabilities can be enhanced by the resonant interaction between EPs and shear Alfvén waves (SAW) during the slowing-down process. A computational simulation is an effective tool for investigating the linear and nonlinear interactions between the EPs and the MHD waves, such as SAW, in 3-dimensional plasma. To this end, a particle-MHD hybrid simulation code, MEGA, has been implemented in the Heliotron J. In the early research phase, the MEGA code failed to reproduce the low-n EP-driven MHD modes observed in the Heliotron J experiments. We solved this problem by extending the code to one with a free boundary condition. This enabled analysis on the clarification of the EP-SAW interactions, including frequency chirping, EP transport, and the mitigation of EP-driven MHD instability, which are useful in promoting our further collaboration research from the viewpoint of both theory and experiment.

Many research topics have made progress with collaborative researchers under the Bilateral Collaboration Program in the Heliotron J project, such as (i) electromagnetic wave measurements, such as multi-line-of-sight interferometry and multi-channel reflectometry, (ii) spectroscopic diagnostics, such as high sensitivity beam emission spectroscopy for local turbulent fluctuation measurements, and fast Stark spectroscopy for pellet ablation clouds, (iii) measurement of peripheral plasma flow and heat flux, and (iv) active diagnostics, such as multi-pass Thomson scattering measurements, event-triggered Thomson scattering and laser blow-off spectroscopy are progressing.

(K. Nagasaki)

Osaka University

Study of Fast Ignition Scheme of Laser fusion with Extremely High-density plasmas

We have performed fundamental research into laser fusion, especially the fast ignition scheme, which enables us to separate the laser fusion process into three phases, i.e., compression, heating, and burning, using the GEKKO XII and LFEX laser systems at the Institute of Laser Engineering, Osaka University. The research included target fabrication, laser development, laser experiments, simulations, and reactor technology development. In FY2021, the following progress was made through the Bilateral Collaboration Research Program with NIFS and other collaborators from universities and institutes (NIFS12KUGK057 as the base project).

Compression of Solid Ball Target

For the fast ignition of laser fusion, we do not need to apply heat in the implosion phase, which means that high implosion velocity is not required, so we can adapt a solid ball target instead of one of thin shell. A solid ball implosion is more robust than a shell implosion from reducing hydro-instabilities. However, to achieve a high-density core, the temporal pulse profile of an implosion laser must be controlled precisely to deliver multiple shocks arriving at the same time at the center. In the experiment of FY2021, intensities of the GEKKO XII laser were increased in three steps by following the optimal pulse profile obtained by a hydrodynamics simulation, PINOCO. Although the pulse profile was set up in three-steps as expected, the outputs of twelve laser beams were not kept stable and thus the core density could not be as high as predicted by PINOCO. We are planning to maintain the laser output of the GEKKO XII in the next fiscal year.

Target Fabrication

In laser fusion, solid tritium (T) and deuterium (D) are used as fuel in the form of a spherical solid with a medium shell. High sphericity and uniformity of the shell thickness are required for these fuels. Optical inspection is an effective method, but thickness measurement with an accuracy of 0.1μm is required. However, due to the difficulty of handling gaseous radioactive materials in the standard state, the refractive indices of solid T2 are only estimated values and have not been measured. In FY2021 we solidified DT in a wedge-shaped cell at temperatures below 19 K, and measured the temperature dependence of the refractive index through a laser at a wavelength of 546 nm. This is the first new physical property of T2 measured in about 60 years. Thus it is an important result that will be useful for fuel inspection in future fusion reactors.

Simulation Research of Compression, Heating, and Ignition

It was confirmed that 1.3 MJ (gain 0.7) of neutrons were produced in response to 1.8 MJ of laser energy input in the NIF experiment at Lawrence Livermore Laboratory in the United States, and that the shell target, which was imploded by the indirect irradiation method, was compressed several thousand times and fusion burning was started. Future

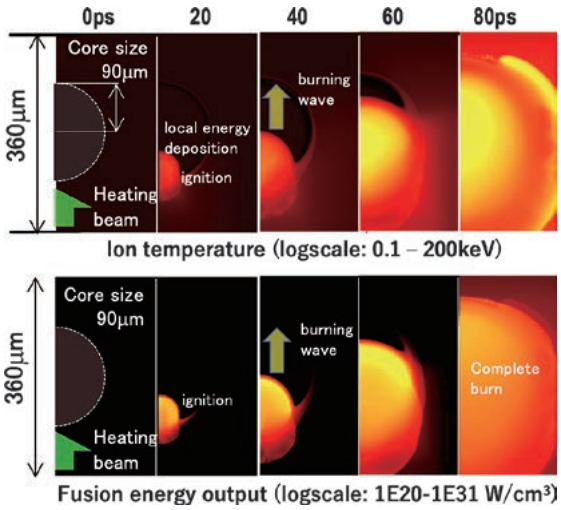

Fig. 1 The required parameters; implosion laser 380 kJ, density of core 500 g/cc, core radius 90 μm, core internal energy 20 kJ, heating laser 200 kJ/30ps (2ω), intensity 3×10^{20} W/cm^2, coupling efficiency 20% (40 kJ to the core).

development will be necessary to establish a high-gain laser fusion design and the identification and solution of elemental problems to realize it. We have designed a high-gain laser fusion (gain x130) by the FIBMET code.

Improvement of GXII and LFEX laser system

The electrical control system of the GXII laser system has not been changed much since its construction and has become obsolete, so a complete review is underway. The trigger signal system is also synchronized with the LFEX laser system, so a complete renovation plan has been prepared and the equipment is gradually being replaced. The monitor system is also under review, and a replacement plan for the energy measurement system has been prepared and will be tested on one beam. We have also developed and tested software for the networking of the beam pattern monitors in the amplification section.

For the LFEX laser system, the alignment laser was replaced with a broadband fiber laser to suppress interference in the beam pattern monitor and improve visibility of the intensity distribution. This has greatly improved the detection accuracy of damage to optical elements and beam kicking. In addition, stray light at the compressor, which could not be detected by alignment lasers, can be now, and countermeasures taken. In the oscillator section, the OPCPA amplification region was completely revised in order to stabilize the seed light, and the design was made to reduce the overall gain by fiberization and OPCPA.

(R. Kodama, H. Shiraga, S. Fujioka, K. Yamanoi, Y. Sentoku, and J. Kawanaka)

Kyushu University

Research activities on QUEST in FY2021

We will summarize the activities on the Advanced Fusion Research Center, the Research Institute for Applied Mechanics in Kyushu University during April 2021 – March 2022. The QUEST experiments were executed during 30th Jun. – 12th Aug. (2021 Spring/Summer, shot no. 45927–46319) and 7th Sep. – 18th Mar. (2021 Autumn/Winter, shot no. 46320–48675). The main topics of the QUEST experiments in FY2019 are listed below.

1) An operation of approximately 673K was carried out and strong fuel particle retention was subdued. The pulse duration at the wall temperature was limited to 40 m, due to wall saturation. Water-cooling of the hot wall had been applied and the pulse duration could be extended to about 4 h. The wall saturation could be avoided during the water-cooling phase, but suffered a reoccurrence when the water-cooling was off.
2) Co-axial helicity injection (CHI) was applied to achieve an efficient plasma start-up. Improvement of a gas-injection system for CHI worked well and electron density of 6×10^{19} m^{-3} could be achieved at an optimized condition of CHI.
3) To realize a double swing of center solenoid current safely, even if the current monitor does not work, the high-speed interlock circuit has been improved so as to mask the switching command in preset time. A plasma current dip during the dead time was decreased and a plasma current of 120 kA with peak electron density of 2.3×10^{18} m^{-3} has been achieved.
4) To study the effect of plasma flow on material transport near the first wall, “directional material probes (DMPs)” were installed. Visual observation revealed that the deposition layers on DMPs were formed with a directionality in a counterclockwise direction in the toroidal direction. Some parts of the deposited layer on a DMP were examined by the glow discharge optical emission spectroscopy (GDOES) in NIFS, and depositions of tungsten, iron, and carbon were observed.
5) The original idea for the direct detection of electron Bernstein wave (EBW) was to utilize a 400 GHz 0.1 ms/50 kW gyrotron as a scattering source. We have decided to change the scattering source to a CW/50 mW HCN-laser (890GHz), expecting the 60 dB source power down could be partly compensated for by an effective integration time of detection.
6) XPS (X-ray Photoelectron Spectroscopy) analyses showed that the major deposits on the plasma facing wall for the QUEST 2020Spring/Summer campaign were carbon and metal oxide. A thick deposit was observed for the Equator wall, whose thickness was about 20 nm, although that for the top and bottom were around 10 nm. Based on TDS (thermal desorption spectroscopy) results, large hydrogen retention was found for the bottom sample, indicating that most of the hydrogen would be trapped as C-H bonds.
7) To double the toroidal field (TF) on QUEST, a module consisting of a Lithium-ion capacitor and a DC-DC buck converter has been designed and developed. The resultant flat-topped-current is 800 A. The wave form in the bench test matches up to the circuit simulation. Assembling the 125 modules in parallel, the coil current reaches 100 kA, and hence the TF is doubled.
8) Tokamak start-up simulations for divertor configuration without RF current drive are demonstrated. Using an axisymmetric MHD simulation code, coupled with a conducting vessel and coils, time evolutions of plasma with a small cross-section to a divertor configuration are investigated and compared with experiments.
9) We study the driving mechanism of toroidal flow by electron cyclotron heating (ECH) related to the 3-D magnetic field, by experimentally verifying the JxB torque by ECH and comparing it with the GNET simulation in QUEST. Assuming a QUEST size tokamak plasma (central temperature 100 eV, density 1.0×10^{18} m^{-3}) we have obtained a significant torque by introducing 0.1% toroidal filed ripples as a 3-D magnetic field.
10) Various waves have been found to emerge in the ion cyclotron range of frequencies to whistler frequencies, in accordance with significant generation of hard X-rays on QUEST. The frequencies of the waves always

chirped in time, even though plasma parameters, which were experimentally measured, were steady for the timescale of their chirps, suggesting rapid evolution of velocity distributions of energetic electrons.

11) In order to accurately understand the surface alteration of plasma-facing materials during steady-state discharges and the associated fuel particle absorption, we plan to clarify the depth profiles of hydrogen isotopes and impurities in the samples exposed to steady-state plasma at QUEST. In this fiscal year, 1) the environmental arrangements of the ion beam analyzer and the nuclear reaction analyzer (NRA), and 2) the installation of samples for analysis at QUEST were carried out.
12) We have jointly developed a large-capacity database with the Pan-Omics Data-Driven Research Innovation Center of Kyushu University, which can register many types of data and provide them with a unified user interface such as a Jupiter notebook. With this provision, researchers will be able to easily access the data they need, and will be able to perform efficient data analysis, which is expected to further advanced research.
13) The potential fluctuation measured by the divertor probes was analyzed in a QUEST divertor configuration. Strong correlation between the fluctuation at different channels was observed. By analyzing the phase delay of each channel, it has been found that the speed of the fluctuation propagation is in the order of several hundred meters per second in a radial direction, and the direction of the propagation changes during the current ramp-up discharges.
14) Experiments to model an ECH assisted Ohmic start-up were performed. It was found that breakdown was slower at higher ECH power above 10 kW and a prefill pressure of ~0.7 mPa. The result was qualitatively similar to LATE and TST-2. Discharge tuning for an Ohmic start-up was also performed. Closed flux surfaces were successfully obtained with EC preionization at ~1.5 mPa.
15) A novel divertor biasing using four toroidally-distributed biased plates has been attempted in low density plasmas produced by ECH. Several current filaments along the scrape-off-layer (SOL) have been generated by the divertor biasing. Enhanced losses of non-thermal electrons leading to ~5% reduction in plasma current, and a noticeable decrease of divertor particle flux have been observed during the biasing. The observed effects are thought to be due to generation of resonant magnetic perturbations produced by the SOL current filaments.
16) For the spectroscopic measurements of (i) hydrogen atom density, (ii) T_e and n_e (with helium puffing), and (iii) Z_{eff} (in high-density discharges), a low-dispersion imaging spectrometer was developed. The spectrometer simultaneously measures 27 spectra in the wavelength range of 400–730 nm with a wavelength resolution of 0.7 nm and a frame rate of up to 23 fps.
17) The circuits with vacuum chamber currents with 58 segments, a pair of horizontal coil and plasma have been solved for the vertical plasma position control system in QUEST. For the central value of the n-index of –0.069, the coil current and voltage required for Ohmic divertor experiments with initial vertical shift of 5.5 cm can be supplied from the power supply system presently being prepared (IHC = 200 A,VHC = 200 V, PHC = 50 kW).

HANADA Kazuaki (Kyushu University) 1), 2)
NAKAMURA Kazuo (Kyushu University) 3)
MASUZAKI Takashi (NIFS) 4)
KUBO Shin (Chubu University) 5)
OYA Yasuhisa (Shizuoka University) 6)
ONCHI Takumi (Kyushu University) 7)
TSUTSUI Hiroaki (Tokyo Institute of Technology) 8)
MURAKAMI Sadayoshi (Kyoto University) 9)
IKEZOE Ryuya (Kyushu University) 10)
YAJIMA Miyuki (NIFS) 11)
HASEGAWA Makoto (Kyushu University) 12)
KOBAYASHI Masahiro (NIFS) 13)
TSUJII Naoto (University of Tokyo) 14)
TOI Kazuo (NIFS) 15)
SHIKAMA Taichi (Kyoto University) 16)
MITARAI Osamu (Institute for Advanced Fusion and Physics Education) 17)

(K. Hanada)

University of Toyama

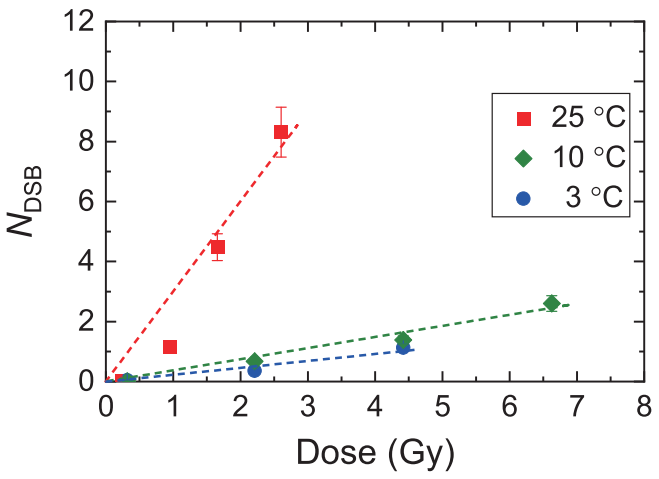

Fig. 1 Number of double-strand breaks, NDSB, of genome-sized DNA molecules of T4 GT7 bacteriophage in high concentration tritiated water (3–4 MBq/cm^3) as a function of β-ray irradiation dose.

Highlight

Research Activities in Hydrogen Isotope Research Center, Organization for Promotion of Research, University of Toyama

A simple experimental system to examine the rate of double strand breaks (DSBs) of genome-sized DNA molecules in tritiated water under well-controlled conditions was established for the validation of computer simulation on interactions of biomolecules and ionizing radiation. Radiation-induced DSBs were clearly recognizable at tritium concentrations of 3–4 MBq/cm^3, while it was unnoticeable at ~ kBq/cm^3. The number of DSBs, N_{DSB}, increased proportionally with the irradiation dose, as shown in Fig. 1. The rate of DSBs showed a clear increase with rising water temperature. These observations indicate that irradiation effects and thermal effects are synergistic with each other. One of the possible mechanisms underlying this synergism is that a single strand break (SSB) induced by radiation developed to DSB by thermal effects and vice versa.

[Double-strand breaks in a genome-sized DNA caused by beta-ray under cellular environment (T. Kenmotsu, Doshisha U.)]

Tritium transport in fusion reactor materials (Y. Hatano, U. Toyama): A nuclear fusion power plant will use a steam turbine to generate electricity. Tritium (T) permeation through steam generator piping results in the risk of uncontrolled T leakage to the environment. Therefore, T permeation must be precisely evaluated and minimized. Nickel alloys are widely used as pipe materials. In this study the permeation of T from/to high temperature, high pressure water through Inconel 600 film was examined.

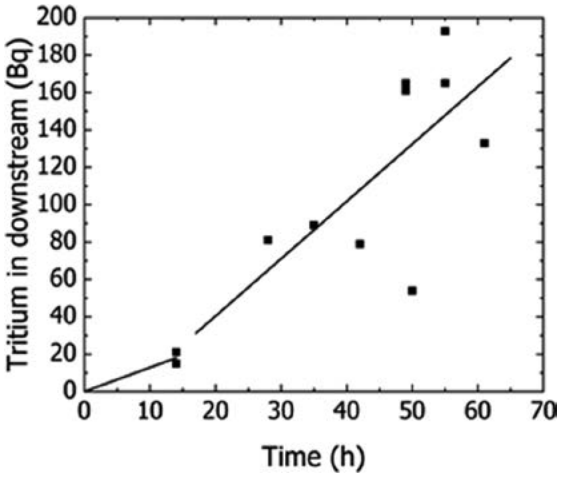

Fig. 2 Change in T permeation with elapse of time.

Thin disks of Inconel 600 were used as samples. The permeation device used was made of type 304 stainless steel and separated into two chambers by a sample disk. The upstream chamber was filled with tritiated water (0.9 MBq/cm^3) and the downstream side was filled with non-radioactive water. The device was placed in a forced convection oven and heated to 280°C for 14–60 h. The vapor pressure of water at this temperature was 6.4 MPa. After heating, the downstream chamber was opened and the concentration of T in water was measured using a liquid scintillation counter. Correlation between heating time and the amount of T permeated to the downstream side is shown in Fig. 2. The initial permeation rate up to 14 h was 1 Bq/h. After 14 h, the data points spread in a relatively wide range but the permeation rate on average was 3 Bq/h after 14 h. Namely, the permeation rate increased after 14 h. Here T cannot permeate through the sample in the form of a HTO molecule. T atoms are liberated by the oxidation of metals and a part of the liberated T atoms permeate to the downstream, together with H atoms. The other part of liberated T is released into the upstream chamber as HT. At the downstream side surface, a T atom is released in the form of HTO, via isotope exchange with H_2O or as HT, via recombination with a H atom. Namely, the partial pressure of HT increases with heating time in both chambers. This increase in HT partial pressure is one of the possible reasons for the increase in permeation rate at 14 h.

Other experimental studies performed in the Hydrogen Isotope Research Center in the fiscal year 2021 are the following:

- *Nano-fiber formation on tungsten alloy by helium plasma irradiation* (Y. Ueda, Osaka U.);
- *High temperature and high flux irradiation effect on hydrogen isotope retention in damaged W* (Y. Oya, Shizuoka U.);
- *Effective tritium removal under vacuum conditions* (N. Ashikawa, NIFS);
- *Effects of heat and particles load on hydrogen isotope retention in tungsten materials* (K. Tokunaga, Kyushu U.);
- *Release behaviors of hydrogen isotopes from tungsten materials exposed to hydrogen isotope plasma* (T. Otsuka, Kindai U.);
- *Suppression of tritium permeation in metals by laser-doping of impurities* (Y. Nobuta, Hokkaido U.);
- *Measurement of transmission of polymer for liquid DT for developments of laser fusion DT fuel* (Y. Arikwa, Osaka U.); and
- *Fabrication of tritium target for 14 MeV neutron irradiation experiments* (M. Kobayashi, NIFS).

9. Activities of Rokkasho Research Center

At Rokkasho village in Aomori Prefecture, the IFERC (International Fusion Energy Research Centre) project and the IFMIF/EVEDA project have been conducted under the Broader Approach (BA) agreement between the EU and Japan from Jun. 2007, in order to complement ITER and to contribute to an early realization of the DEMO reactor. The roles of the NIFS Rokkasho Research Center (RCE) established in May 2007 are to assist NIFS and universities in cooperating with those activities, and to prepare the environment for promoting various collaborative research activities, including technology, between Rokkasho and universities. As cooperation activities, the head of the NIFS RCE was undertaking tasks as the IFERC Project Leader (PL) from Sep. 2010 to May 2020 and those as the IFERC Deputy PL (D-PL) from Jun. 2020 to Mar. 2022. The role of PL was to coordinate the activities by EU and JA implementing agencies and the role of D-PL was to support PL.

BA activities have two Phases; BA Phase I from Jun. 2007 to Mar. 2020 and BA Phase II from Apr. 2020 to Mar. 2025 or beyond. FY 2021 has been a year of continuation of re-organization to orient IFERC activities according to the priorities given by BA Steering Committee (SC) for BA Phase II, and of a start-up of collaboration with ITER.

The original IFERC project plan for BA Phase II, including long and short-term objectives for a period of five years or more, was approved by SC in BA SC-25 (Jul. 2020) and updated year by year.

The long-term objectives of IFERC project are

- to build on the past successful collaboration in the CSC, in order to provide support to the ITER and JT-60SA projects, by fostering state-of-the-art modelling tools development and providing computer simulation resources, as well as remote experimentation facilities;
- to provide support for the JT-60SA, and eventually ITER exploitation by promoting simulation projects to develop reliable scenarios;
- to provide support to the IFMIF validation and design projects, both those taking place in the Rokkasho site (LIPAc) and the projected DONES and Advanced Fusion Neutron Source (A-FNS), including making use of the licensed materials laboratory;
- to consolidate and further the know-how on analysis/design of fusion reactors (e.g. DEMO) in strong collaboration with JT-60SA and ITER.

The short-term objectives of IFERC project are

- to provide support for ITER, IFMIF/EVEDA, and JT-60SA (STP);
- to consolidate the know-how for future fusion reactors (e.g. DEMO) through the production of databases, inputs to engineering handbooks, and a review of lessons learned in existing fusion projects, building on the results of BA Phase I.

Regarding the collaboration with ITER, a Cooperation Arrangement between the Broader Approach Activities and the ITER Project was signed in Nov. 2019 between F4E, QST and ITER Organization for promoting and furthering academic and scientific cooperation and establishing a collaboration between ITER and BA Activities. Regarding the IFERC project, following the approval of a new annex to the Cooperation Arrangement for IFERC, the Implementing Arrangement No. 2 of the Cooperation Arrangement was concluded in Jun. 2021. In Oct. 2021, the Coordination Committee approved the Work Programme 2021/2022. Based on the Work Programme 2021/2022, collaborations have started in the area of remote participation in ITER between ITER CODAC/IT and IFERC-REC, and in CSC with the provision of CSC resources to collaborative simulation projects in high priority areas related to disruption studies and edge/SOL/divertor. Collaboration with ITER in the preparation of DEMO design guidelines and knowledge management will also be considered.

Based on the Work Programme 2021/2022 including

- Participation in joint simulation projects, on the subjects defined by ITER as high priority: Modelling of disruptions in ITER, and ITER edge/SOL/divertor plasma simulations
- Participation of IO in HPC Follow-up Working Group,

collaborative activities between IFERC-CSC and ITER were implemented in 2021. Both activities started immediately after approval of the Work Programme. Regarding the Participation in joint simulations projects, ITER scientists joined two existing CSC simulation projects ("MHD" for disruption studies in ITER and "MISONIC" for ITER edge/SOL/divertor plasma simulations) while additional subjects were included. Resources for these projects were increased in JFRS-1 by reallocating unused resources assigned to other BA simulation projects. This allocation was concluded in Dec. 2021. Regarding the second activity, the ITER responsible person for the CSC collaboration has been invited and regularly attends the meetings of the HPC Follow-up Working Group.

The activity plan for cooperation with ITER CODAC was discussed at a kick-off meeting held in Sep. 2021, where the main points of the collaboration and the contact persons of each party for this collaboration were agreed. The Work Programme 2021/2022 includes:

- Construction of a connection environment using Layer 2 VPN (L2VPN)
- CODAC Application Testing
- Remote data access to ITER database
- Live data viewing of ITER operation status in REC
- Fast data transfer from ITER to REC.

The collaborative tests with IO have started. Real-time monitoring tests of the ITER facility from REC room are ongoing. The server installation in F4E Barcelona has been completed and will allow the installation of remote IO-CODAC virtual machines that will be used in the testing activities. The procurement of a 100Gbps network switch and the related work have been completed for better network connection in accordance with the upgrade of SINET. The ITER Dashboard installed at REC was tested as a "Live data viewing tool", using the L2VPN dedicated line between REC and CODAC. In parallel, the collaboration with IFMIF/EVEDA on remote participation has enabled the commissioning and operation activities of LIPAc.

As for DEMO Design Activity, the progress of activities resulted in 54 publications. It was also reported that the first intermediate Check and Review of JA DEMO programme, similar to G1 Gate Review for EU in 2020, was successfully completed. The efforts to recover from problems caused by COVID-19 were implemented. In DEMO R&D Activity, steady progress in four task areas covering R&D in tritium technology, structural materials, functional materials, and corrosion database led to 52 publications, of which five were joint papers. The population of engineering databases had started. One concern is that the recent Russian situation would result in delays of activities in the task of functional materials, where irradiations in Russian reactors have been cancelled.

Additionally, the head of the NIFS RCE was working until Mar. 2022 as the leader of the general coordination group of the Joint Special Team for a Demonstration Fusion Reactor (DEMO) design, which is the organization as an all-Japan collaboration set in May 2015, for establishing technological bases required for the development of DEMO.

In summary, the NIFS RCE contributes widely not only to the success of ITER but also to the realization of fusion energy through the continuous efforts mentioned above.

(N. Nakajima)

10. Research Enhancement Strategy Office

The Research Enhancement Strategy Office (RESO) was established on November 1, 2013, to strengthen the research activities of the Institute by planning various support programs for the researchers and conducting public relations programs for making fusion science more understandable in society. Three University Research Administrators (URAs) are working in the following five Task Groups:

(1) The IR (Institutional Research)/Evaluation Task Group
(2) The Young Researchers and their Career-path Development Task Group
(3) The Collaboration Research Enhancement Task Group
(4) The Public Relations Enhancement Task Group
(5) The Financial Basis Strengthening Task Group

(1) IR/Evaluation

The task group for IR and evaluation has continued its role to make systematic analyses of the present research activities of the institute. The statistical data of publications and scientific reports were collected using the NIFS article information system (NAIS), with complementary data obtained through the SCOPUS and WoS public research resource supplying companies. The outcome results of the collaboration activities were collected through the annual collaboration reports of NIFS.

(2) Supporting Young Researchers

In the activities for supporting young researchers, three research startups were encouraged, to enhance their basic research skills. Applications were reviewed by the Young Researchers Development Task Group, and the following programs were supported in FY2021:

1. *Understanding Fine structure of Magnetic Field in Anisotropic Plasmas* (Tomoko Kawate),
2. *New Electron Cyclotron Heating Using Optical Vortices* (Toru Tsujimura),
3. *Development of Functional Optical Devices by Femtosecond Laser Micro-processing* (Hiyori Uehara).

RESO also assisted with the applications of young scientists to the 'Grants-in-aid Scientific Research' program. Nineteen application documents were reviewed and suggestions were given to the authors for improvement.

(3) Enhancing Collaboration Research

Much international collaboration researches with various institutes and universities in Asia, Europe and United States was performed, although experiments or meetings in person were still not available.

NIFS has concluded international exchange agreements with overseas research institutes, of which joint research with research institutes in Europe, the United States, and China has been strengthened. For the W7-X of Max Planck Institute of Plasma Physics (Germany), we focused on joint research on common issues of helical equipment by utilizing plasma diagnostic instruments. Strengthened joint research activities took

Fig. 1 A modular coil in the winding process

place using helical devices at the University of Wisconsin (USA) and the CIEMAT Research Institute (Spain).

On the other hand, as for the CFQS (Chinese First Quasi-axisymmetric Stellarator) project, based on the bilateral agreement on General Collaboration and Exchange between NIFS and Southwest Jiaotong University (China), machine construction proceeded in Hefei, China, amid the pandemic. Manufacturing of modular coils was vigorously performed, and five coils completed the first vacuum impregnation process.

(4) Enhancing public relations

1) Dissemination of research achievements through EurekAlert!
   Three topics were released: i) "Developing a novel joint technique for copper alloy", ii) "A self-sustained divertor oscillation mechanism identified in fusion plasma experiment" and iii) "Plasma turbulence spreading by magnetic fluctuation reduces heat load on a fusion device wall". These topics were also released to the media in Japan. Some topics attracted attention from the international media.
2) Information release about NIFS and fusion science
   Eight research results were released in the press and disseminated on SNS (twitter and facebook) . NIFS's web design was re-examined to enhance the dissemination of information on research results.
3) Outreach activities based on the fusion community
   RESO joined a discussion of fusion science outreach headquarters with QST, universities and the Ministry of Education, Culture, Sports, Science and Technology.
4) Others
   RESO introduced interesting science topics to the public on the occasion of the Science Talk in the Open Campus Online of NIFS, as shown in Figure 2. RESO produced movies, briefly introducing researchers' activities.

(5) Strengthening Financial Base

Activities are being carried out with the aim of strengthening the financial base of the institute. Support activities were carried out by holding briefing sessions to obtain competitive research funds such as Grants-in-Aid for Scientific Research (KAKENHI), JST, and NEDO, and by supporting the preparation of application forms.

Fig. 2　The Science Talk in the Open Campus Online of NIFS.
Prof. Mito talked about superconductivity to the public online.
(T. Morisaki, T. Muroga, T. Mito and K. Yaji)

11. The Division of Health and Safety Promotion

The Division of Health and Safety Promotion is devoted to preventing work-related accidents, to ensuring safe and sound operation of machinery and equipment, and to maintaining a safe and healthful environment for researchers, technical staff, co-researchers, and students. This division consists of ten offices, and various subjects related to health and safety are discussed by office chiefs once a month.

1. Environmental Safety Control Office

This office has the responsibility to maintain a safe workspace and environment.

A) Management to solve problems pointed out by the safety and health committee.
B) Maintenance of a card-key system for the gateways of controlled areas.
C) Maintenance and management of the vehicle gate at the entrance of the experimental zone.
D) Maintenance of the fluorescent signs of the evacuation routes and the caution marks.
E) Management of sewage drainage from NIFS.
F) Monitoring of discharging water to prevent water pollution.

2. Health Control Office

The main role of this office is to keep the workers in the institute healthy, including co-researchers and students.

A) Medical checkups both for general and special purposes and immunization for influenza.
B) Mental health care services and health consultation.
C) Accompany the inspections of the health administrator and the occupational physician.
D) Maintenance of AEDs.
E) Alerts and response to COVID-19.

Various lectures were held for physical and mental health. An online stress-check was held in October 2021.

3. Fire and Disaster Prevention Office

The main role of this office is to prevent or minimize damage caused by various disasters.

A) Making self-defense plans for fires and disasters, and implementation of various training.
B) Promotion of first-aid workshops and the AED class.
C) Maintenance of fire-defense facilities and attending on-site inspections by the local fire department.
D) Review and update disaster prevention rules and disaster prevention manuals.

All workers must attend disaster prevention training held every year, and a disaster simulation exercise is also held. Figure 1 shows fire extinguisher training in LHD.

Fig. 1 Fire extinguisher training in LHD

4. Radiation Control Office

The main role of this office is to maintain radiation safety for researchers and the environment. Legal procedures for radiation safety and regular education for the radiation area workers are also important roles of this office.

A) Maintain radiation safety for workers.
B) Registration and dose control for radiation area workers.
C) Observation of radiation in radiation-controlled and peripheral areas.
D) Maintenance of the radiation monitor.
E) Applications for radiation equipment to the national agencies and local governments.
F) Revise official regulations and establish new rules.

An educational lecture for radiation area workers was held on March 18, 2022. We provided an opportunity to view a DVD of it for absentees. Non-Japanese workers were educated and trained in English.

5. Electrical Equipment and Work Control Office

The main role of this office is to maintain electrical safety for researchers, technical staff members and students.

A) Check and control the electrical facilities according to technical standards.
B) Safety lecture for researchers and workers.
C) Annual check of the electric equipment in case of a blackout.

The annual inspection of the academic zone was carried out on May 23, 2021, and that of the experimental zone was carried out on June 12 and June 13, 2021.

6. Machinery and Equipment Control Office

The main role of this office is to maintain the safe operation of cranes. The tasks of this office are as follows.

A) Inspection and maintenance of cranes.
B) Management of the crane license holders and safety lectures for the crane users.
C) Schedule management of crane operations.

7. High Pressure Gas Control Office

The main role of this office is for safe operation and maintenance of high pressure facilities with cooling system such as LHD.

A) Safe operation and maintenance of high-pressure gas handling facilities in NIFS.
B) Daily operation, maintenance, system improvement, and safety education according to the law.
C) Safety lectures for researchers and workers.

8. Hazardous Materials Control Office

The main role of this office is management of the safe treatment of hazardous materials and maintaining safety for researchers against hazardous events.

A) Research requests for hazardous materials and their storage status.
B) Management to ensure safe storage of the waste.
C) Implementation of a chemical substance risk assessment.

9. New Experimental Safety Assessment Office

The main role of this office is to check the safety of experimental devices except for LHD. For this purpose, researchers who want to set up new experimental apparatus must apply for a safety review. Two reviewers are assigned from members of this office and other specialists to check the safety of these devices.

A) Examine new experiments for safety problems and advise on safety measures.
B) Improve safety in each experiment and reinforce a safety culture at NIFS from annual reviews by NIFS employees.

10. Safety Handbook Publishing Office

The tasks of this office are to publish the Safety Handbook in Japanese and in English, and it is updated every year. Regular safety lectures were held on May 13, 2021. All workers, including co-researchers and students, must attend this safety lecture every year.

(S. Sakakibara)

12. Division of Deuterium Experiments Management

A deuterium experiment has been carried out in LHD since March 7th, 2017. Objectives of the deuterium experiments are (1) to realize high-performance plasmas by confinement improvement and better heating devices and other facilities, (2) to explore an isotope effect study, (3) to demonstrate the confinement capability of energetic particles (EPs) in a helical system and to explore their confinement studies in toroidal plasmas, and (4) to continue extended studies on Plasma-Material Interactions (PMI) with longer time scales.

The Division of Deuterium Experiments management was founded to establish a safety management system and to consolidate experimental apparatus related to the deuterium experiments. After the start of the deuterium experiment in LHD, the function of this division was shifted to the management of a safe and reliable operation of the deuterium experiment. Under this division, a taskforce named 'Deuterium Experiment Management Assistance Taskforce' was founded. The main jobs of the taskforce were (1) the establishment and improvement of manuals to operate LHD and peripheral devices safely during deuterium experiments, (2) check and improve regulations related to continuing the deuterium experiments safely, (3) an upgrade of LHD itself, its peripheral devices and the interlock systems for its safe operation during the deuterium experiments, (4) upgrade and optimization of heating devices and diagnostic systems for the deuterium experiments, (5) remodeling the LHD building and related facilities, and so on. These jobs are accomplished with the cooperation of the LHD board and the Division of Health and Safety promotion. In addition, the necessary tasks related to the Safety Evaluation Committee founded by NIFS and those related to the Safety Inspection Committee of the National Institute for Fusion Science (NIFS) founded by local government bodies are carried out in this division. The publication of an annual report for radiation management of the LHD deuterium experiment is another important task of this division.

During the fiscal year of 2021, the Safety Evaluation Committee met once. The main topic of the committee was the evaluation of an annual report about radiation management in the deuterium experiment and an evaluation of the safety operation of the deuterium experiment in the experiment campaign of 2020.

Cooperation with the Safety Inspection Committee of the NIFS is an important task for the division of the deuterium experiments management. Environmental neutron dose monitoring at NIFS and tritium concentration monitoring in the water around the NIFS environment has been done by the committee since 2015. In 2021 FY, these monitoring activities were performed twice, as scheduled with the cooperation of the Division of Deuterium Experiments management.

(a)

(b)

(c)

Photographs of (a) environmental water sampling and (b) measuring the environmental radiation dose rate by the secretariat of the Safety Inspection Committee. (c) The front cover of the annual report on radiation management of the first LHD deuterium experiment (written in Japanese).

(M. Osakabe and M. Isobe)

13. Division of Information and Communication Systems

NIFS handles a great deal of information, including experimental data. As a center of excellence in fusion science, NIFS is in a position to exchange information both domestically and internationally and is required to open and protect such information. The Division of Information and Communication Systems (ICS) works on open science and network security by centralizing the development and operation of the information and communication systems. Open science is an initiative that aims "to create new knowledge that transcends fields", "to ensure transparency in research", and "to return the results of the studies to society" by widely open research data and results. And it is becoming a major international trend. NIFS also provides open access to research data and results to researchers worldwide and the public. Internet communication systems for handling various types of information are increasingly important to support open science. We are working on network security to ensure the safe and appropriate handling of information.

The Department of Information and Communication System (ICS) was founded in 2014 in order to develop and maintain the information and network systems of NIFS efficiently. All the information system experts in NIFS belong to the ICS. There are one office and four TASK groups which correspond to the job classifications in NIFS. The Information Security Office, established in 2020, oversees the overall information security of the institute. The Network Operation task group manages and maintains the communication systems in NIFS, such

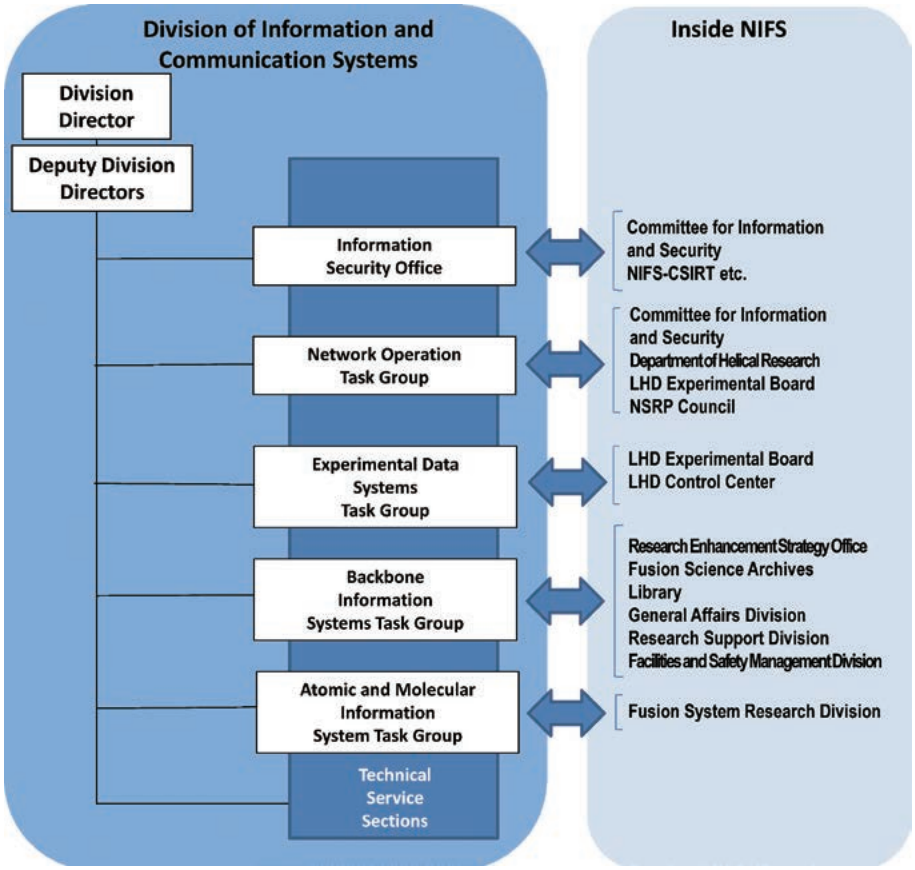

Fig. 1 Structure of Division for Information and Communication Systems.

as the E-mail system including security issues. The Experimental Data System task group performs operation and development of data acquisition systems for the LHD experiment. The Backbone Information Systems task group, which was created by merging the Institutional Information Task Group and Integrated ID management and Authentication System task group in 2021, carries out the maintenance and development of the management systems for collaboration research and its output. The Atomic and Molecule Database task group maintains the atom and molecule database which is open to researchers around the world.

The ICS works as follows: the request for the maintenance, improvement, and development of the information and communication system from each section is submitted to the ICS. The deputy division directors of ICS check all the requests, establish the priority among them, and assign them to the appropriate Task Group. Because all the experts belong to the Technical Service Section of ICS, each Task Group Leader asks the Section Leader to allot the required number of experts for a prescribed period to finish the job.

In NIFS, three research projects extend across the research divisions. It can be said that the ICS is another "project" which lies across all the divisions in the institute for keeping the information and communication systems stable, secure, and up to date.

(R. Sakamoto)

14. International Collaboraiton

Many research activities in NIFS are strongly linked with international collaborations with institutes and universities around the world. These collaborations are carried out in various frameworks, such as 1) coordination with foreign institutes, 2) bilateral coordination with intergovernmental agreements, and 3) multilateral coordination under the International Energy Agency (IEA).

Coordination with foreign institutes is important as a basis for collaborative research. From 1991, NIFS concluded 32 coordinations through FY2019.

NIFS is the representative institute for three bilateral coordinations with intergovernmental agreements (Japan-US, Japan-Korea, and Japan-China), and four multilateral coordinations under the IEA (Plasma Wall Interactions (PWI), the Stellarator-Heliotron concept, Spherical Tori, and the Steady State Operation). For the three bilateral coordinations, and the multilateral coordination PWI Technology Collaboration Program (TCP), NIFS coordinates the collaborative research between researchers in foreign institutes and researchers in domestic universities and NIFS. The activities of bilateral and multilateral coordination activities are reported in the following subsections.

For the COVID-19 pandemic, social activities have still been strongly limited to prevent its outbreak all over the world since the beginning of 2020. Many international activities with personal exchanges could not be conducted, and many international conferences were postponed or held online. Online communications drastically increased, and people became very familiar with such communications, though the time difference was a serious problem when holding an international online conference.

Under such a situation, the 30th International Toki Conference on Plasma and Fusion Research was held in Toki, Japan from 16 – 19 November 2021, and NIFS hosted the meeting. For reducing the risk of the spread of COVID-19, the conference was held using an online connection for video conferencing. Reflecting the new policy of NIFS, which aims for interdisciplinary development of fusion science, 26 keynote lectures and 111 guest lectures were given by invited researchers, not only from the field of fusion science, but also from a wide range of other fields, and more than 466 researchers from 18 countries participated.

(S. Masuzaki)

Academic Exchange Agreements

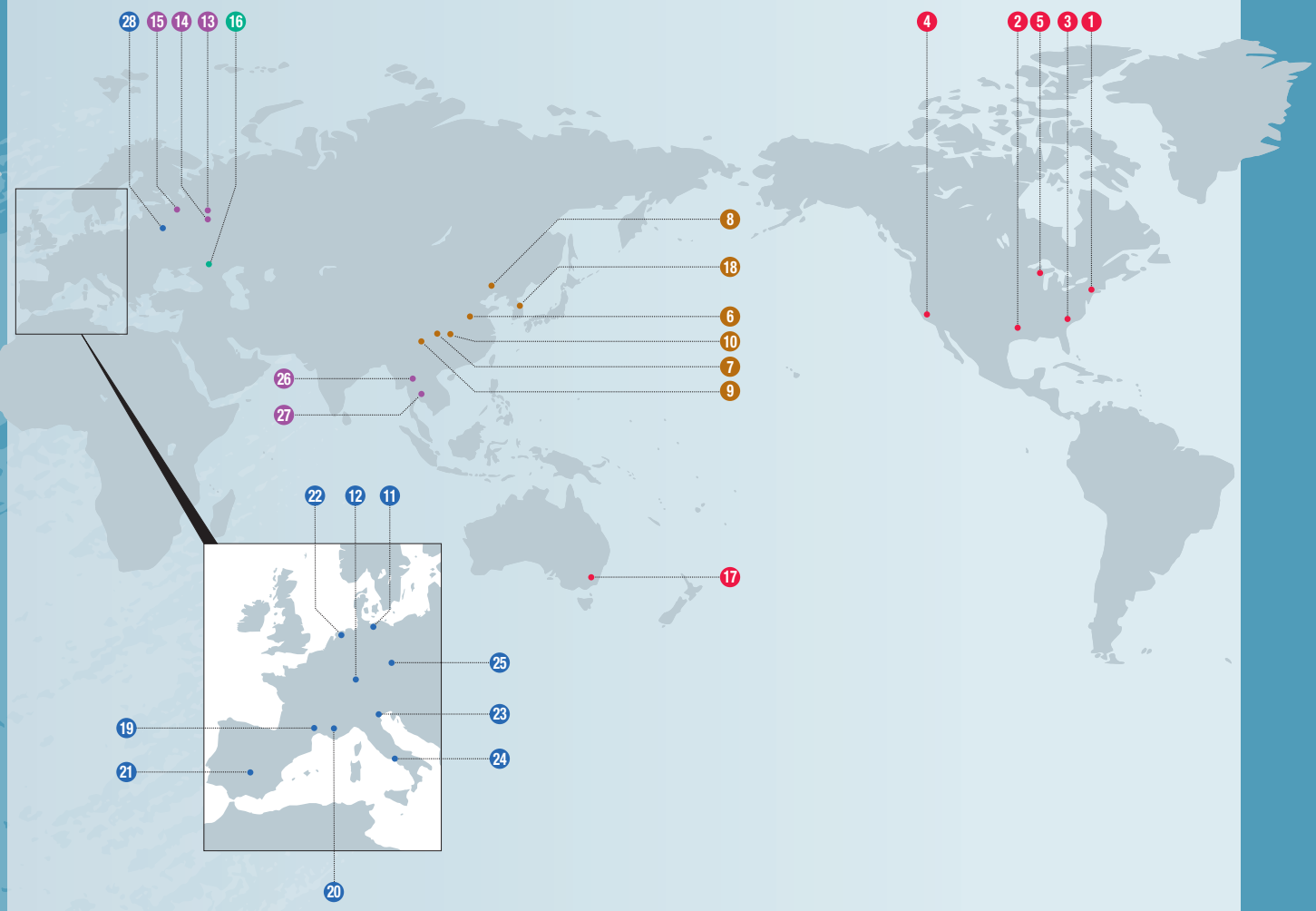

U.S.A. 1 Princeton Plasma Physics Labolatory (PPPL)
2 Institute for Studies, The University of Texas at Austin (IFS)
3 Oak Ridge National Laboratory (ORNL)
4 Center for Energy Science and Technology Advanced Research, University of California, Los Angelse (UCLA)
5 College of Engineering, University of Wisconsin, Madison

China 6 Institute of Plasma Physics, Chinese Academy of Sciences (ASIPP)
7 Southwestern Institute of Physics (SWIP)
8 Peking University
9 Southwest Jiaotong University (SWJTU)
10 Huazhong University of Science and Technology

Germany 11 Max Planck Institute for Plasma Physics (IPP)
12 Karlsruhe Institute of Technology (KIT)

Russia 13 Russian Research Center, Kurchatov Institute (KI)
14 A. M. Prokhorov General Physics Institute, Russian Academy of Sciences (GPI)
15 Peter the Great St. Petersburg Polytechnic University

Ukraine 16 National Science Center of the Ukraine Khar'kov Institute of Physics and Technology Institute of Plasma Physics (KIPT)

Australia 17 Australian National University (ANU)

South Korea 18 National Fusion Research Institute (NFRI)

France 19 Aix-Marseille University (AMU)
20 Commissariat à l'énergie atomique et aux énergies alternatives (CEA)

Spain 21 National Research Center for Energy, Environment and Technology (CIEMAT)

Netherlands 22 Dutch Institute for Fundamental Energy Reseearch (FOM)

Italy 23 CONSORZIO RFX
24 Institute of Lonized Gas (IGI)

Czech 25 HiLASE Center, Institute of Physics CAS (FZU)

Tailand 26 Chiang Mai University
27 Thailand Institute of Nuclear Technology (TINT)

Poland 28 Institute of Plasma Physics and Laser Microfusion (IPPLM)

The ITER International Fusion Energy Organization (ITER)

US – Japan (Universities) Fusion Cooperation Program

US-Japan Joint Activity has continued from 1977. The 42th CCFE (Coordinating Committee for Fusion Energy) meeting was held on April 13, 2021 via video conference system. Representatives from the MEXT, the DOE, universities and research Institutes from both Japan and the US participated. At the meeting the current research status of both countries was reported, together with bilateral technical highlights of the collaborations. FY 2021 cooperative activities were reviewed, and FY 2022 proposals were approved. It should be noted that because of the continuing COVID-19 pandemic, most of the personnel exchange and workshops were canceled. However, some collaborative activities were maintained by remote participation and web meetings.

(1) Fusion Technology Planning Committee (FTPC)

In this category of US-Japan collaboration, there are six research fields, namely, superconducting magnets, low-activation structural materials, plasma heating related technology, blanket engineering, in-vessel/high heat flux materials and components, and power plant studies and related technologies. In fiscal year 2021, due to the continuation of the COVID-19 pandemic, most of the personal exchanges either differed or were canceled, including four Japan-to-US personal exchanges (differed), one Japan-to-US personal exchange (canceled), and one US-to-Japan personal exchange (differed). One workshop was also canceled. Despite this situation, one US-to-Japan personal exchange was successfully performed online, which had the title "Depth profile of D retention in RAFM steels: effect of surface layers". In this collaboration, the devices on both sides (the plasma-surface interactions research facility PISCES at UCLA and characterization devices such as the EDX, the TEM, and the GDOES at NIFS) were best utilized for preparing samples and for characterizing them. One workshop was also held online, which was titled "Workshop on fusion reactor design and critical issues of fusion engineering". There were 18 oral presentations (US: 9, Japan: 9), and a total of 33 participants (US: 15, Japan: 18). Regarding all the differed or canceled collaborations, information exchanges were done among responsible members and participants via e-mails and/or video conferencing to make an agreement about the resumption of each program in the coming fiscal year 2022.

(2) Fusion Physics Planning Committee (FPPC)

In the area of fusion physics, one committee meeting, two workshops and 29 personnel exchanges were performed remotely, amid the continuing COVID-19 pandemic. In a newly established collaboration style during the pandemic, scientists from both sides have endeavored to continue their collaborative research activities. Every experiment was carried out with remote participation, enabled by tele-communication tools and data transport systems which have been drastically improved in this year. As one of the most excellent results, a boron powder injection experiment in LHD, with collaboration between NIFS and Princeton Plasma Physics Laboratory, was summarized and published in Nature Physics (Fig. 1).

Fig. 1 Cover page of the Nature Physics. https://www.nature.com/articles/s41567-021-01460-4

(3) Joint Institute for Fusion Theory (JIFT)

Some of workshops and personal exchanges that had been scheduled for the 2021–2022 JIFT programs were canceled due to the influence of COVID-19. A workshop

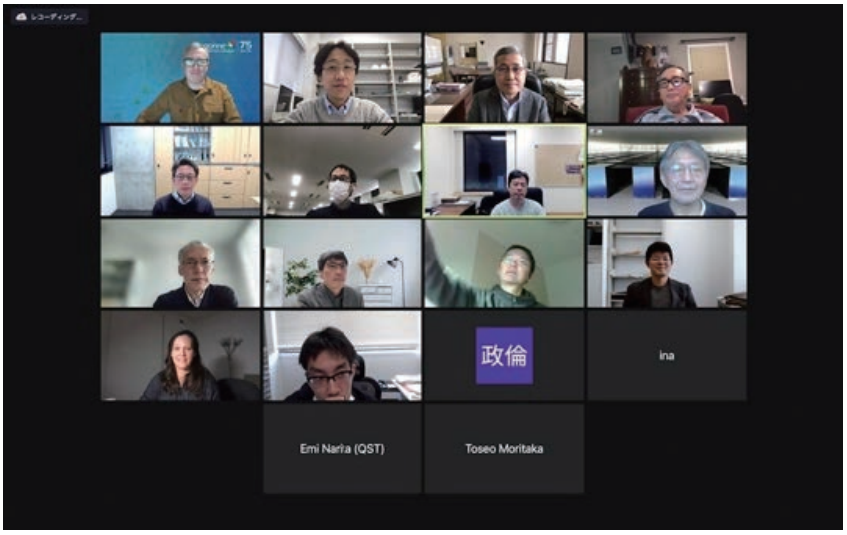

Fig. 2 Snapshot of the Workshop on "US-Japan collaborations on co-designs of fusion simulations for extreme scale computing" held online in January 2022.

"US-Japan collaborations on co-designs of fusion simulations for extreme scale computing" was held online in January 2022 (Fig. 2). A personnel exchange program (Japan to US) for a Visiting Researcher on "Theoretical study related to two-fluid equilibria" was carried out successfully from January to February in 2022. Four Japan to US and three US to Japan personnel exchange programs were carried out as remote collaborations. The status of JIFT activities for 2021–2022 was reviewed and recommendation plans for 2022–2023 were discussed by email among members of the JIFT Steering Committee in December 2021. The JIFT discussion meeting was held online on September 17, 2021, in the Plasma Simulator Symposium.

(4) US-Japan Joint Project: FRONTIER

The FRONTIER collaboration started in April 2019 to provide the scientific foundations for reaction dynamics in interfaces of plasma facing components for DEMO reactors. This project consists of four tasks: Irradiation Effects on Reaction Dynamics at Plasma-Facing Material/Structural Material Interfaces (Task 1), Tritium Transport through Interface and Reaction Dynamics in Accidental Conditions (Task 2), Corrosion Dynamics on Liquid-Solid Interface under Neutron Irradiation for Liquid Divertor Concepts (Task 3) and Engineering Modeling (Task 4). The project performs neutron irradiation in the High Flux Isotope Reactor (HFIR) at Oak Ridge National Laboratory (ORNL) and examines neutron-induced modifications in microstructure, mechanical strength, tritium transport, corrosion behavior, etc. Twenty-five irradiation capsules were designed and fabricated, and the majority of them were irradiated in the HFIR at 300, 500 and 800 °C for one and three cycle(s). Post-irradiation examinations will be carried out in the coming years. A corrosion test in flowing Sn was performed for steel specimens using a thermal convection loop for 1000 h at a peak temperature of 400 °C and a 55 °C temperature gradient. Significant mass loss was observed in the hot leg, and specimen characterization is in progress to understand corrosion mechanisms.

(T. Morisaki, N. Yanagi, H. Sugama and Y. Hatano)

Plasma Wall Interaction (PWI) Collaboration

This collaboration is based on the IEA Technical Collaboration Programme (TCP) of the "Development and Research on Plasma Wall Interaction Facilities for Fusion Reactors" (in short, PWI TCP) which involves Japan, Europe, the United States, and Australia. The objective of this TCP is to advance the physics and technologies of plasma-wall interaction research by strengthening cooperation among plasma-wall interaction facilities (in particular, by using dedicated linear plasma devices), to enhance the research and development effort related to a fusion reactor's first wall materials and components shown in the figure below.

NIFS collects proposals for international collaborative studies based on the PWI TCP, from domestic universities every year. The proposals are reviewed by the PWI technical committee whose members are domestic senior researchers in universities, QST and NIFS, and some of the proposals are approved. Proponents of the approved collaborative research go to foreign institutes with support from NIFS and the conduct the studies.

Unfortunately, for because of COVID-19 pandemic, collaborative activities based on the PWI TCP could not be conducted in FY2021.

(S. Masuzaki)

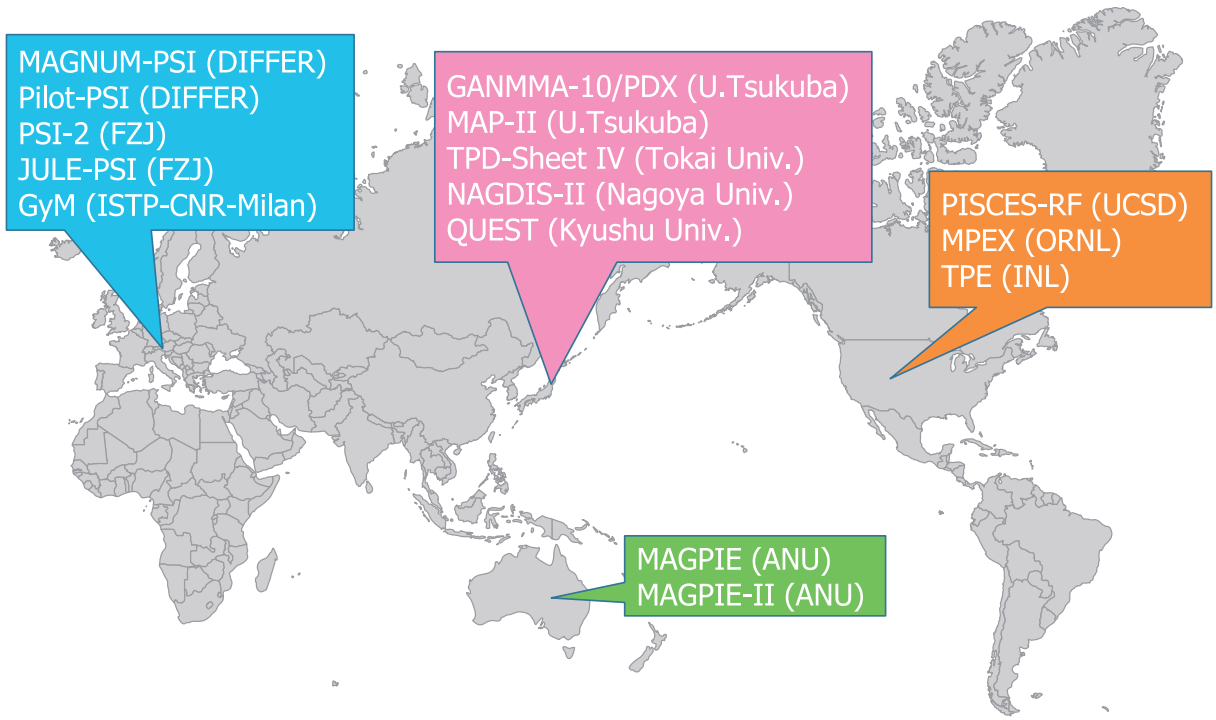

Main Plasma-Wall Interaction facilities in member countries

IEA (International Energy Agency) Technology Collaboration Programme for Cooperation in Development of the Stellarator-Heliotron (SH) Concept ("IEA SH-TCP")

Highlight

IEA SH-TCP
Programmatic collaborations have been further extended in the next step of SH research

The SH TCP's objective is to improve the physics base of the Stellarator-Heliotron concept and to enhance the effectiveness and productivity of research by strengthening co-operation among member countries. All collaborative activities of the worldwide stellarator and heliotron research are combined under the umbrella of this programme, which promotes the exchange of information among the partners, the assignment of specialists to facilities and research groups of the contracting parties, joint planning and coordination of experimental programmes in selected areas, joint experiments, workshops, seminars and symposia, joint theoretical and design and system studies, and the exchange of computer codes. The joint-programming and research activities are organized via Coordinated Working Group Meetings (CWGM), an interactive workshop to facilitate agreements on joint research actions, experiments and publications under the auspices of the SH-TCP.

The Executive Committee (ExCo) of the SH-TCP has been working hard to extend the agreement and has now been granted an extension for the period 2021–2026.

Major achievements in 2021

In 2021, major achievements were the deuterium plasma campaign in the Large Helical Device (LHD) and the start of the first Island Divertor campaign of the Wendelstein 7-X (W7-X). Main highlights will be reported in many presentations at the 23rd International Stellarator-Heliotron Workshop (ISHW) in Warsaw, Poland.

The LHD project will be terminated in March 2023. Until then, it is intended to maximize scientific output by promoting open science and open data, and by further increasing the number of international collaborators above the current record level of 30 %. Colleagues from abroad are strongly encouraged to participate in the next campaign and improved software and a better website have been prepared to facilitate remote participation while the pandemic makes it difficult to come to the site in person. Also, Japan is ready to participate in the next W7-X campaign when the Covid situation improves.

At the Heliotron-J, experiments started in September and will continue until the beginning of February. The current focus is on confinement transport and energetic particle turbulence. Upgrades of the NBI heating system and diagnostics are done. Financial support for personnel exchange was received by the JSPS, but the pandemic makes this difficult to achieve. International collaborators will be invited to participate in Heliotron-J experiments remotely.

Completion of the W7-X is coming to an end. All in-vessel components have been installed – most notably

the actively cooled high-heat-flux (HHF) divertor for heat fluxes of up to 10 MW/m^2, with its cooling water supply and helium connections of the cryo pumps. The NBI system has been extended to four sources, and the new ICRH system has been installed. In-vessel components and diagnostics have been hardened for steady state operation. This was important for addressing the mission of the W7-X: to demonstrate high performance plasmas in optimized magnetic fields and go step by step to longer pulses, towards 30 min at 10 MW heating power.

50th S-H TCP executive committee meeting

The 50th Executive Committee (ExCo) meeting of the S-H TCP took place remotely on November 10, 2021, via Zoom. The meeting was attended by representatives from all seven contracting parties: Australia, China, the European Union, Japan, Russia, Ukraine, and the United States of America. A membership invitation to Costa Rica is still pending.

21st Coordinated Working Group Meeting (CWGM)

Coordinated Working Group Meeting activity has been pursued despite the difficulties due to the Covid pandemic. The 21st CWGM was held as a virtual meeting on November. 22–24, 2021. The meeting had its focus the perspectives for stellarators as fusion reactors. About 130 people registered for three consecutive days of one-hour video conferences, to allow attendance from different time zones. In order to facilitate the scientific discussion further, the meeting sessions were recorded. Additionally, the presentation slides and notes were in an electronic documentation system running INDICO software. The material is available for registered participants working in laboratories that are members of the IEA TCP.

Each of the three sessions had introductory presentations addressing ‘Open questions for a fast track to stellarator reactors (Allen Boozer, Columbia University, USA), ‘What can we learn for the first W7-X campaigns for a HELIAS reactor?’ (Robert Wolf, Max-Planck-Institut für Plasmaphysik, Greifswald, Germany) and ‘Multi-ion physics and isotope effects in helical devices’ (Hiroshi Yamada, University of Tokyo, Japan). An essential outcome of the sessions was ensured by structured discussions guided by expert chairpersons (Arturo Alonso (CIEMAT), Felix Warmer (IPP) and Friedrich Wagner (IPP)).

(Y. Suzuki (Hiroshima Univ.), K. Ida, and K. Nagasaki (Kyoto Univ.))

Japan–China Collaboration for Fusion Research (Post–CUP Collaboration)

I. Post–CUP collaboration

The post-Core University Program (Post-CUP) collaboration is motivated by collaboration on fusion research with institutes and universities in China, including the Institute of Plasma Physics, the Chinese Academy of Science (ASIPP), the Southwestern Institute of Physics (SWIP), Peking University, Southwestern Jiaotong University (SWJTU), Huazhong University of Science and Technology (HUST) and other universities both in Japan and China. Post-CUP collaboration is carried out for both studies on plasma physics and fusion engineering. Based on the following implementation system, Post-CUP collaboration is executed.

Table 1 Implementation system of Japan-China collaboration for fusion research

Category	① Plasma experiment				② Theory and simulation	③ Fusion engineering research
Subcategory	①-1	①-2	①-3	①-4	—	—
Operator	A. Shimizu	Y. Yoshimura	M. Isobe	T. Oishi	G. Kawamura	T. Tanaka

①-1: Configuration optimization, transport, and magnetohydrodynamics, ①-2: Plasma heating and steady-state physics, ①-3: Energetic particles and plasma diagnostics, ①-4: Edge plasma and divertor physics, and the atomic process

II. Primary research activities of collaboration in FY 2021

The fourth steering committee meeting for the NIFS-SWJTU joint project for the CFQS quasi-axisymmetric stellarator, was held on Nov. 12, 2021, online as shown in Fig. 1. The progress of engineering design, the current status of the construction of modular coils (MCs), and the vacuum vessel (VV) were reviewed [1]. At this time, the first vacuum pressure impregnation process for five MCs has been completed. For the VV, one quarter of a toroidal section has been manufactured. Completion of renovation of an experiment building in the Jiuli campus

Fig. 1 The 4th steering committee meeting of the NIFS-SWJTU joint project for the CFQS, held on Nov. 12, 2021 online. Top left, top right and bottom pictures show participants from NIFS, Hefei Keye, and SWJTU, respectively.

in SWJTU was also reported. Also, it was decided that the first plasma will be produced in this experiment building under conditions of 0.1 T operation.

In the research of energetic particles, NIFS and ASIPP have been discussing execution of collaborative research to measure a velocity distribution function of neutral beam (NB)-injected energetic ions in EAST and LHD through deuterium-deuterium (DD) fusion born neutron spectroscopy, based on ^{7}Li-enriched Cs_2LiYCl_6: the Ce (CLYC-7) fast-neutron scintillation detector having a tangential sightline in LHD. A significant shift of DD neutron energy, according to the direction of tangential NB injection, was clearly observed. This result was summarized and published as a joint outcome between NIFS and ASIPP [2]. As for DD fusion born 1 MeV triton confinement research, NIFS developed a scintillating-fiber (Sci-Fi) detector optimized for the HL-2M, and the Sci-Fi detector was exported to SWIP.

In research of edge and divertor plasmas, M. Sakamoto of Tsukuba Univ. and N. Ashikawa joined the EAST experiment on "Hydrogen recycling properties by fueling termination in EAST" by remote communication in 2021. Density decay after fueling termination was measured in a lower single null (LSN) configuration. It is clearly shown that hydrogen recycling is enhanced by a repeat of the discharge. The density decay time of the ohmic discharge does not depend on the fitting period, in contrast to the density decay of the LHCD discharges, suggesting a difference in hydrogen recycling properties without fueling, in the both discharges [3]. A collaborative study on extreme-ultraviolet (EUV) and vacuum-ultraviolet (VUV) spectroscopy has also continued progress. The results of emission line spectra measurement of tungsten impurity ions over a wide range of charge states, from neutral to 46+ are compared, and an extension of the observable charge states is discussed. A paper summarizing tungsten emission line spectra measured at LHD, EAST, and HL-2A was also published [4].

In research of theory and simulation, a Particle-In-Cell (PIC) simulation model for the estimation of tritium flux distribution on a divertor tile with a spherical dust grain has been developed by G.J. Niu of ASIPP and G. Kawamura, and geometric and physical factors on deposition distribution were discussed [5].

In research of fusion engineering, tritium release characteristics from Li_4TiO_4-Li_2TiO_2 mixed materials developed in SWIP have been examined in Shizuoka University. The results have been presented orally at ICFRM-20 (online, Nov. 2021). In association with this work, the Japan-China joint paper was published [6].

[1] The CFQS TEAM, "*NIFS-SWJTU JOINT PROJECT FOR CFQS – PHYSICS AND ENGINEERING DESIGN – VER. 4.1*." NIFS-PROC-122, 2022.

[2] S. Sangaroon, K. Ogawa *et al*., "*Neutron energy spectrum measurement using CLYC7-based compact neutron emission spectrometer in the Large Helical Device*", JINST **16**, C12025 (2021).

[3] M. Sakamoto, Y. W. Yu, N. Ashikawa *et al*., "*Evaluation of hydrogen recycling properties by fueling termination in the EAST superconducting tokamak*", PSI-15 conference 2022, Poster P148(C), Nuclear Materials and Energy **33**, 101286 (2022).

[4] S. Morita, C. F. Dong *et al*., "*Recent Progress on Identifications of Spectral Lines from Tungsten Ions in Low and High Ionization Stages Using Laboratory Plasmas for Fusion Research and Its Application to Plasma Diagnostics*", Proceedings of the International Conference on Atomic, Molecular, Optical & Nano Physics with Applications, Springer Proceedings in Physics **271**, pp. 23–36 (2022).

[5] Guo-Jian Niu, Gakushi Kawamura *et al*., "*A numerical study on the effect of dust particles on tritium deposition on plasma-facing materials*", Nuclear Materials and Energy **31**, 101169 (2022).

[6] S. Hirata, K. Ashizawa, F. Sun *et al*., "*Tritium recovery behavior for tritium breeder Li_4SiO_4-Li_2TiO_3 biphasic material*", Journal of Nuclear Materials **567**, 153838 (2022).

(M. Isobe, A. Shimizu, K. Ogawa, T. Oishi, G. Kawamura and T. Tanaka)

Japan-Korea Fusion Collaboration Programs
FY 2021 Japan-Korea Diagnostics Collaboration

Japan and Korea have been collaborating on the development of plasma diagnostics since 2004. The topics have included Thomson scattering, ECE, CXS, bolometer, energetic ion and neutron diagnostics, ECEI and RF diagnostics, SXCCD and VUV cameras and automated integrated data analysis. On January 25th, 2022, we held an online meeting to discuss the collaboration (See Figure 1).

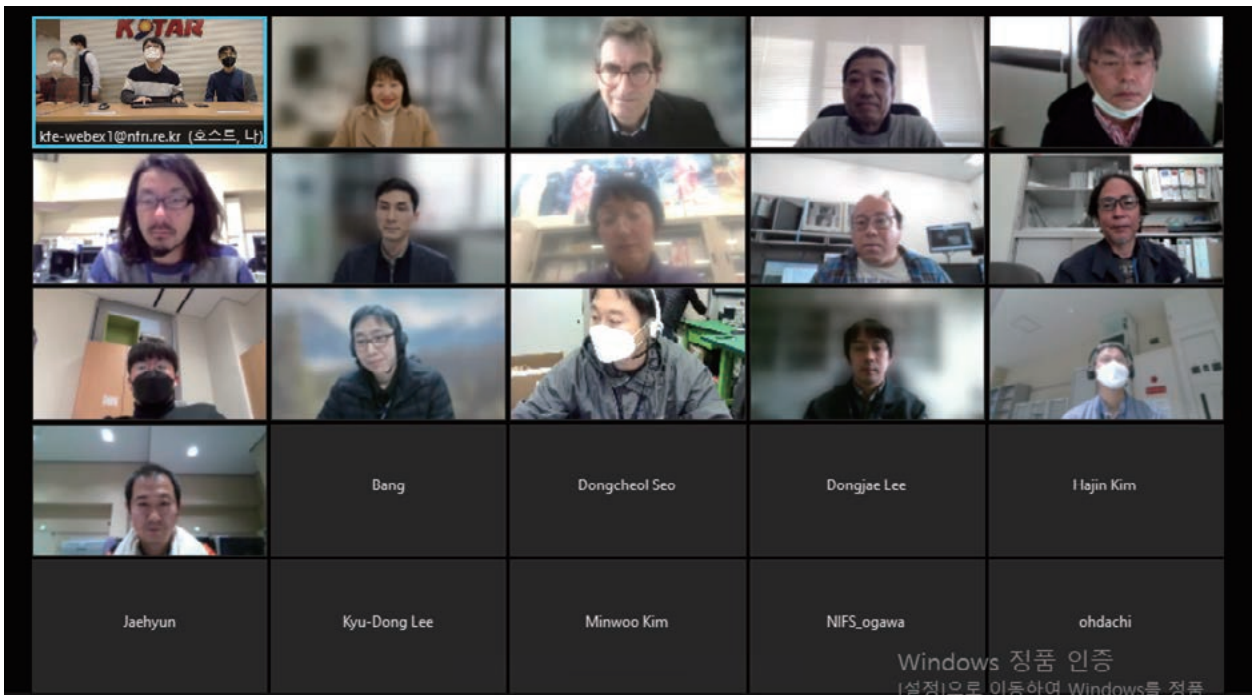

Fig. 1 Image from online meeting regarding the Japan-Korea diagnostics collaboration

Bolometer diagnostics

At KSTAR, disruption mitigation experiments by Shattered Pellet Injection (SPI) will be carried out in preparation for the ITER experiment. We discussed with the KSTAR team about the applicability of the bolometer to the radiation intensity measurement. We also discussed the re-installation of the resistive bolometer on KSTAR. In addition, we introduced various equipment necessary for fabricating and calibrating thin-film detectors for infrared imaging video bolometers and improved the method for evaluating the calibration coefficients of the fabricated detectors. Conventionally, regarding the temperature distribution when irradiating a thin film with a laser, ANSYS heat transfer calculations assuming a calibration coefficient are compared with experimental data, and the calibration coefficient is evaluated by changing the ANSYS calibration coefficient and converging iteratively. This time, we created a temperature distribution database for various calibration coefficients by ANSYS in advance and changed the method to determine the calibration parameters by error evaluation. As a result, we were able to shorten the analysis time from about a week to just a few minutes. In addition, the analysis environment can be migrated to Python, which does not require a software license, and joint research can be conducted smoothly in the future.

Charge Exchange Recombination Spectroscopy (CXS)

At KSTAR, experiments are being conducted to suppress the occurrence of edge localized modes (ELMs) in the H mode by applying perturbation magnetic fields to the periphery of the plasma. When a resonant perturbation magnetic field (RMP) is applied, the heating power required for the transition from L-mode to H-mode increases as the perturbation magnetic field strength increases. One of the reasons for this is thought to be that the rotational shear of the peripheral plasma is reduced by the perturbation magnetic field. However, when a non-resonant magnetic perturbation (NRMP) is applied, even if the perturbation magnetic field strength is increased, the power threshold does not increase. Therefore, investigating the difference in the depth of influence of the resonant perturbed magnetic field (RMP) and the non-resonant perturbed magnetic field (NRMP) on the plasma rotation shear is the key to understanding the power threshold difference.

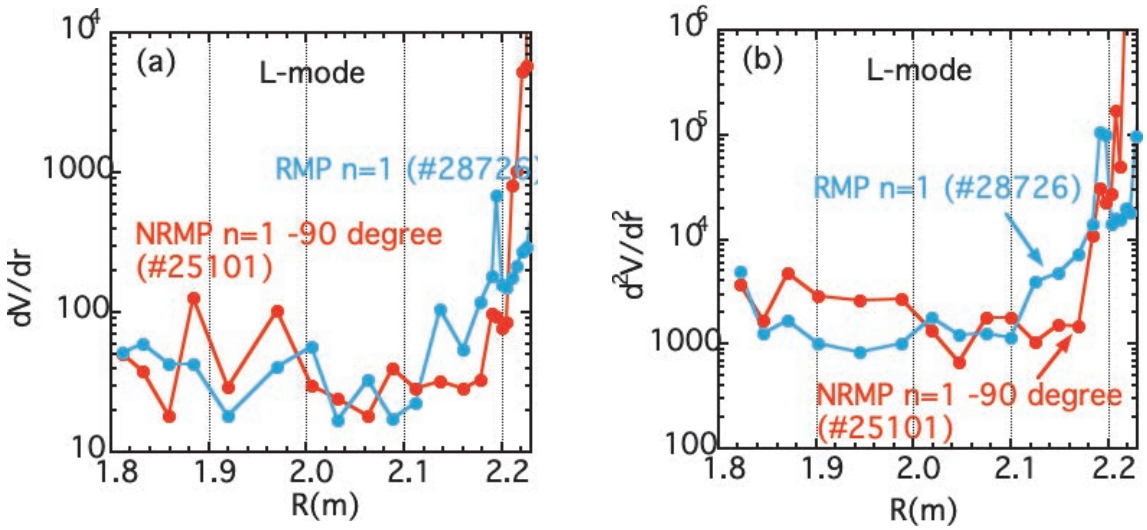

Fig. 2 Spatial distribution of (a) gradient of toroidal rotation velocity and (b) modulation amplitude of curvature due to resonant perturbation magnetic field (RMP)

Figure 2 shows the responses of the resonant perturbed magnetic field (RMP) and the non-resonant perturbed magnetic field (NRMP) to the toroidal rotational velocity gradient and curvature in an L-mode plasma. Compared to the resonant perturbed magnetic field (RMP), the non-resonant perturbed magnetic field (NRMP) causes the rotational shear (decrease in rotational shear due to the perturbed magnetic field) to be localized in the periphery and not to the interior.

(Byron Peterson - High Temperature Plasma Research Division)

15. Division of External Affairs

The Division of External Affairs, as a core organization responsible for public relations and outreach activities, promotes “dialogue” with society, including the local area, through a variety of activities. The organization underwent a review in 2019 and now consists of five offices: the Society Cooperation Office, the Content Production Office, the Event Planning Office, the Public Relations and Tour Guide Office, and the Outreach Promotion Office. A summary of the offices is depicted in Fig. 1. Many NIFS staff are active as members of the department. Its main activities are : holding academic lectures for the public (Fig. 2), providing tours of NIFS facilities (Fig. 3), and science classroom activities (Fig. 4). Face-to-face activities have been limited due to COVID-19, but new activities online have been initiated.

Fig. 1 Organization chart of Division of External Affairs

Activities held in 2021 include the following.

- Tours of NIFS facilities (any time) held 77 times; more than 771 people participated
- Open academic lectures for the public, held online; These were accessed 127 times
- Science classroom activities, held 16 times
- Release of information through web pages, mailing lists, and SNS (Twitter and Facebook)
- Publication of NIFS official pamphlet (in Japanese and English)
- Publication of public relations magazine: NIFS News (6 issues) (Fig. 5)
- Publication of public relations magazine: Letters from Helica-chan (5 issues)

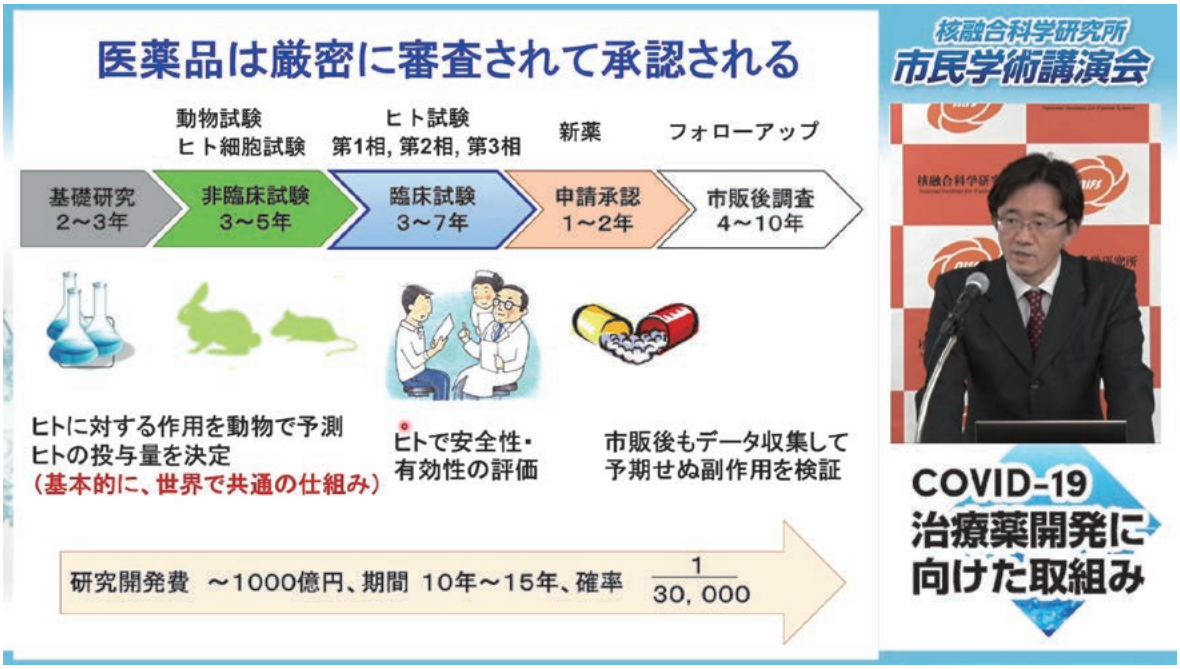

Fig. 2　Online academic lectures

Fig. 3　Tour of NIFS facilities

Fig. 4　Science classroom

Fig. 5　Public relations magazine: NIFS News

16. Department of Engineering and Technical Services

The Department of Engineering and Technical Services covers a wide range of work in the design, fabrication, construction, and operation of experimental devices in the fields of software and hardware.

The department consists of the following five divisions. The Fabrication Technology Division oversees the construction of small devices and the quality control of parts for all divisions. The Device Technology Division works on the Large Helical Device (LHD) and its peripheral devices, except for heating and diagnostic ones. The Plasma Heating Technology Division supports ECH, ICRF and NBI systems. The Diagnostic Technology Division supports plasma diagnostic and radiation measurement devices, and oversees radiation control. Finally, the Control Technology Division concentrates on central control, cryogenic and current control systems, and the NIFS network.

The total number of staff is now 57 (2021). We have carried out development, operation and maintenance of the LHD and those peripheral devices, together with approximately 57 operators.

In FY2021 the Symposium on Technology in Laboratories and the 5th Symposium on computational technology, using finite element methods, were held at NIFS under the auspices of the Department of Engineering and Technical Services.

(Hiromi Hayashi)

1. Fabrication Technology Division

The main work of this division is the fabrication of experimental equipment. We also take care of technical consultation and experimental parts supplies related to the LHD experiment. In addition, we manage the administrative procedures of the department.

The number of machined requests was 84, and the production parts total number was 291 in this fiscal year (FY). The total numbers of electronic engineering requests and articles were 16 and 23, respectively. The details of some of this division's activities follow below.

(M. Yokota)

(1) Focusing mirror for ECE

We have fabricated a focusing mirror (Fig. 1) for the Electron Cyclotron Emission (ECE) diagnostic. It has a spherical shape, and a radius of 1200 mm.

The material of the mirror is an aluminum alloy; the size of the mirror is 500 mm length and 350 mm width. It took 26 hours to complete the cutting process. This is the largest focusing mirror we have ever fabricated.

(K. Okada)

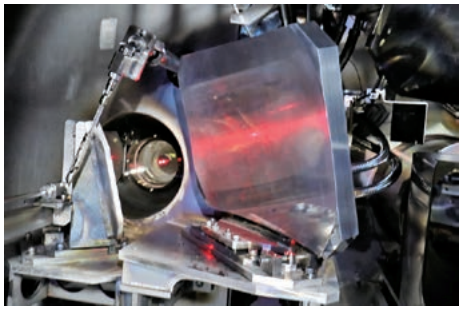

Fig. 1 Focusing mirror for ECE.

(2) 154 GHz Notch filter

We have fabricated a notch filter (Fig. 2) for ECE. It has four cavities and a waveguide in an internal space.

In order to decide the parameter of the cavity, we have analyzed the electromagnetic field.

The cavity has a diameter of 1.5 mm and a depth of 0.655 mm. The rectangular waveguide has a length of 1.651 mm and a width of 0.826 mm.

(T. Shimizu)

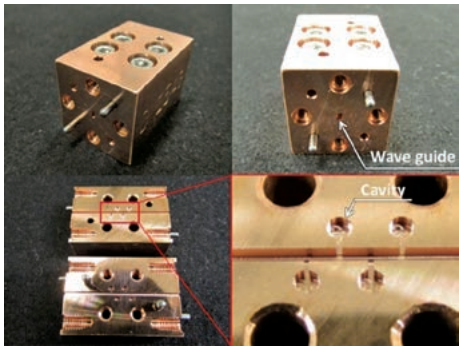

Fig. 2 154GHz Notch filter.

(3) Fabrication of DC offset voltage canceller

The circuits are cancelling DC offset voltage included in the output signal of ECE diagnostics.

The circuits of 12 channels are manufactured with an isolation amplifier (Fig. 3).

(Y. Ito)

Fig. 3 DC offset voltage canceller.

(4) 4ch LPF Amplifier

This LPF (Fig. 4) was made for ECE measurement.

An amplifier with an amplification factor of 1 to 6 times was mounted in the previous stage. A pie-type filter consisting of one inductor and two capacitors was mounted in the middle stage. The cutoff frequency was designed around 1.25 MHz. A buffer amplifier with an amplification factor of 1 was mounted in the latter stage.

We have succeeded in manufacturing products according to the required specifications and they are used for measurement.

(H. Furuta)

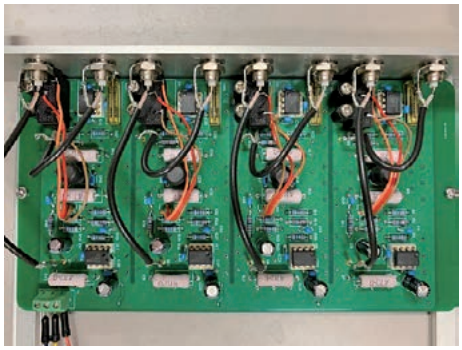

Fig. 4 4ch LPF Amplifier.

2. Device Technology Division

This Division supports the operation, improvement, and maintenance of the LHD.

(1) LHD operation

We started pumping the cryostat vessel for cryogenic components on August 19, 2021 and pumping the plasma vacuum vessel on August 20, 2021. Subsequently we checked for air leakage from the flanges on the plasma vacuum vessel. Thirty flanges were inspected. Consequently, we did not observe any leakage.

The pressure of the cryostat vessel reached an adiabatic condition ($< 2 \times 10^{-2}$ Pa) on August 20, 2021, and the pressure of the plasma vacuum vessel was below 1×10^{-5} Pa on August 30, 2021.

The LHD experiments of the 23rd LHD experimental campaign were started on October 14, 2021 and carried out until February 17, 2022. The total number of days of the plasma experiments was 61.

During this experimental campaign, the vacuum pumping system and the LHD utilities (for example, compressed air, water-cooling and GN2-supply systems) continued to operate without problems. The LHD operation was completed on March 11, 2022.

(N. Suzuki)

(2) Installation of an additional pumping system

To increase the pumping speed for helium we installed an additional pumping system with two turbo molecular pumps at the 6O port of the LHD, as shown in Fig. 5. The reason for increasing the pumping speed for helium was to support the helium beam experiments by NBI#5. The design pumping speed for helium was estimated at 10 m^3/s. The measurement result of the pumping speed was about 9.5 m^3/s for helium.

Fig. 5 The additional pumping system with two turbo molecular pumps.

(N. Suzuki)

(3) Development of tungsten divertor component via advanced bonding technique

We developed a technique for bonding tungsten (W) to chromium zirconium copper (CuCrZr) alloy, i.e., the powder solid bonding method (PSB). In this fiscal year, a W divertor component was fabricated via the PSB method. The divertor component comprises W plates, a CuCrZr alloy and a backplate made of SUS316. Helical cooling channels are provided inside the CuCrZr alloy. Helical flow pulls away the thick temperature boundary layer between the coolant and the CuCrZr alloy, and the contact heat transfer coefficient is effectively increased. Thus, the heat removal performance of the W divertor component is significantly better than that of a straight cooling channel. In the 24th experimental campaign, the W divertor component will be employed in an insertable divertor test module, installed at the 9.5L port of the LHD, to verify material damage in the plasma experimental environment, shown in Fig. 6.

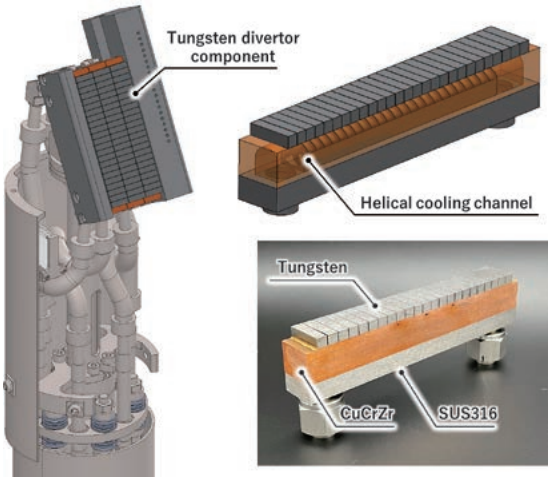

Fig. 6 Tungsten divertor component employed in an insertable divertor test module.

(T. Murase)

3. Plasma Heating Technology Division

The main tasks of this division are the operation and maintenance of three different individual types of plasma heating devices and their common facilities. We have also provided technical support for improving, developing and newly installing these devices. In this fiscal year, we mainly carried out device improvement and modification for the deuterium plasma experiments. The details of these activities are as follows.

(T. Kondo)

(1) ECH

During the 23rd experimental campaign, we injected power up to 5MW to assist plasma experiments. That contributed to achieving high performance plasma with high ion and electron temperatures. Low power and long pulse injection can sustain ECH plasma. Some trouble occurred, but all ECH technical staff of the LHD experimental group contributed to the various plasma experiments.

We developed a switching device for a corrugated waveguide for 154GHz-ECH plasma heating. It can switch from the normal pathway to an experimental one with flat and spiral-mirrors by remote-controlled switching ones. (Fig. 7)

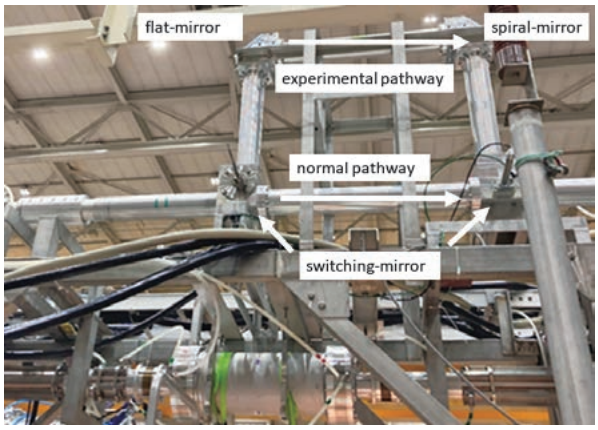

Fig. 7 A picture of the switching device for the ECH waveguide.

(Y. Mizuno and T. Takeuchi)

(2) ICH

(a) The operation of ICH in the 23rd experimental campaign of LHD experiments

In the 23rd experimental campaign, we carried out the LHD experiment with a total of two antennas with four straps, that is, the HAS (Handshake type) antenna with two straps at the 3.5U&L ports and the FAIT (Field-Aligned Impedance-Transforming) antenna with two straps at the 4.5U&L ports of the LHD. We decided on the combination of an RF transmitter and an antenna strap. Then the transmitter of #3 and #4 were connected to the 3.5U&L antenna straps and the transmitters of #6A and #6B were connected to the 4.5U&L antenna straps. The total injection power from the four antenna straps into the plasma reached about 3.2 MW in a short pulse of 0.6 seconds at an RF wave frequency of 38.47 MHz.

(b) Pump control for improved impedance matching

In the Ion Cyclotron Range of Frequencies (ICRF) heating, the oil level inside the stub tuner was controlled only by the cylinder, which reduced reflected power from the antenna. However, since the rate of change of the liquid level became insufficient, due to antenna improvement, a pump was also used for its control. Fig. 8 shows the experimental results. The updated system reduced the reflected power.

(G. Nomura and M. Kanda)

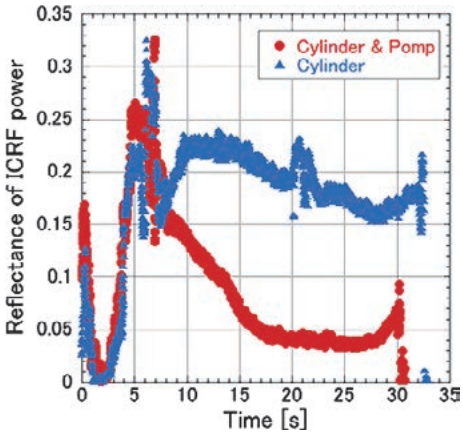

Fig. 8 A Reflectance of ICRF power.

(3) NBI

(a) The operation of NBI in the 23rd campaign of LHD experiments

In the 23rd campaign, approximately 8,000 shots of beams were injected into the LHD plasmas with three negative-NBIs (BL1, BL2, and BL3). The maximum injection power in this campaign was about 12 MW. As for the positive-NBIs (BL4 and BL5), the maximum total injection power was about 20 MW.

(b) Maintenance of the liquid nitrogen supply facility in LHD-NBIs

The transfer tube for liquid nitrogen consumed in the cryopumps of LHD-NBIs has a double-layered structure, composed of an inner and an outer tube. The space between these tubes is constantly evacuated to thermally insulate from the outer tube the inner ones, which reaches liquid nitrogen temperature when the cryopumps are operating. But we must evacuate this vacuum insulation layer of the transfer tubes periodically, because the degree of vacuum in this space gradually degrades over time. Thus, after the 23rd LHD experimental campaign, the vacuum insulation layer of the transfer tubes in NBI #5 was evacuated by a turbo-molecular pump up to 5×10^{-4} Pa at the pump head.

(M. Sato and H. Sekiguchi)

(4) Motor-Generator (MG) and Cooling water facility

(a) MG

An MG is used to supply pulsed power to NBI and ECH for the LHD. The MG has supplied power for 19,991 shots in this fiscal year and 694,464 since its construction. The operation time was 1,081 hours. A diagnosis of the insulation was performed for the generator and motor. Neither had a problem except for a corona discharge. There is no ozone odor, and we continue using it.

(b) Cooling water facility

The cooling water facility supplies pure water to ECH, ICH, and NBI. A 450A electric butterfly valve for ECH, a 350A one for ICH and a 350A glove valve for ICH were replaced as they had become too old. Two pump

motors were serviced at the factory. For one, a stator wedge was missing, which was in a dangerous state.

(Y. Mizuno)

4. Diagnostics Technology Division

This division mainly supports the development, operation and maintenance of plasma diagnostic and radiation measurement devices for the LHD. In addition, we also have taken charge of radiation control.

(T. Kobuchi)

(1) Plasma diagnostic device

Some plasma diagnostics devices have functioned for more than 20 years and thus require maintenance.

In the Nd:YAG Thomson scattering system, the CAMAC control PC sometimes did not start normally. The system applies high voltage to the polychromator, and is an old one, working on Windows NT. We renewed the CAMAC controller and its control program that is compatible with Windows 10, then we replaced the PC with a new one at the end of the fiscal year. The new CAMAC controller is shown in Fig. 9. And it was confirmed that the new system operates normally.

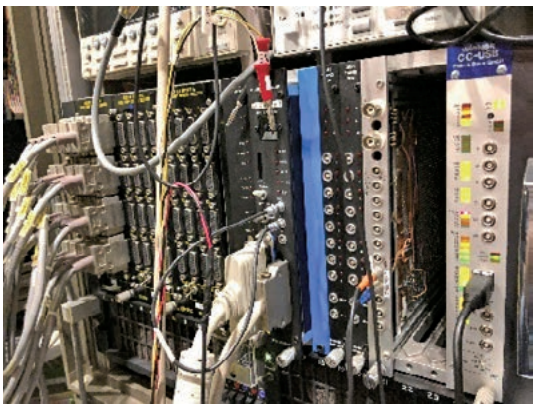

Fig. 9 The rightmost module is the newly added controller.

There are many observation windows on the LHD, and there is a shutter system that protects them from coating. Because the system uses serial communication, we improved it by use of Ethernet last year. We also renewed the operational program. Because we used the new standard Ethernet, equipment replacement has become easier. Even if the equipment breaks down, we can find a replacement. And the operability has been improved by updating the operation program. Though there were seven operational windows for each of the seven PLCs in the old program, they were combined into one window. It became easier to find the switch to operate. The old and new operation screens are shown in Figs. 10 and 11.

Fig. 10 The old operation screen.

Fig. 11 The new operation screen.

(Hiroshi Hayashi and T. Nishimura)

(2) LHD data acquisition (DAQ) system

The LHD data acquisition system operated almost steadily and acquired a total data volume of approximately 320 TB in compressed size in the 23rd experimental campaign. Before this campaign, we had prepared many spare HDD RAIDs and much optical storage, but we increased it further because the capacity of the optical disk

became insufficient at the end of this campaign. Now the cartridge of the optical disk storage system is full. Therefore there is a possibility that a major change for long-term storage systems will be required before the 24th experimental campaign.

(M. Ohsuna)

(3) NIFS Article Information System (NAIS) and Zoom reservation system development

In order to streamline registration jobs in the NIFS Repository, we arranged for its manuscripts to be uploaded from the NIFS Article Information System (NAIS) and published to the Internet. As a result, registration information of the NIFS Repository can be shared on NAIS, and research deliverables can be published to the Internet, using the information of NAIS.

Regarding reservations for using Zoom in NIFS, we have changed the application process for submitting an Excel file, so that instead, a form can be submitted from a web browser. This saves the applicant the effort of creating an Excel file. In addition, since the application details are described and sent in an email, the person requiring the reservation does not have to open the Excel file, and the work can be streamlined. (Link: http://resomini.nifs.ac.jp/~sakamoto/zoom/index.html)

(M. Nonomura)

(4) Radiation control

In order to have stable management of radiation safety control, we have carried out the operation and maintenance of three high-purity germanium (HPGe) detectors, seven liquid scintillation counters, a 2π gas-flow counter, an auto well gamma system, three stack tritium monitoring systems, two gas ones, two dust and a drain water one.

A 2π gas-flow counter and an auto well gamma system are used for smear inspection. There are about 1,300 samples with about 150 smear inspection requests a year. These requests used to be put in by a paper application form and were approved by circulation of them by a few department managers. The approval took several days. Therefore, for the purpose of making it paperless, speeding up the approval process, and automatic evaluation of measurement results, we have developed a web-based application system to apply and to approve them online. The automatic evaluation has made it possible to report results faster and more accurately than before. This has made it possible to obtain approval on the same day of evaluation.

(M. Nakada and S. Hashimoto)

5. Control Technology Division

The Control Technology Division is in charge of important engineering tasks in the LHD project, such as system development, project management and system operation, which are mainly targeted on the central control and cryogenic systems, coil power supply and super-conducting coils.

We are also responsible for the IT infrastructure, e.g. the LHD experiment network, NIFS campus information network and internet servers, in every phase of the projects, including requirements analysis, system design, implementation, operation and user support.

The essential topics of activities for the last fiscal year are described below.

(H. Ogawa)

(1) LHD cryogenic system for superconducting coils

The cryogenic system operation in the 23rd experimental campaign was performed without a significant

accident. Fig. 12 shows the operation result. From August 25th 2021, the He purification operation in the LHD cryogenic system was begun. After that the coil cool-down operation was started on September 8th 2021 and finished on October 4th 2021. (Cool-down time was 622 hours) After approximately five months of plasma experiments, the coil warm-up operation was performed from February 18th to March 11th 2022 (warm-up time was 482 hours). He compressors continuously operated during the cryogenic system operation phase, without any accidents suspending their operation. The total operation period of He compressors was 4750 hours and their operation rates were 100 %.

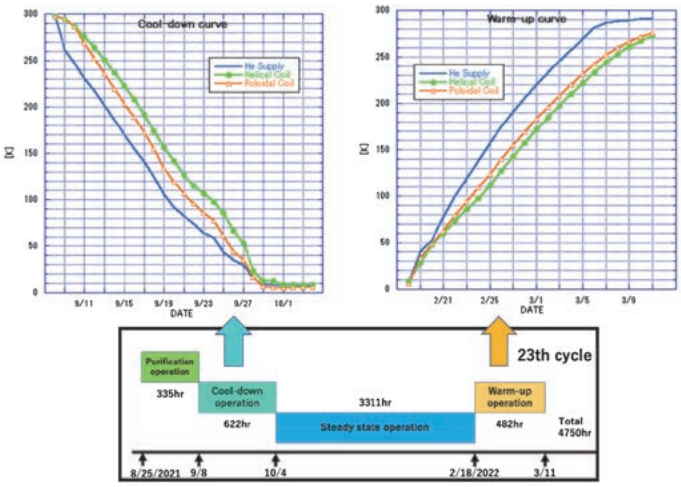

Fig. 12 The operation result of the LHD Cryogenic system for the 23rd experimental campaign.

(H. Tanoue and H. Noguchi)

(2) Implementation of remote operation system for Oroshhi2

In the Oroshhi2, we have been modifying the control system to realize a more secure and efficient operation. In F.Y. 2021, we introduced a touch-panel emulator which is compatible with Windows OS. It enables operation and monitoring not only from a physical touch-panel, but also from a remote Windows terminal. The terminal maintains a high level of security by allowing remote desktop connection under strict user management and connection source management policy.

We will develop additional functions, e.g. automated alert notification through email and customizable data logging, to improve usability.

(H. Ogawa)

(3) Network management

The NIFS campus information networks consist of several clusters. We manage the Research Information Cluster (NIFS-LAN) and the LHD Experiment Cluster (LHD-LAN).

The achievements in FY 2021 are as follows:

(a) Replacement of the barrier L3 switch

The replacement plan was to expand the uplink from 10GbE to 100GbE. However, due to SINET access line procurement, we decided to maintain the current speed of 10GbE x 4 for the time being.

(b) Update the SSL-VPN system

We updated the SSL-VPN system from BIG-IP (F5 Networks) to PSA5000 (Pulse Secure).

Security level is enhanced by introducing two-factor authentications, using a client certificate in cooperation with an authentication server (NetAttest EPS).

(c) LHD-LAN

Our security policy requires that the network management staff needs to be present when connecting a new device to the LHD-LAN.

In FY2021 43 new devices were connected to the LHD-LAN and 53 devices were updated. Furthermore, 36 IP addresses became available due to device removal (disconnection from LHD-LAN).

(T. Inoue and O. Nakamura)

6. Symposium on Technology in Laboratories

The Symposium on Technology in Laboratories was held online, using Zoom Cloud Meeting, on March 10–11 2022. The National Institute for Fusion Science (NIFS) hosted this event. There were 253 participants from 43: Japanese universities, national laboratories, and technical colleges. Fig. 13 shows a gallery view of some participants of the Zoom meeting.

35 oral reports were presented in five technical groups. After each oral session we tried to have an exchange session, with each presenter using the breakout room in a Zoom meeting. This attempt was well received because it was possible to freely discuss matters, as in a poster session.

In addition, we had two online tours, each to show the Large Helical Device and the Helium liquefaction refrigeration system. About 100 participants engaged. The tours were also well received because participants could see areas they were not able to enter and view in the onsite tours.

Fig. 13 Participants in the Zoom meeting.

(T. Kobuchi)

7. Fifth technical exchange meeting: "Computational technology using finite element method"

On March 29 2022 we held a technical exchange meeting to discuss numerical computational technology, based on the finite element method. This meeting, the fifth hitherto, was attended by seven presenters and 43 participants, including those who used a remote web conference application (ZOOM), as shown in Figure 14. In this meeting, two talks by invitation were presented under the titles of "Introduction of ANSYS-centric solutions provided by Cybernet Systems, Inc." and "Optimization of electromagnetic analyses using the finite element method for the design of ICRF antennas in the LHD." In addition, five general talks were presented, all of which resulted in lively discussions.

(T. Murase)

Fig. 14 Group photos of the technical exchange meeting, (a) at the NIFS site and (b) in the ZOOM system.

17. Department of Administration

The Department of Administration handles planning and external affairs, general affairs, accounting, research support, and facility management work.

The major operations of this department are to support the promotion of the Institute's regular research and the development of the collaborative research.

The department consists of the following four divisions, namely, the General Affairs Division, the Financial Affairs Division, the Research Support Division, and the Facilities and Safety Management Division. Details of these divisions are described below.

General Affairs Division

The General Affairs Division handles administrative work and serves as the contact point with the outside. This Division consists of four sections. The General Affairs Section is in charge of secretarial work for the Director General and the Deputy Director General, support for the Advisory Committee meetings, and enacting rules and regulations. The Planning and Evaluation Section is in support for assessment of the institution's performance including scientific achievement and management efficiency. The Personnel and Payroll Section is in charge of general personnel affairs, salary, and public welfare. And the Communications and Public Affairs Section focuses on outreach and publicity activities.

Number of Staff Members (※ This list was compiled as of March 31, 2022.)

Director General	1
Researchers	114
Technical and Engineering Staff	44
Administrative Staff	43
Employee on Annual Salary System	15
Research Administrator Staff	3
Visiting Scientists	0
Total	220

Financial Affairs Division

The Financial Affairs Division consists of six sections: The Audit Section, the Financial Planning Section, the Accounts and Properties Administration Section, the Contracts Section, the Procurement Section, and the Purchase Validation Section.

The major responsibilities of the division are to manage and execute the budget, to manage corporate property, revenue/expenditure, and traveling expenses of staff, and to purchase supplies and receive articles.

The budget is 8,300,000,000 yen. (JFY 2021)

Research Support Division

The Research Support Division consists of four sections and one center. These are the Graduate Student Affairs Section, the Academic Information Section which includes the Library at NIFS, the Research Support Section and the International Collaboration Section, which is in charge of inter-university coordination and arranging international cooperation. The Visitor Center assists collaborating researchers and visitors.

Collaboration Research Programs (JFY 2021)

	Applications Applied	Applications Accepted	Researchers Accepted
LHD Project Collaboration Research	35	30	350
Joint Research	190	189	1,022
Joint Research Using Computers	99	99	777
Workshops	35	34	1,049
Bilateral Collaboration Research	100	98	1,445
Total	459	450	4,643

Number of Graduate School Students
(SOKENDAI: The Graduate University for Advanced Studies) (As of March 31, 2022)

Doctoral Course					
Grade 1	Grade 2	Grade 3	Grade 4	Grade 5	Total
4	5	3	4	4	20

(The Joint Program of Graduate Education)

Graduate course education is given in NIFS apart from SOKENDAI in joint programs with the Department of Energy Science and Engineering of the Graduate School at Nagoya University, Division of Particle and Astrophysical Science of the Graduate School of Science at Nagoya University, Division of Quantum Science of the Graduate School of Engineering at Hokkaido University, Department of Energy Science of the Graduate School of Science and Engineering at University of Toyama, Interdisciplinary Graduate School of Engineering Science in Kyushu University and the Graduate School of Engineering at Tohoku University. In total, 29 graduate students are involved in the programs as of March 31, 2021.

The Special Research Collaboration Program for Education (As of March 31, 2022)

Affiliation \ Degree	Bachelor's Course	Master's Course	Doctoral Course	Total
National Graduate School	9	12	8	29
Public Graduate School	0	0	0	0
Private Graduate School	0	0	0	0
Total	9	12	8	29

Books and Journals (JFY 2021)

Books in Japanese	20,283
Books in Other Languages	49,891
Total (volumes)	70,174
Journals in Japanese	282
Journals in Other Languages	844
Total (titles)	1,126

Facilities and Safety Management Division

The Facilities and Safety Management Division consists of three sections: The Safety and Health Management Section, the Facilities Planning Section, and the Facilities Maintenance Section. They are in charge of planning, designing, making contracts, supervising the construction and maintenance of all facilities at NIFS, such as buildings, campus roads, electricity, telephone, power station, air conditioning, water service, gas service, elevators, and cranes. The Facilities and Safety Management Division submits a budget request and administers the budget for those facilities.

The Safety and Health Management Section also arranges medical examination and disaster drills. These three sections promote facilities' environment better for all staff.

Site and Buildings (JFY 2021)

Toki	
Site	464,445 m^2
Buildings	
Total Building Area	39,557 m^2
Total Floor Space	71,830 m^2

APPENDIX

APPENDIX 1. Organization of the Institute

NATIONAL INSTITUTE for FUSION SCIENCE

Organization

APPENDIX 2. Members of Committees

Advisory Committee

UEDA, Yoshio	Professor Graduate School of Engineering, Osaka University
OHNO, Noriyasu	Professor Graduate School of Engineering, Nagoya University
OZAWA, Tohru	Professor Department of Applied Physics, Waseda University
KANEKO, Toshiro	Professor Graduate School of Engineering, Tohoku University
KISHIMOTO, Yasuaki	Professor Graduate School of Energy Science, Kyoto University
KURIHARA, Kenichi	Managing Director, Fusion Energy Research and Development Directorate, National Institutes for Quantum and Radiological Science and Technology
FUJISAWA, Akihide	Professor Research Institute for Applied Mechanics, Kyushu University
MATSUOKA, Ayako	Professor Graduate School of Science, Kyoto University
YAMADA, Hiroshi	Professor Graduate School of Frontier Sciences, The University of Tokyo
YONEDA, Hitoki	Professor Institute for laser science, The University of Electro-Communications
WATANABE, Tomo-hiko	Professor Department of Physics, Nagoya University

※ This list was compiled as of March 31, 2022

APPENDIX 3. Advisors, Fellows, and Professors Emeritus

Professors Emeritus

ICHIKAWA, Yoshihiko (1993)
MIZUNO, Yukio (1994)
FUJITA, Junji (1996)
KURODA, Tsutomu (1997)
AMANO, Tsuneo (1998)
MOMOTA, Hiromu (1998)
IIYOSHI, Atsuo (1999)
HATORI, Tadatsugu (1999)
TANAHASHI, Shugo (2000)
KAWAMURA, Takaichi (2000)
SATO, Tetsuya (2001)
FUJIWARA, Masami (2002)
KAMIMURA, Tetsuo (2003)
HAMADA, Yasuji (2007)
KATO, Takako (2007)
NODA, Nobuaki (2008)
WATARI, Tetsuo (2008)
MOTOJIMA, Osamu (2009)
SATOH, Kohnosuke (2010)
OHYABU, Nobuyoshi (2010)
MATSUOKA, Keisuke (2010)
TOI, Kazuo (2012)
NARIHARA, Kazumichi (2012)
KUMAZAWA, Ryuhei (2012)
UDA, Tatsuhiko (2012)
SATO, Motoyasu (2012)
YAMAZAKI, Kozo (2013)
KAWAHATA, Kazuo (2013)
OKAMURA, Shoichi (2014)
KOMORI, Akio (2015)
SUDO, Shigeru (2015)
SKORIC, Milos (2015)
MUTO, Takashi (2016)
NAGAYAMA, Yoshio (2017)
NAKAMURA, Yukio (2017)
SAGARA, Akio (2017)
ITOH, Kimitaka (2017)
HORIUCHI, Ritoku(2017)
HIROOKA, Yoshihiko (2018)
MORITA, Shigeru (2019)
NISHIMURA, Arata (2019)
KUBO, Shin (2020)
MITO, Toshiyuki (2020)
NISHIMURA, Kiyohiko (2020)
ISHIGURO, Seiji (2021)
MUROGA, Takeo (2021)
NAJIMA, Noriyoshi (2021)
SHIMOZUMA, Takashi (2021)

※ This list was compiled as of March 31, 2022

APPENDIX 4. List of Staff

Director General

YOSHIDA, Zensho

Deputy Director General

MUROGA, Takeo

Department of Helical Plasma Research

Prof. IDA, Katsumi (Director)

High-Density Plasma Physics Research Division

Prof. MORISAKI, Tomohiro (Director)
Prof. WATANABE, Kiyomasa
Prof. SAKAMOTO, Ryuichi
Prof. MORISAKI, Tomohiro
Prof. OHDACHI, Satoshi
Assoc. Prof. YOSHIMURA, Shinji
Assoc. Prof. SHOJI, Mamoru
Assoc. Prof. TOKUZAWA, Tokihiko
Assoc. Prof. KOBAYASHI, Masahiro
Assoc. Prof. MOTOJIMA, Gen
Asst. Prof. NARUSHIMA,Yoshiro
Asst. Prof. TAKEMURA, Yuki
Asst. Prof. OISHI, Tetsutaro
Asst. Prof. NISHIMURA, Shin
Asst. Prof. HAYASHI, Yuki
Asst. Prof. KAWAMOTO, Yasuko
Asst. Prof. GOTO, Yuki
Specially Asst. Prof. OHTSUBO, Yohko

High-Temperature Plasma Physics Research Division

Prof. IDA, Katsumi (Director)
Prof. SAKAKIBARA, Satoru
Prof. TANAKA, Kenji
Prof. ISOBE, Mitsutaka
Prof. PETERSON, Byron Jay
Assoc. Prof. GOTO, Motoshi
Assoc. Prof. TAMURA, Naoki
Assoc. Prof. YAMADA, Ichihiro
Assoc. Prof. YASUHARA, Ryo
Assoc. Prof. OZAKI, Tetsuo
Assoc. Prof. NAKANISHI, Hideya
Assoc. Prof. OGAWA, Kunihiro
Asst. Prof. KOBAYASHI, Tatsuya
Asst. Prof. MUTO, Sadatsugu
Asst. Prof. FUNABA, Hisamichi
Asst. Prof. YOSHINUMA, Mikirou
Asst. Prof. SUZUKI, Chihiro
Asst. Prof. SHIMIZU, Akihiro
Asst. Prof. EMOTO, Masahiko
Asst. Prof. MUKAI, Kiyofumi
Asst. Prof. UEHARA, Hiyori
Asst. SHI, Quan

Plasma Heating Physics Research Division

Prof. NAGAOKA, Kenichi (Director)
Prof. SIMOZUMA, Takashi
Prof. OSAKABE, Masaki
Prof. TSUMORI, Katsuyoshi
Assoc. Prof. YOSHIMURA, Yasuo
Assoc. Prof. NISHIURA, Masaki
Assoc. Prof. KASAHARA, Hiroshi
Assoc. Prof. IGAMI, Hiroe
Assoc. Prof. TAKAHASHI, Hiromi
Assoc. Prof. SAITO, Kenji
Assoc. Prof. SEKI, Tetsuo
Assoc. Prof. NAKANO, Haruhisa
Asst. Prof. IKEDA, Katsunori
Asst. Prof. SEKI, Ryosuke
Asst. Prof. NUGA, Hideo
Asst. Prof. YANAI, Ryohma
Asst. Prof. KENMOCHI, Naoki

Device Engineering and Applied Physics Research Division

Prof. MITO, Toshiyuki (Director)
Prof. TAKAHATA, Kazuya
Prof. IMAGAWA, Shinsaku
Prof. YANAGI, Nagato
Prof. NISHIMURA, Kiyohiko
Prof. HIRANO, Naoki
Assoc. Prof. IWAMOTO, Akifumi
Assoc. Prof. HAMAGUCHI, Shinji
Assoc. Prof. CHIKARAISHI, Hirotaka
Assoc. Prof. TAKAYAMA, Sadatsugu
Assoc. Prof. TANAKA, Masahiro
Assoc. Prof. SAZE, Takuya
Asst. Prof. TAKADA, Suguru
Asst. Prof. OBANA, Tetsuhiro
Asst. Prof. KOBAYASHI, Makoto
Asst. Prof. ONODERA, Yuta

Fusion Systems Research Division

Prof. MURAKAMI, Izumi (Director)
Prof. MUROGA, Takeo
Prof. MIYAZAWA, Junichi
Prof. MASUZAKI, Suguru
Prof. NAGASAKA, Takuya
Assoc. Prof. TANAKA, Teruya
Assoc. Prof. TAMURA, Hitoshi
Assoc. Prof. HISHINUMA, Yoshimitsu
Assoc. Prof. ASHIKAWA, Naoko
Assoc. Prof. KATO, Daiji
Assoc. Prof. TOKITANI, Masayuki
Asst. Prof. GOTO, Takuya
Asst. Prof. NOTO, Hiroyuki
Asst. Prof. SAKAUE, Hiroyuki
Asst. Prof. HAMAJI, Yukinori
Asst. Prof. YAJIMA, Miyuki
Asst. Prof. KAWATE, Tomoko
Asst. Prof. SHEN, Jingjie

Fusion Theory and Simulation Research Division

Prof. TODO, Yasushi (Director)
Prof. SUGAMA, Hideo
Prof. ICHIGUCHI, Katsuji
Prof. YOKOYAMA, Masayuki
Assoc. Prof. MIZUGUCHI, Naoki
Assoc. Prof. TODA, Shinichiro
Assoc. Prof. SATAKE, Shinsuke
Assoc. Prof. KANNO, Ryutaro
Assoc. Prof. NUNAMI, Masanori
Assoc. Prof. NAKATA, Motoki
Asst. Prof. YAMAGISHI, Osamu
Asst. Prof. ISHIZAKI, Ryuichi
Asst. Prof. MATSUOKA, Seikichi
Asst. Prof. WANG, Hao
Asst. Prof. KAWAMURA, Gakushi
Asst. Prof. SATO, Masahiko
Asst. Prof. YAMAGUCHI, Hiroyuki

Fundamental Physics Simulation Research Division

Prof. ISHIGURO, Seiji (Director)
Prof. MIURA, Hideaki
Prof. NAKAMURA, Hiroaki
Prof. SAKAGAMI, Hitoshi
Assoc. Prof. USAMI, Shunsuke
Assoc. Prof. OHTANI, Hiroaki
Assoc. Prof. ITO, Atsushi M.
Assoc. Prof. TOIDA, Mieko
Assoc. Prof. YAMAMOTO, Takashi
Asst. Prof. HASEGAWA, Hiroki
Asst. Prof. MORITAKA, Toseo
Asst. Prof. ITO, Atsushi
Asst. Prof. TAKAYAMA, Arimichi

Rokkasho Research Center

Prof. NAKAJIMA, Noriyoshi
Asst. Prof. SATO, Masahiko (Additional Post)

Project

Large Helical Device Project

Prof. IDA, Katsumi
Prof. OSAKABE, Masaki

Numerical Simulation Reactor Research Project

Prof. SUGAMA, Hideo

Fusion Engineering Research Project

Prof. MUROGA, Takeo
Prof. YANAGI, Nagato

Research Enhancement Strategy Office
Prof. YOSHIDA, Zensho (Director)
Specially Appointed Prof. OKAMURA, Shoichi
Specially Appointed Prof. CARR, Stephen
Specially Appointed Prof. YAJI, Kentaro
Specially Appointed Prof. MITO, Toshiyuki

Division of Health and Safety Promotion
Prof. NISHIMURA, Kiyohiko (Division Director)

Division for Deuterium Experiments Management
Prof. OSAKABE, Masaki (Division Director)

Division of Information and Communication Systems
Prof. ISHIGURO, Seiji (Division Director)

Division of External Affairs
Prof. TAKAHATA, Kazuya (Division Director)

Fusion Science Archives
Prof. IMAGAWA, Shinsaku (Director)

Library
Prof. MURAKAMI, Izumi (Director)

※ This list was compiled as of March 31, 2022

Guest Professor
(None)

COE Research Fellows
IDOUAKASS, Malik
ADULSIRISWAD, Panith
SHI, Quan
Priti

Research Fellow (Science research)
(None)

Research Fellow (Industrial-Academic coordination)
(None)

JSPS Research Fellow
(None)

Department of Administration

NISHIYAMA, Kazunori	Department Director

General Affairs Division

NISHIO, Naoaki	Director
ICHIOKA, Akihiro	Senior Advisor
ARAI, Masanori	Chief/General Affairs Section
SHIMIZU, Kazuma	Chief/Planning and Evaluation Section
UESUGI, Kohtaro	Chief/Employee Section
MURASE, Itaru	Chief/Personnel and Payroll Section
MATSUBARA, Tomohisa	Chief/Communications and Public Affairs Section

Financial Affairs Division

SHIMIZU, Naomi	Director
OHBA, Ryo	Deputy Director
HIBINO, Atsushi	Chief/Financial Planning Section
KONDO, Takahiko	Chief/Accounts and Properties Administration Section
FUKUOKA, Miwa	Chief/Audit Section
IWASHIMA, Itsuki	Chief/Procurement Section

Research Support Division

KUMAZAWA, Shuhei	Director
URUSHIHARA, Satona	Deputy Director
SUZUKI, Takayuki	Chief/Research Support Section
SOGA, Shihoko	Chief/International Collaboration Section
KAWAI, Sanae	Chief/Graduate Student Affairs Section
OHTA, Masako	Chief/Academic Information Section
URUSHIHARA, Satona	Leader/Visitor Center (Additional Post)
HAYASHI, Tomomi	Chief/Visitor Center

Facilities and Safety Management Division

SHIRAHIGE, Tamio	Director
WAKASHIMA, Masahiro	Senior Specialist.
MIYATA, Kazuaki	Chief/Facilities Section (Additional Post)
IKEDA, Katsumi	Chief/Equipment Section

※ This list was compiled as of March 31, 2022

APPENDIX 5. List of Publications I (NIFS Reports)

NIFS-1129
To achieve both economic activity and suppression of COVID-19
—Based on the analogy between the SIR model and the controlled fusion—

MITARAI Osamu and YANAGI Nagato

May 23, 2021 (In Japanese)

NIFS-MEMO-88
Report on Administrative Work for Radiation Safety
From April 2019 to March 2020

Radiation Control Office / Division of Health and Safety Promotion
National Institute for Fusion Science

Mar. 5, 2021 (In Japanese)

NIFS-MEMO-89
Report on Administrative Work for Radiation Safety
From April 2020 to March 2021

Radiation Control Office / Division of Health and Safety Promotion
National Institute for Fusion Science

March 08, 2022 (In Japanese)

NIFS-PROC-121
Frontier of Advanced Pulsed Power Technology and its Application to Plasma and Particle Beam

Edited by Hiroaki Ito and Tetsuo Ozaki

Nov. 08, 2021

NIFS-PROC-122
NIFS-SWJTU JOINT PROJECT FOR CFQS
–PHYSICS AND ENGINEERING DESIGN–
VER. 4.1 2022. JAN.

CFQS Team
National Institute for Fusion Science, National Institutes of Natural Sciences
Institute of Fusion Science, School of Physical Science and Technology,
Southwest Jiaotong University
Hefei Keye Electro Physical Equipment Manufacturing Co. Ltd.

Feb. 10, 2022

※ This list was compiled as of March 31, 2022

APPENDIX 6. List of Publications II (Journals, etc.)

1. Adulsiriswad P., Todo Y., Kado S., Yamamoto S., Kobayashi S., Ohshima S., Okada H., Minami T., Nakamura Y., Ishizawa A., Konoshima S., Mizuuchi T., Nagasaki K.
   Numerical investigation into the peripheral energetic-particle-driven MHD modes in Heliotron J with free boundary hybrid simulation
   Nuclear Fusion 61 11 116065 -2021

2. Akata N., Kakiuchi H., Tanaka M., Ishikawa Y., Kurita N., Furukawa M., Hegedüs M., Kovács T., Gusyev M., Sanada T.
   Isotope and chemical composition of monthly precipitation collected at Sapporo, northern part of Japan during 2015-2019
   Fusion Engineering and Design 168 112434 -2021

3. Arellano F., Yoshinuma M., Ida K.
   Charge exchange spectroscopy using spatial heterodyne spectrometer in the large helical device
   Review of Scientific Instruments 93 3 33503 -2022

4. Chen H., Yao W., Uehara H., Yasuhara R.
   Actively Q-switched Tb:LiYF4 green lasers
   Optics Letters 14 6 -2021

5. Du X., Zeeland M., Heidbrink W., Gonzalez-martin J., Lin D., Collins C., Austin M., McKee G., Yan Z., Todo Y.
   Visualization of Fast Ion Phase-Space Flow Driven by Alfven Instabilities
   Physical Review Letters 127 23 235002 -2021

6. Era S., Kato D., Sakaue H., Umezaki T., Nakamura N., Murakami I.
   Emission Lines in 290–360 nm of Highly Charged Tungsten Ions W20+–W29+
   Atoms 9 63 63 -2021

7. Feng S., Kajita S., Yasuhara R., Imazawa R., Tokitani M.
   Optical Properties of Fiberform Nanostructured Tungsten in the Infrared Wavelength Range
   Plasma and Fusion Research 16 Regular Issue 1206098 -2021

8. Fujita K., Satake S., Nunami M., Garcia-Regana J., Velasco J., Calvo I.
   Study on impurity hole plasmas by global neoclassical simulation
   Nuclear Fusion 61 8 86025 -2021

9. Fujiwara S., Hatano Y., Nakamura H.
   Mechanism of DNA Damage by Tritium – Fluorescence Microscope Observation of Double-Strand Breaks and Simulation
   BUTSURI 77 1 35-41 -2022

10. Fujiwara S., Kawanami R., Li H., Nakamura H., Omata K.
    A theoretical approach to structural change of a polymer induced by beta decays of substituted tritium based on the linear response theory
    Journal of Advanced Simulation in Science and Engineering 8 2 211-222 -2021

11. Fukushima J., Tanaka M., Takayama S., Hirotsugu T.
    Kinetics of CO_2 splitting by microwave irradiation using honeycomb-like pellets of Fe_3O_4/FeO
    Chemical Engineering Journal 428 131087 -2022

12. Goto T., Ichiguchi K., Tamura H., Miyazawa J., Satake S., Yamaguchi H., Yanagi N.
    Effect of the Pitch Modulation of Helical Coils on the Core Plasma Performance of the LHD-Type Helical Fusion Reactor
    Plasma and Fusion Research 16 Regular Issue 1405085 -2021

13. Goto T., Tanaka T., Tamura H., Miyazawa J., Iwamoto A., Yanagi N., Fujita T., Kodama R., Mori Y.
    Feasibility study of tokamak, helical and laser reactors as affordable fusion volumetric neutron sources
    Nuclear Fusion 61 12 126047 -2021

14. Goto Y., Kubo S., Tsujimura T.
Coherent Cyclotron Emission with a Helical Wavefront from Multi-electron System Accelerated by the Circularly Polarized Wave
New Journal of Physics 23 63021 -2021

15. Goto Y., Kubo S., Tsujimura T., Kobayashi T.
Direct Measurement of the Millimeter Wave Phase Singularity with Helical Wavefront using Heterodyne Detection System at Two Spatial Points
Plasma and Fusion Research 17 Special Issue 1 2401007 -2022

16. Goto Y., Tokuzawa T., Kuwahara D., Ichinose K., Tsuchiya H., Nishiura M., Shimizu T., Kubo S., Yamada I.
Development of the Q-band ECE Imaging system in the large helical device
Journal of Instrumentation 17 C01016 -2022

17. Goya K., Koyama Y., Nishijima Y., Tokita S., Yasuhara R., Uehara H.
A fluoride fiber optics in-line sensor for mid-IR spectroscopy based on a side-polished structure
Sensors and Actuators B: Chemical 351 130904 -2022

18. Haba Y., Aramaki M., Tsumori K., Osakabe M., Ikeda K., Nakano H., Nagaoka K.
Abundance ratio of multiple velocity distribution components in a single negative ion beamlet produced by a cesium-seeded negative ion source
AIP Advances 12 3 35223 -2022

19. Hamaguchi S., Moriuchi S., Noguchi H., Tanoue H., Mito T.
Reliable long-term operation of superconducting bus lines for the LHD
Journal of Physics: Conference Series 1857 12014 -2021

20. Hasegawa H., Tanaka H., Ishiguro S.
Linear Analysis of Cross-field Dynamics with Feedback Instability on Detached Divertor Plasmas
Nuclear Fusion 61 12 126005 -2021

21. Hata M., Sano T., Sentoku Y., Nagatomo H., Sakagami H.
Pulse duration constraint of whistler waves in magnetized dense plasma
Physical Review E 104 3 35205 -2021

22. Hayashi Y., Kobayashi M., Mukai K., Masuzaki S., Murase T., The LHD Experimental Group.
Divertor heat load distribution measurements with infrared thermography in the LHD helical divertor
Fusion Engineering and Design 165 112235 -2021

23. Hayashi Y., Masuzaki S., Motojima G., Hwangbo D., Fujiwara Y., The LHD Experimental Group.
Observation of arc trails with significant damage due to glow discharge wall conditioning in the Large Helical Device
Plasma and Fusion Research 16 Regular Issue 1202061 -2021

24. Hirano N., Nakamura M., Kawamura K., Ishii Y., Iwatani Y., Nagaya S., Watanabe T.
Research and Development of SMES for Instantaneous Voltage Drop Compensation
Journal of the Cryogenic Society of Japan 56 5 262-268 -2021

25. Hishinuma Y., Shimada Y., Hata S., Tanaka T., Kikuchi A.
Superconducting Properties and Microstructure of In-situ Cu Addition Low Activation MgB2 Multifilamentary Wires Using Different Boron-11 Isotope Powders
Journal of the Cryogenic Society of Japan 57 1 31-38 -2022

26. Hu K., Koyamada K., Ohtani H., Goto T., Miyazawa J.
Visualization of plasma shape in the LHD-type helical fusion reactor, FFHR, by a deep learning technique
Journal of Visualization 24 6 1141-1154 -2021

27. Ichiguchi K., Suzuki Y., Todo Y., Sakakibara S., Ida K., Takemura Y., Sato M., Sugiyama L., Carreras B.
Non-resonant global mode in LHD partial collapse with net toroidal current
Nuclear Fusion 61 12 126056 -2021

28. Ichiki R., Komatsu T., Yakushiji K., Tachibana K., Furuki T., Kanazawa S., Yoshimura S.
Ignition-area extension of dielectric barrier discharge under high temperature
Results in Physics 29 104791 -2021

29. Ida K.

Non-local transport nature revealed by the research in transient phenomena of toroidal plasma
Reviews of Modern Plasma Physics 6 1 2 -2022

30. Ida K., Mcdermott R., Holland C., Choi M., Yu L., Kobayashi T., Kwon J., Kosuga Y.

Joint meeting of 9th Asia Pacific-Transport Working Group (APTWG) & EU-US Transport Task Force (TTF) workshop
Nuclear Fusion 62 3 37001 -2022

31. Idouakass M., Todo Y., Wang H., Wang J., Seki R., Sato M.

Precession drift reversal and rapid transport of trapped energetic particles due to an energetic particle driven instability in the Large Helical Device
Physics of Plasmas 28 8 80701 -2021

32. Igami H., Yanai R., Ito S., Yoshimura Y., Kubo S., Takahashi H., Shimozuma T., Tsujimura T., Mizuno Y.

Development of the molybdenum millimeter wave target tile for ECRH antenna alignment after the evacuation in LHD
Plasma and Fusion Research 16 Special Issue 1 2405066 -2021

33. Ikeda K., Kisaki M., Nakano H., Tsumori K., Nagaoka K., Fujiwara Y., Masaki S., Rattanawongnara E., Osakabe M.

Validation of the Distribution of Stripping Loss Neutrals in the Accelerator of the Negative Ion Source
AIP conference proceedings 2373 1 60001 -2021

34. Imagawa S., Chikaraishi H., Hamaguchi S., Obana T., Iwamoto A., Yanagi N., Takahata K., Mito T.

Effect of Direction of External Magnetic Field on Minimum Propagation Current of A Composite Conductor for LHD Helical Coils
IEEE Transactions on Applied Superconductivity 31 5 3059606 -2021

35. Imagawa S., Kajitani H., Obana T., Takada S., Hamaguchi S., Chikaraishi H., Onodera Y., Takahata K., Matsui K., Koizumi N.

Measurement of Decay Time Constant of Shielding Current in ITER-TF Joint Samples
Journal of Physics: Conference Series 1857 12013 -2021

36. Imagawa S., Kajitani H., Obana T., Takada S., Hamaguchi S., Chikaraishi H., Onodera Y., Takahata K., Matsui K., Koizumi N.

Simulation of Decay of Shielding Currents in ITER-TF Joint Samples
Plasma and Fusion Research 17 Special Issue 1 2405021 -2022

37. Ishihara H., Kuzmin A., Kobayashi M., Shikama T., Sawada K., Saito S., Nakamura H., Fujii K., Hasuo M., The LHD Experimental Group.

Ro-vibrational population distribution in the ground state of hydrogen isotopologues in LHD peripheral plasmas deduced from emission spectroscopy
Journal of Quantitative Spectroscopy and Radiative Transfer 267 107592 -2021

38. Islam M., Ishiguro S., Hasegawa H., Pianpanit T.

Study of energy loss processes during hydrogen gas puffing by the PIC simulation
Nuclear Materials and Energy 27 100995 -2021

39. Isobe M., Ogawa K., Sangaroon S., Kamio S., Fujiwara Y., Osakabe M.

Recent development of neutron and energetic-particle diagnostics for LHD deuterium discharges
Journal of Instrumentation 17 C03036 -2022

40. Isobe M., Ogawa K., Sangaroon S., Zhong G., Fan T.

Recent Progress of Neutron Spectrometer Development for LHD Deuterium Plasmas
Plasma and Fusion Research 17 Special Issue 1 2402008 -2022

41. Iwamoto A., Kodama R.

Core size effects of laser fusion subcritical research reactor for fusion engineering research
Nuclear Fusion 61 11 116075 -2021

42. Iwamoto A., Mori Y., Shigemori K.

Progress of Laser Fusion -Fuel gain achievement and industrial applications- 4 Grappling with high repetition operation
The Journal of The Institute of Electrical Engineers of Japan 141 9 563-566 -2021

43. Iwano K., Iwamoto A., Yamanoi K., Arikawa Y., Nagatomo H., Nakai M., Norimatsu T.
Preliminary Cryogenic Layering by the Infrared Heating Method Modified with Cone Temperature Control for the Polystyrene Shell FIREX Target
Plasma and Fusion Research 16 Regular Issue 1404099 -2021

44. Iwano K., Zhang J., Iwamoto A., Iwasa Y., Shigemori K., Hara M., Hatano Y., Norimatsu T., Yamanoi K.
Refractive index measurements of solid deuterium-tritium
Scientific Reports 12 2223 -2022

45. Kambara N., Kawate T., Oishi T., Kawamoto Y., Sakaue H., Kato D., Nakamura N., Hara H., Murakami I.
Evaluation of Fe XIV Intensity Ratio for Electron Density Diagnostics by Laboratory Measurements
Atoms 9 3 60 -2021

46. Kamio S., Moiseenko V., Kovtun Y., Kasahara H., Saito K., Seki R., Kanda M., Nomura G., Seki T., Takemura Y., Wauters T., Brakel R., Dinklage A., Hartmann D., Laqua H., Stange T., Alonso A., Lazerson S., Kazakov Y., Ongena J., Thomsen H., Fuchert G., Garkusha I.
First experiments on plasma production using field-aligned ICRF fast wave antennas in the Large Helical Device
Nuclear Fusion 61 11 114004 -2021

47. Kamio S., Saito K., Seki R., Kasahara H., Kanda M., Nomura G., Seki T.
Study of ion cyclotron range of frequencies heating characteristics in deuterium plasma in the Large Helical Device
Nuclear Fusion 62 1 16004 -2022

48. Kamitani A., Takayama T., Saitoh A., Nakamura H.
Linear-System Solver for EFG-Type Saddle-Point Problem without Using QR Decomposition
Plasma and Fusion Research 17 Special Issue 1 2403014 -2022

49. Kato D., Sakaue H., Murakami I., Goto M., Oishi T., Tamura N., Funaba H., Morita S.
Assessment of W density in LHD core plasmas using visible forbidden lines of highly charged W ions
Nuclear Fusion 61 11 116008 -2021

50. Kawamoto Y., Morita S., Goto M., Oishi T.
Qualitative Improvement of Zeff Diagnostic Based on Visible Bremsstrahlung Profile Measurement by Changing Observation Cross Section in LHD
Plasma and Fusion Research 16 Special Issue 1 2402072 -2021

51. Kawamoto Y., Ogawa K., Isobe M., Sangaroon S., Zhong G., Osakabe M.
Initial Measurement of Doppler-Shifted DD Neutron Energy Spectrum using CLYC7 Scintillator in LHD
Plasma and Fusion Research 16 Regular Issue 1202108 -2021

52. Kawamura G., Hasuo M., Saito S., Nakamura H., Sawada K., Kobayashi M., Hanada K., Shikama T., Fujii K., Kuzmin A., Yoneda N., Goto M.
Special Topic Articles: The New Phase in Transport Studies of Hydrogen Atoms and Molecules in Magnetic Confinement Fusion Devices
Journal of Plasma and Fusion Research 98 1 3-36 -2022

53. Kenmochi N., Yokota Y., Nishiura M., Saitoh H., Sato N., Nakamura K., Mori T., Ueda K., Yoshida Z.
Inward diffusion driven by low frequency fluctuations in self-organizing magnetospheric plasma
Nuclear Fusion 62 2 26041 -2022

54. Kimura K., Matsuura H., Kawamoto Y., Oishi T., Goto M., Ogawa K., Nishitani T., Isobe M., Osakabe M.
Fast deuteron diagnostics using visible light spectra of 3He produced by deuteron–deuteron reaction in deuterium plasmas
Review of Scientific Instruments 92 5 53524 -2021

55. Kobayashi M., Kawamura G., Suzuki Y., Tanaka H., Ohno N.
Special Topic Articles:Three-Dimensional Effects in the Edge Plasma Region of Fusion Devices
Journal of Plasma and Fusion Research 97 8 433-473 -2021

56. Kobayashi M., Shimada M., Chase T., Nobuta Y., Hatano Y., Oya Y.
Numerical analysis of deuterium migration behaviors in tungsten damaged by fast neutron by means of gas absorption method
Fusion Engineering and Design 168 112635 -2021

57. Kobayashi M., Suzuki N., Saze T., Miyake H., Nishimura K., Hayashi H., Kobuchi T., Ogawa K., Isobe M., Osakabe M.

The Evaluation of a Simple Measurement Method using NaI(Tl) Scintillation Survey-Meter for Radiation Safety Management of Radioactivated Armor Tiles of LHD Vacuum Vessel
Radiation Safety Management 20 20-28 -2021

58. Kobayashi M., Tanaka K., Ida K., Hayashi Y., Takemura Y., Kinoshita T.

Turbulence Spreading into an Edge Stochastic Magnetic Layer Induced by Magnetic Fluctuation and Its Impact on Divertor Heat Load
Physical Review Letters 128 12 125001 -2022

59. Kobayashi T., Nishizawa T., Sasaki M., Yoshinuma M., Ida K.

Method for estimating the frequency-wavenumber resolved power spectrum density using the maximum entropy method for limited spatial points
Plasma Physics and Controlled Fusion 63 4 45011 -2021

60. Kobayashi T., Takahashi H., Nagaoka K., Tanaka K., Seki R., Yamaguchi H., Nakata M., Sasaki M., Yoshinuma M., Ida K.

Characterization of isotope effect on ion internal transport barrier and its parameter dependence in the Large Helical Device
Nuclear Fusion 61 12 126013 -2021

61. Koga M., Takenaka R., Tsuchiya H., Manabe R., Iwama N., Yamamoto S., Yamaguchi S.

Three-Dimensional Electromagnetic Field Calculation for Microwave Holography
Plasma and Fusion Research 16 Regular Issue 1402063 -2021

62. Koike F., Suzuki C., Murakami I., Kato D., Tamura N., Nakamura N.

Z-dependent crossing of excited-state energy levels in highly charged galliumlike lanthanide atomic ions
Physical Review A 105 3 32802 -2022

63. Kondo M., Pint B., Jun J., Russell N., Mcduffee J., Akiyoshi M., Tanaka T., Oono N., Miyazawa J., Geringer J., Katoh Y., Hatano Y.

Conceptual Design of HFIR Irradiation Experiment for Material Compatibility Study on Liquid Sn Divertor
Plasma and Fusion Research 16 Special Issue 1 2405040 -2021

64. Kotani T., Toida M., Moritaka T., Taguchi S.

PIC Simulation of Energetic-ion Injection Effects on Nonlinear Development of Lower Hybrid Wave Instabilities
Journal of the Physical Society of Japan 90 12 124501 -2021

65. Lazerson S., Ford O., Akaslompolo S., Bozhenkov S., Slaby C., Vanó L., Spanier A., Mcneely P., Rust N., Hartmann D., Poloskei P., Buttenschön B., Burhenn R., Tamura N., Bussiahn R., Wegner T., Drevlak M., Turkin Y., Ogawa K., Knauer J., Brunner K., Pasch E., Beurskens M., Damm H., Fuchert G., Nelde P., Scott E., Pablant N., Langenberg A., Traverso P., Valson P., Hergenhahn U., Pavone A., Rahbarnia K., Andreeva T., Schilling J., Brandt C., Neuner U., Thomsen H., Chaudhary N., Höefel U., Stange T., Weir G., Marushchenko N., Jakubowski M., Ali A., Gao Y., Niemann H., Sitjes A., Koenig R., Schroeder R., Harder N., Heinemann B., Hopf C., Riedl R., Wolf R., W7-x team T.

First neutral beam experiments on Wendelstein 7-X
Nuclear Fusion 61 9 96008 -2021

66. Le T., Suzuki Y., Hasegawa H., Moritaka T., Ohtani H.

Particle Simulation of Controlling Particle and Heat Flux by Magnetic Field
Plasma and Fusion Research 16 Regular Issue 1401103 -2021

67. Li E., Uehara H., Yao W., Tokita S., Potemkin F., Yasuhara R.

High-efficiency, continuous-wave Fe:ZnSe mid-IR laser end pumped by an Er:YAP laser
Optics Express 29 26 44118-44128 -2021

68. Li H., Todo Y., Wang H., Idouakass M., Wang J.

Simulation study of energetic-particle driven off-axis fishbone instabilities in tokamak plasmas
Nuclear Fusion 62 2 26013 -2022

69. Li H., Zhang X., Xu Y., Lei G., Tang C., Tsumori K., Okamura S., Isobe M., Shimizu A., Liu Q., Ni Y., Cui Z., Liu Y., Li M., Geng S., Liu H., Wang X., Huang J., Liu H., Cheng J.

The effect of O impurity particle adsorption on the Cs/Mo (110) surface
Fusion Engineering and Design 172 112859 -2021

70. Masaki S., Nakano H., Kisaki M., Rattanawongnara E., Nagaoka K., Ikeda K., Fujiwara Y., Osakabe M., Tsumori K.

Development of the Directional Langmuir Probe for the Charged Particle Flow Measurement
AIP conference proceedings 2373 1 90003 -2021

71. Matsuoka S., Sugama H., Idomura Y.

Neoclassical transport simulations with an improved model collision operator
Physics of Plasmas 28 6 64501 -2021

72. Matsuura H., Kimura K., Umezaki D., Ogawa K., Isobe M., Nishitani T., Kawamoto Y., Oishi T., Goto M., Tamura N., Osakabe M., Sugiyama S.

Effect of nuclear elastic scattering on the D(d,n)^{3}He fusion reactivity induced by energetic protons observed in the large helical device
Nuclear Fusion 61 9 94001 -2021

73. Matsuyama A., Sakamoto R.

Results of ITER DMS pellet material (neon) injection into Large Helical Device
Plasma and Fusion Research 17 Special Issue 1 2402017 -2022

74. McCarthy K., Ascasíbar E., Tamura N., Panadero N., García-cortes I., Milligen B., Cappa A., García R., Hernández-sánchez J., Liniers M., Motojima G., Navarro M., Pastor I.

The interpretation of magnetic activity associated with pellet injections into plasmas created in the stellarator TJ-II
Nuclear Fusion 61 7 76014 -2021

75. Mito T., Onodera Y., Hirano N., Takahata K., Yanagi N., Iwamoto A., Hamaguchi S., Takada S., Baba T., Otsuji M., Chikumoto N., Kawagoe A., Kawanami R.

Improvement of Ic degradation of HTS Conductor (FAIR Conductor) and FAIR Coil Structure for Fusion Device
IEEE Transactions on Applied Superconductivity 31 5 4202505 -2021

76. Miura H., Hamba F.

Sub-grid-scale model for studying Hall effects on macroscopic aspects of magnetohydrodynamic turbulence
Journal of Computational Physics 448 110692 -2021

77. Miyazawa J., Goto T., Hamaji Y., Kobayashi M.

Coordinated Design of the Cartridge-type Blanket and the Ceramic Pebble Divertor for the Helical Reactor FFHR-b3
Nuclear Fusion 61 12 126062 -2021

78. Miyazawa J., Goto T., Hamaji Y., Kobayashi M.

Novel features of the helical volumetric neutron source FFHR-b2
Nuclear Fusion 61 11 116030 -2021

79. Miyazawa T., Hishinuma Y., Nagasaka T., Muroga T.

Effect of tantalum addition on the tensile properties of V-Ta-4Cr-4Ti quaternary alloys
Fusion Engineering and Design 165 112191 -2021

80. Mori Y., Ishii K., Hanayama R., Okihara S., Kitagawa Y., Nishimura Y., Komeda O., Hioki T., Motohiro T., Sunahara A., Sentoku Y., Iwamoto A., Sakagami H., Miura E., Johzaki T.

Ten hertz bead pellet injection and laser engagement
Nuclear Fusion 62 3 36028 -2022

81. Morita S., Dong C., Zhang L., Oishi T., Fujii K., Goto M., Hasuo M., Kato D., Kawamoto Y., Murakami I., Nakamura N., Sakaue H.

Recent Progress on Identifications of Spectral Lines from Tungsten Ions in Low and High Ionization Stages Using Laboratory Plasmas for Fusion Research and Its Application to Plasma Diagnostics
Springer Proceedings Physics 271 23-36 -2022

82. Moritaka T., Cole M., Hager R., Ku S., Chang C., Ishiguro S.

Improving Gyrokinetic Field Solvers toward Whole-Volume Modeling of Stellarators
Plasma and Fusion Research 16 Special Issue 1 2403054 -2021

83. Mukai K., Masuzaki S., Hayashi Y., Oishi T., Suzuki C., Kobayashi M., Tokuzawa T., Tanaka H., Tanaka K., Kinoshita T., Sakai H., Peterson B.

Steady-state sustainment of divertor detachment with multi-species impurity seeding in LHD
Nuclear Fusion 61 12 126018 -2021

84. Mukai K., Ogino Y., Kobayashi M., Bakr M., Yagi J., Ogawa K., Isobe M., Konishi S.
Evaluation of tritium production rate in a blanket mock-up using a compact fusion neutron source
Nuclear Fusion 61 4 46034 -2021

85. Mukai K., Peterson B., Ezumi N., Shigematsu N., Ohshima S., Miyashita A., Matoike R.
Sensitivity Improvement of Infrared Imaging Video Bolometer for Divertor Plasma Measurement
Review of Scientific Instruments 92 6 63521 -2021

86. Muroga T., Hatano Y., Clark D., Katoh Y.
Characterization and qualification of neutron radiation effects – Summary of Japan-USA Joint Projects for 40 years –
Journal of Nuclear Materials 560 153494 -2022

87. Nakagawa S., Hochin T., Nomiya H., Nakanishi H., Shoji M.
Prediction of unusual plasma discharge by using Support Vector Machine
Fusion Engineering and Design 167 112360 -2021

88. Nakamura H., Fujiwara S., Hatano Y.
Commentary:Molecular dynamics simulation on tritium-induced damage of biopolymers and experimental system for validation
Journal of Plasma and Fusion Research 97 10 561-567 -2021

89. Nakamura H., Saito S., Sawada T., Sawada K., Kawamura G., Kobayashi M., Hasuo M.
Isotope Effect of Rovibrational Distribution of Hydrogen Molecules Desorbed from Amorphous Carbon
Japanese Journal of Applied Physics 61 SA SA1005 -2022

90. Nakamura N., Numadate N., Kono Y., Murakami I., Kato D., Sakaue H., Hara H.
Electron Density Dependence of Extreme Ultraviolet Line Intensity Ratios in Ar XIV
The Astrophysical Journal 921 2 115 -2021

91. Nakanishi H., Ito Y., Maeno H., Ohsuna M.
Research and Technology Notes:Study of White Rabbit-based sub-nanosecond precision timing distribution for fusion experiments
Journal of Plasma and Fusion Research 97 10 597-603 -2021

92. Nakanishi H., Yamanaka K., Tokunaga S., Ozeki T., Ishii Y., Homma Y., Ohtsu H., Nakajima N., Emoto M., Yamamoto T., Ohsuna M., Ito T., Imazu S., Nonomura M., Yokota M., Ogawa H., Maeno H., Aoyagi M., Yoshida M., Inoue T., Nakamura O., Abe S., Urushidani S.
Design for the Distributed Data Locator Service for Multi-site Data Repositories
Fusion Engineering and Design 165 112197 -2021

93. Naoi Y., Iwata M., Yokota D., Gaigalas G., Kato D., Murakami I., Sakaue H., Sekiguchi Y., Tanaka M., Tanuma H., Wanajo S., Nakamura N.
Laser induced breakdown spectroscopy of Er II for transition probability measurements
Applied Sciences 12 4 2219 -2022

94. Narushima Y., Terazaki Y., Onodera Y., Yanagi N., Hirano N., Hamaguchi S., Chikaraishi H., Baba T., Miyazawa J.
Test of 10 kA-class HTS WISE conductor in high magnetic field facility
Plasma and Fusion Research 17 Special Issue 1 2405006 -2022

95. Nishimura A., Ono Y., Umezawa O., Kumagai S., Kato Y., Kato T., Yuri T., Komatsu M.
Study on development policy for new cryogenic structural material for superconducting magnet of fusion reactor
Nuclear Materials and Energy 30 101125 -2022

96. Noto H., Hishinuma Y., Muroga T., Tanaka T.
Thermal change of microstructure and mechanical properties of dispersion strengthened tungsten
Nuclear Fusion 61 11 116001 -2021

97. Nuga H., Seki R., Ogawa K., Kamio S., Fujiwara Y., Yamaguchi H., Osakabe M., Isobe M., Murakami S., Yokoyama M.
Analysis of NB Fast-Ion Loss Mechanisms in MHD Quiescent LHD Plasmas
Plasma and Fusion Research 16 Special Issue 1 2402052 -2021

98. Obana T., Yanagi N.

Measurements of self-field and voltage for the REBCO stacked tapes assembled in rigid structure (STARS) conductor at 77 K
Cryogenics 115 103278 -2021

99. Ogawa K., Isobe M., Nuga H., Kamio S., Fujiwara Y., Kobayashi M., Sangaroon S., Takada E., Seki R., Yamaguchi H., Murakami S., Jo J., Osakabe M.

A study of beam ion and deuterium–deuterium fusion-born triton transports due to energetic particle-driven magnetohydrodynamic instability in the large helical device deuterium plasmas
Nuclear Fusion 61 9 96035 -2021

100. Ogawa K., Isobe M., Nuga H., Seki R., Ohdachi S., Osakabe M.

Evaluation of Alpha Particle Emission Rate Due to the p-11B Fusion Reaction in the Large Helical Device
Fusion Science and Technology 78 3 175 -2022

101. Ogawa K., Isobe M., Sangaroon S., Takada E., Nakada T., Murakami S., Jo J., Zhong G., Zhang Y., Tamaki S., Murata I.

Time-resolved secondary triton burnup 14 MeV neutron measurement by a new scintillating fiber detector in middle total neutron emission ranges in deuterium large helical device plasma experiments
AAPPS Bulletin 31 20 -2021

102. Ogawa K., Isobe M., Seki R., Nuga H., Yamaguchi H., Sangaroon S., Shimizu A., Okamura S., Takahashi H., Oishi T., Kinoshita S., Murase T., Nakagawa S., Tanoue H., Osakabe M., Liu H., Xu Y.

Feasibility Study of Fast Ion Loss Diagnostics for CFQS by Beam Ion Loss Calculation on Vacuum Vessel
Journal of Instrumentation 16 C09029 -2021

103. Ogawa K., Isobe M., Seki R., Nuga H., Yamaguchi H., Sangaroon S., Shimizu A., Okamura S., Takahashi H., Oishi T., Kinoshita S., Murase T., Nakagawa S., Tanoue H., Osakabe M., Liu H., Xu Y.

Feasibility Study of Deuterium-deuterium Fusion Profile Diagnostics Using Fusion Born 3 MeV Proton for CFQS
Plasma and Fusion Research 17 Special Issue 1 2402012 -2022

104. Ogawa K., Isobe M., Sugiyama S., Spong D., Sangaroon S., Seki R., Nuga H., Yamaguchi H., Kamio S., Fujiwara Y., Kobayashi M., Jo J., Osakabe M.

Characteristics of neutron emission profile from neutral beam heated plasmas of the Large Helical Device at various magnetic field strengths
Plasma Physics and Controlled Fusion 63 6 65010 -2021

105. Ogawa K., Isobe M., Yokoyama M.

Extending the total neutron emission rate of steady-state deuterium large helical plasma guided by a data-driven approach
Fusion Engineering and Design 167 112367 -2021

106. Ogawa K., Zhang Y., Zhang J., Sangaroon S., Isobe M., Liu Y.

Predictive analysis for triton burnup ratio in HL-2A and HL-2M plasmas
Plasma Physics and Controlled Fusion 63 4 45013 -2021

107. Oishi T., Ashikawa N., Nespoli F., Masuzaki S., Shoji M., Gilson E., Lunsford R., Morita S., Goto M., Kawamoto Y., Suzuki C., Sun Z., Nagy A., Gates D., Morisaki T., The LHD Experimental Group.

Line identification of boron and nitrogen emissions in extreme- and vacuum-ultraviolet wavelength ranges in the impurity powder dropping experiments of the Large Helical Device and its application to spectroscopic diagnostics
Plasma Science and Technology 23 8 84002 -2021

108. Oishi T., Morita S., Kato D., Murakami I., Sakaue H., Kawamoto Y., Kawate T., Goto M.

Simultaneous observation of tungsten spectra of W0 to W46+ ions in visible, VUV and EUV wavelength ranges in the Large Helical Device
Atoms 9 3 69 -2021

109. Okamoto M., Tomita H., Watanabe K., Sato M., Takemura Y., Sakakibara S., Ida K., Yoshinuma M., LHD Experiment Group.

Linear MHD analyses of locked-mode-like instabilities in LHD
Nuclear Fusion 61 4 46005 -2021

110. Oyola P., Gonzalez-martin J., Garcia-munoz M., Galdon-Quiroga J., Birkenmeier G., Viezzer E., Dominguez-palacios J., Rueda-Rueda J., Rivero-rodriguez J., Todo Y., ASDEX Upgrade T.

Implementation of synthetic fast-ion loss detector and imaging heavy ion beam probe diagnostics in the 3D hybrid kinetic-MHD code MEGA
Review of Scientific Instruments 92 4 43558 -2021

111. Ozaki T., Abe Y., Arikawa Y., Okihara S., Miura E., Sunahara A., Ishii K., Hanayama R., Komeda O., Sentoku Y., Iwamoto A., Sakagami H., Johzaki T., Kawanaka J., Tokita S., Miyanaga N., Jitsuno T., Nakata Y., Tsubakimoto K., Mori Y., Kitagawa Y.

Hot Electron and Ion Spectra in Axial and Transverse Laser Irradiation in the GXII-LFEX Direct Fast Ignition Experiment
Plasma and Fusion Research 16 Special Issue 1 2404076 -2021

112. Peterson B., Reichle R., Pandya S., O'mullane M., Mukai K.

Consideration of signal to noise ratio for an imaging bolometer for ITER
Review of Scientific Instruments 92 4 43534 -2021

113. Reman B., Dendy R., Akiyama T., Chapman S., Cook J., Igami H., Inagaki S., Saito K., Seki R., Kim M., Thatipamula S., Yun G.

Density dependence of ion cyclotron emission from deuterium plasmas in the Large Helical Device
Nuclear Fusion 61 6 66023 -2021

114. Saito K., Seki T., Kasahara H., Seki R., Kamio S., Nomura G., Kanda M.

Upgrade of ICRF antennas by utilizing impedance transformers in LHD
Plasma and Fusion Research 17 Special Issue 1 2405009 -2022

115. Saito S., Nakamura H., Kenmotsu T., Oya Y., Hatano Y., Tamura Y., Fujiwara S., Ohtani H.

Image processing method for automatic measurement of number of DNA breaks
Journal of Advanced Simulation in Science and Engineering 8 2 173-193 -2021

116. Sanders M., Ida K., Yoshinuma M., Suzuki C., Yoshimura Y., Seki R., Emoto M., Yoshida M., Kobayashi T.

Analysis of the Motional Stark Effect (MSE) diagnostic to measure the rotational transform and current profile in the Large Helical Device
Review of Scientific Instruments 92 5 53503 -2021

117. Sangaroon S., Ogawa K., Isobe M., Kobayashi M., Conroy S., Zhang Y., Fan T., Osakabe M.

Neutron and gamma-ray transport calculations in support of the design of the radiation shielding for the TOFED neutron spectrometer at LHD
Fusion Engineering and Design 166 112296 -2021

118. Sangaroon S., Ogawa K., Isobe M., Kobayashi M., Fujiwara Y., Kamio S., Yamaguchi H., Seki R., Nuga H., Takada E., Murakami S., Zhong G., Osakabe M.

Observation of significant Doppler shift in deuterium-deuterium neutron energy caused by neutral beam injection in the Large Helical Device
AAPPS Bulletin 32 1 5 -2022

119. Sangaroon S., Ogawa K., Isobe M., Kobayashi M., Fujiwara Y., Kamio S., Yamaguchi H., Seki R., Nuga H., Toyama S., Miwa M., Matsuyama S., Takada E., Murakami S., Zhong G., Osakabe M.

Neutron energy spectrum measurement using CLYC7-based compact neutron emission spectrometer in the Large Helical Device
Journal of Instrumentation 16 C12025 -2021

120. Sato M., Todo Y.

Kinetic thermal ion effects on maintaining high beta plasmas above the Mercier criterion in the Large Helical Device
Nuclear Fusion 61 11 116012 -2021

121. Sharov I., Sergeev V., Miroshnikov I., Tamura N., Sudo S.

Spatial characteristics of luminous hydrocarbon pellet clouds in the Large Helical Device
Plasma Physics and Controlled Fusion 63 6 65002 -2021

122. Shimizu A., Kinoshita S., Isobe M., Okamura S., Ogawa K., Nakata M., Yoshimura Y., Suzuki C., Osakabe M., Murase T., Nakagawa S., Tanoue H., Xu Y., Liu H., Liu H., Huang J., Wang X., Cheng J., Xiong G., Tang C., Yin D., Wan Y.

Recent developments in engineering design for the quasi-axisymmetric stellarator CFQS
Nuclear Fusion 62 1 16010 -2022

123. Shoji M., Masuzaki S., Kawamura G., Romazanov J., Kirschner A., Brezinsek S.

Simulation analysis of the carbon deposition profile on directional material probes in the Large Helical Device using the ERO2.0 code
Plasma and Fusion Research 17 Special Issue 1 2403010 -2022

124. Suzuki C., Koike F., Murakami I., Oishi T., Tamura N.

Spectra of Ga-like to Cu-like praseodymium and neodymium ions observed in the Large Helical Device
Atoms 9 3 46 -2021

125. Suzuki T., Zhang M., Nomura M., Tsukahara T., Tanaka M.

Engineering study on lithium isotope separation by ion exchange chromatography
Fusion Engineering and Design 168 112478 -2021

126. Suzuki Y., Huang J., Wang N., Ding Y.

Design of simple stellarator using tilted toroidal field coils
Fusion Engineering and Design 173 112843 -2021

127. Takada D., Itoh T., Kobayashi M., Nakamura H.

A Mesh-Generation Scheme for the Large Helical Device Based on the Structure of Magnetic-Field Lines
Plasma and Fusion Research 16 Special Issue 1 2401086 -2021

128. Takahashi T., Asai T., Mizuguchi N., Matsuura H., Mitarai O., Johzaki T., Momota H., Takeno H., Goto T., Yanagi N., Sagara A.

Special Topic Articles “Advanced-Fuel Fusion Research -Current Status and Development-”
Journal of Plasma and Fusion Research 98 2 63-98 -2022

129. Takahata K.

Explosive boiling of liquid nitrogen in a long thin tube and its application to the detection of a local temperature rise
Cryogenics 122 103419 -2022

130. Takemura Y., Yasuhara R., Funaba H., Uehara H., Den hartog D., Watanabe K., Sakakibara S., Narushima Y., Ohdachi S.

Mode Structure of Locked-Mode-Like Instability in LHD and Its Effects on Confinement Degradation
Plasma and Fusion Research 16 Regular Issue 1402091 -2021

131. Takenaka K., Shinohara N., Hashida M., Kusaba M., Sakagami H., Sato Y., Masuno S., Nagashima T., Tsukamoto M.

Delay times for ablation rate suppression by femtosecond laser irradiation with a two-color double-pulse beam
Applied Physics Letters 119 23 231603 -2021

132. Tamura N., Hayashi H., Uejima N., Maeno H., Ito Y., Yokota M., Ogawa H.

Development of a double-barreled Tracer Encapsulated Solid Pellet (TESPEL) injection system for LHD
Journal of Instrumentation 16 C08003 -2021

133. Tamura N., Yoshinuma M., Ida K., Suzuki C., Goto M., Oishi T., Shoji M., Mukai K., Funaba H.

Simultaneous observation of silicon and boron impurity behaviors in the core region of a mid-density LHD plasma
Plasma and Fusion Research 16 Regular Issue 1202094 -2021

134. Tamura N., Yoshinuma M., Yin X., Ida K., Suzuki C., Shoji M., Mukai K., Funaba H.

A new multi-tracer technique in the TESPEL method for a simultaneous study of behaviors of Low- and Mid/High-Z impurities in high-temperature plasmas
Review of Scientific Instruments 92 6 63516 -2021

135. Tanaka K., Nagaoka K., Ida K., Yamada H., Kobayashi T., Satake S., Nakata M., Kinoshita T., Ohtani Y., Tokuzawa T., Takahashi H., Warmer F., Mukai K., Murakami S., Nakano H., Osakabe M., Morisaki T., Nunami M., Tala T., Tsujimura T., Takemura Y., Yokoyama M., Seki R., Igami H., Yoshimura Y., Kubo S., Shimozuma T., Akiyama T., Yamada I., Yasuhara R., Funaba H., Yoshinuma M., Goto M., Oishi T., Morita S., Motojima G., Shoji M., Masuzaki S., Michael C., Vacheslavov L., Sakamoto R.

Isotope effects on transport in LHD
Plasma Physics and Controlled Fusion 63 9 94001 -2021

136. Tanaka M., Kato H., Suzuki N., Chimura H.

Detection of Ammonia and Deuterated Hydrocarbons in Exhaust Gas by Infrared Absorption Spectroscopy during Wall Conditioning
Plasma and Fusion Research 16 Special Issue 1 2405062 -2021

137. Tanaka M., Kato H., Suzuki N., Chimura H., Masuzaki S., Takahashi H., Seki T., Osakabe M.

Removal of tritium from vacuum vessel by RF heated plasmas in LHD
Physica Scripta 96 12 124007 -2021

138. Tanaka M., Seki T., Wang J., Kamimura Y., Uda T., Fujiwara O.

A New Wide-area Monitoring System of Electromagnetic Fields around Megawatt-class Amplifiers for Ion Cyclotron Range of Frequency Heating at a Fusion Test Facility
IEEE Transactions on Plasma Science 49 4 1475-1483 -2021

139. Tanaka M., Suzuki N., Kato H., Chimura H.

Estimation of Tritium Inventory in Exhaust Detritiation System for Fusion Test Device in the Initial Tritium Recovery Operation
Fusion Engineering and Design 172 112808 -2021

140. Terasaka K., Yoshimura S.

Plasma–neutral coupling allows electrostatic ion cyclotron waves to propagate below ion cyclotron frequency
Physics of Plasmas 29 2 22103 -2022

141. Todo Y., Sato M., Wang H., Idouakass M., Seki R.

Magnetohydrodynamic hybrid simulation model with kinetic thermal ions and energetic particles
Plasma Physics and Controlled Fusion 63 7 75018 -2021

142. Tokitani M., Hamaji Y., Hiraoka Y., Masuzaki S., Tamura H., Noto H., Tanaka T., Tsuneyoshi T., Tsuji Y., Muroga T., Sagara A., Group F.

Advanced multi-step brazing for fabrication of a divertor heat removal component
Nuclear Fusion 61 4 46016 -2021

143. Tokuzawa T., Tanaka K., Tsujimura T., Kubo S., Emoto M., Inagaki S., Ida K., Yoshinuma M., Watanabe K., Ejiri A., Saito T., Yamamoto K., LHD Experiment Group.

W-band millimeter-wave back-scattering system for high wave number turbulence measurements in LHD
Review of Scientific Instruments 92 4 043536 -1 -4 -2021

144. Tsujimura T., Kobayashi T., Tanaka K., Ida K., Nagaoka K., Yoshinuma M., Yamada I., Funaba H., Seki R., Satake S., Kinoshita T., Tokuzawa T., Kenmochi N., Igami H., Mukai K., Goto M., Kawamoto Y.

Direct observation of the non-locality of non-diffusive counter-gradient electron thermal transport during the formation of hollow electron-temperature profiles in the Large Helical Device
Physics of Plasmas 29 3 32504 -2022

145. Ueda K., Nishiura M., Kenmochi N., Yoshida Z., Nakamura K.

Calibration of coherence imaging spectroscopy using spectral line sources
Review of Scientific Instruments 92 7 73501 -2021

146. Ueno Y., Nagamoto N., Kawagoe A., Obana T., Takayasu M.

Evaluation AC Losses in Large-Scale Conductors Consisting of Stacked REBCO Tapes
Plasma and Fusion Research 16 Special Issue 1 2405071 -2021

147. Usami S., Horiuchi R.

Pseudo-Maxwellian Velocity Distribution Formed by the Pickup-Like Process in Magnetic Reconnection
Frontiers in Astronomy and Space Sciences 9 846395 -2022

148. Varela J., Spong D., Garcia L., Ohdachi S., Watanabe K., Seki R., Ghai Y.

Theoretical analysis of the saturation phase of the 1/1 energetic-ion-driven resistive interchange mode
Nuclear Fusion 61 12 126016 -2021

149. Xu H., Nomura S., Isobe T., Chikaraishi H., Tsutsui H.

Calculation Methods for the Self-inductance of Electromagnets with a Wide Air Gap
IEEJ Transactions on Industry Applications 141 11 912-920 -2021

150. Yamaguchi H., Satake S., Nakata M., Shimizu A., Suzuki Y., W7-x team T.

Optimization of modular and helical coils applying genetic algorithm and fully-three-dimensional B-spline curves
Nuclear Fusion 61 10 106004 -2021

151. Yamamoto T., Takayama A., Inoue T., Nakamura O.

Construction and evaluation of a quarantine authentication system as an information security measure
Journal for Academic Computing and Networking 25 1 2022/9/20 -2021

152. Yamamoto Y., Murakami S., Chang C., Takahashi H., Ida K., Yoshinuma M., Ko W.
Effects of Electron Cyclotron Heating on the toroidal flow in LHD plasmas
Physics of Plasmas 28 10 102501 -2021

153. Yamashita T., Tokitani M., Hamaji Y., Noto H., Masuzaki S., Muroga T., Group F.
Development of the brazing technique of W and JLF-1 by Ni-P filler material
Fusion Engineering and Design 170 112687 -2021

154. Yanai R., Tsujimura T., Kubo S., Yoneda R., Yoshimura Y., Nishiura M., Igami H., Takahashi H., Shimozuma T.
Upgrading LHDGauss code by including obliquely propagating wave absorption effect for ECH
Plasma and Fusion Research 16 Special Issue 1 2402084 -2021

155. Yanai R., Tsujimura T., Kubo S., Yoshimura Y., Takeuchi T., Ito S., Mizuno Y., Nishiura M., Igami H., Kenmochi N., Takahashi H., Shimozuma T., Osakabe M., Morisaki T.
Development of a 56 GHz ECH system for deuterium plasma experiments of a low magnetic field in LHD
Fusion Engineering and Design 173 112862 -2021

156. Yang H., Chen H., Li E., Uehara H., Yasuhara R.
Electro-optically Q-switched operation of a high-peak-power Tb:LiYF4 green laser
Optics Express 29 20 31706-31713 -2021

157. Yao W., Li E., Uehara H., Yasuhara R.
Efficient diode-pumped Er:YAP master-oscillator power-amplifier system for laser power improvement at 2920 nm
Optics Express 29 16 24606-24613 -2021

158. Yoshimura S., Terasaka K., Aramaki M.
Application of optical vortex to laser-induced fluorescence velocimetry of ions in a plasma
Journal of Advanced Simulation in Science and Engineering 9 1 150-159 -2022

159. Zeeland M., Bardoczi L., Gonzalez-martin J., Heidbrink W., Podesta M., Austin M., Collins C., Du X., Duarte V., Garcia-Munoz M., Munaretto S., Thome K., Todo Y., Wang X.
Beam modulation and bump-on-tail effects on Alfvén eigenmode stability in DIII-D
Nuclear Fusion 61 6 66028 -2021

160. Zhang Y., Ge L., Hu Z., Sun J., Li X., Ogawa K., Isobe M., Sangaroon S., Liao L., Yang D., Gorini G., Nocente M., Tardocchi M., Fan T.
Design and optimization of an advanced time-of-flight neutron spectrometer for deuterium plasmas of the large helical device
Review of Scientific Instruments 92 5 53547 -2021

161. Zou Y., Chan V., Zeeland M., Heidbrink W., Todo Y., Chen W., Wang Y., Chen J.
Prediction of the Energetic Particle Redistribution by an Improved Critical Gradient Model and Analysis of the Transport Threshold
Physics of Plasmas 29 3 32304 -2022

※ This list was compiled as of March 31, 2022

National Institute for Fusion Science

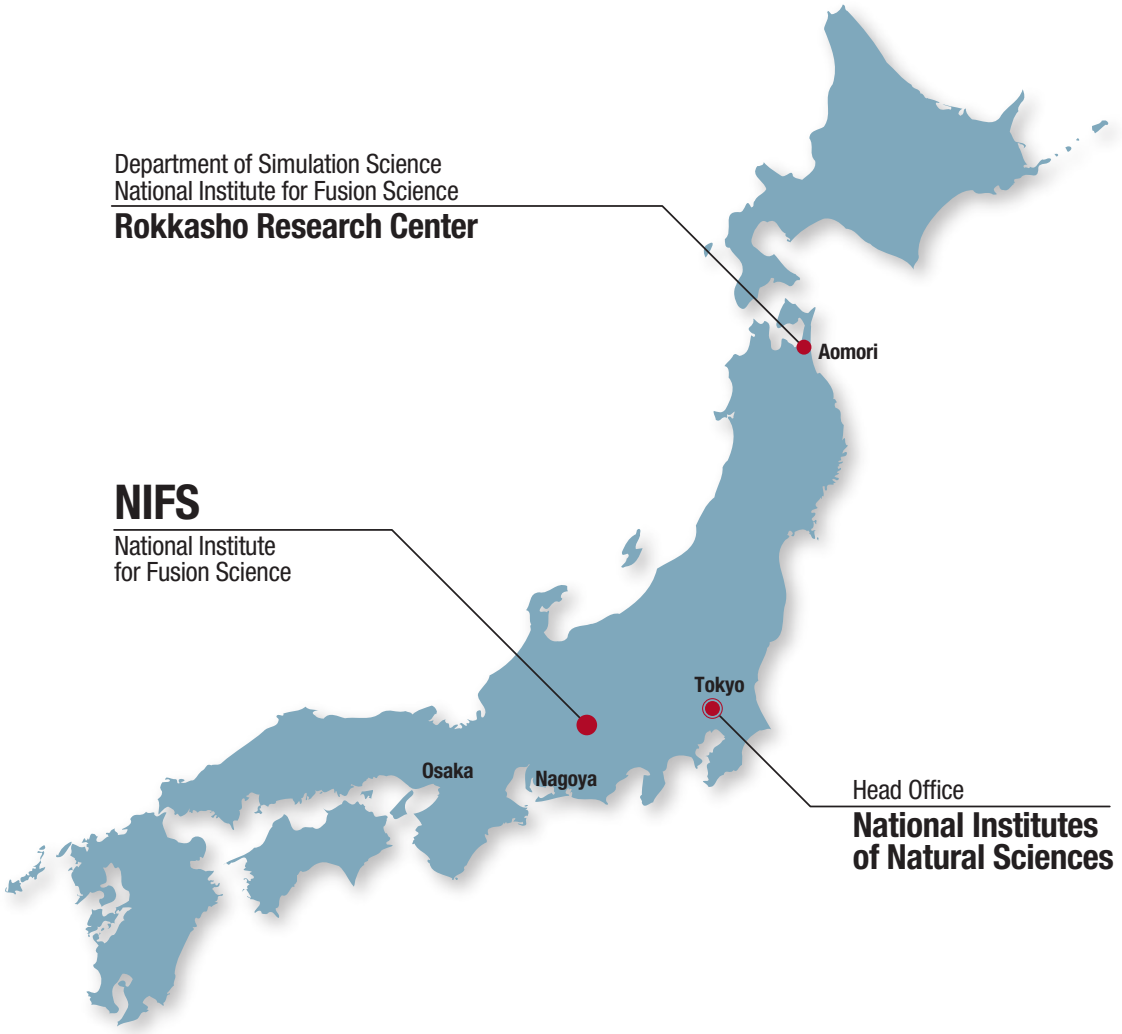

National Institute for Fusion Science
National Institutes of Natural Sciences
(TOKI Area)

322-6 Oroshi-cho
Toki-city, GIFU
509-5292

TEL: 0572-58-2222 FAX: 0572-58-2601

Rokkasho Research Center
Department of Helical Plasma Research
Located in the Aomori Research and Development Center
Japan Atomic Energy Agency

2-166 Oaza-Obuchi-Aza-Omotedate,
Rokkasho-mura, Kamikita-gun,
AOMORI
039-3212

TEL/FAX: 0175-73-2151

How to Reach National Institute for Fusion Science

☐ACCESS

When you use the public transportation facility

◇from Centrair (Central Japan International Airport)

Centrair–(μ-sky)–**Meitetsu Kanayama Sta. (36km)**
about 25min

JR Kanayama Sta.–(JR Chuo Line)–**JR Tajimi Sta. (33km)**
about 33min (express)

JR Tajimi Sta.–(Totetsu Bus)–**Kenkyuugakuentoshi (7km)**
about 15min

◇from JR Nagoya Sta.

JR Nagoya Sta.–(JR Chuo Line)–**JR Tajimi Sta. (36km)**
about 22min (limited express) / about 30min (lapid) / about 40min (local)

JR Tajimi Sta.–(Totetsu Bus)–**Kenkyuugakuentoshi (7km)**
about 15min

◇from Nagoya Airport

(Obihiro•Akita•Yamagata•Niigata•Kouchi• Matsuyama•Fukuoka•Kumamoto•Nagasaki)

Nagoya Airport–(Taxi)–**JR Kachigawa Sta. (4km)**
about 10min

Nagoya Airport–(Meitetsu Bus)–**JR Kachigawa Sta. (4km)**
about 19min

JR Kachigawa Sta.–(JR Chuo Line)–**JR Tajimi Sta. (21km)**
about 20min

JR Tajimi Sta.–(Totetsu Bus)–**Kenkyuugakuentoshi (7km)**
about 15min

When you use a car

from Chuo Expressway Toki I.C. or Tajimi I.C. (8km)
about 20min

from Tokai-Kanjo Expressway Tokiminami Tajimi I.C. (2km)
about 5min

How to Reach Rokkasho Research Center

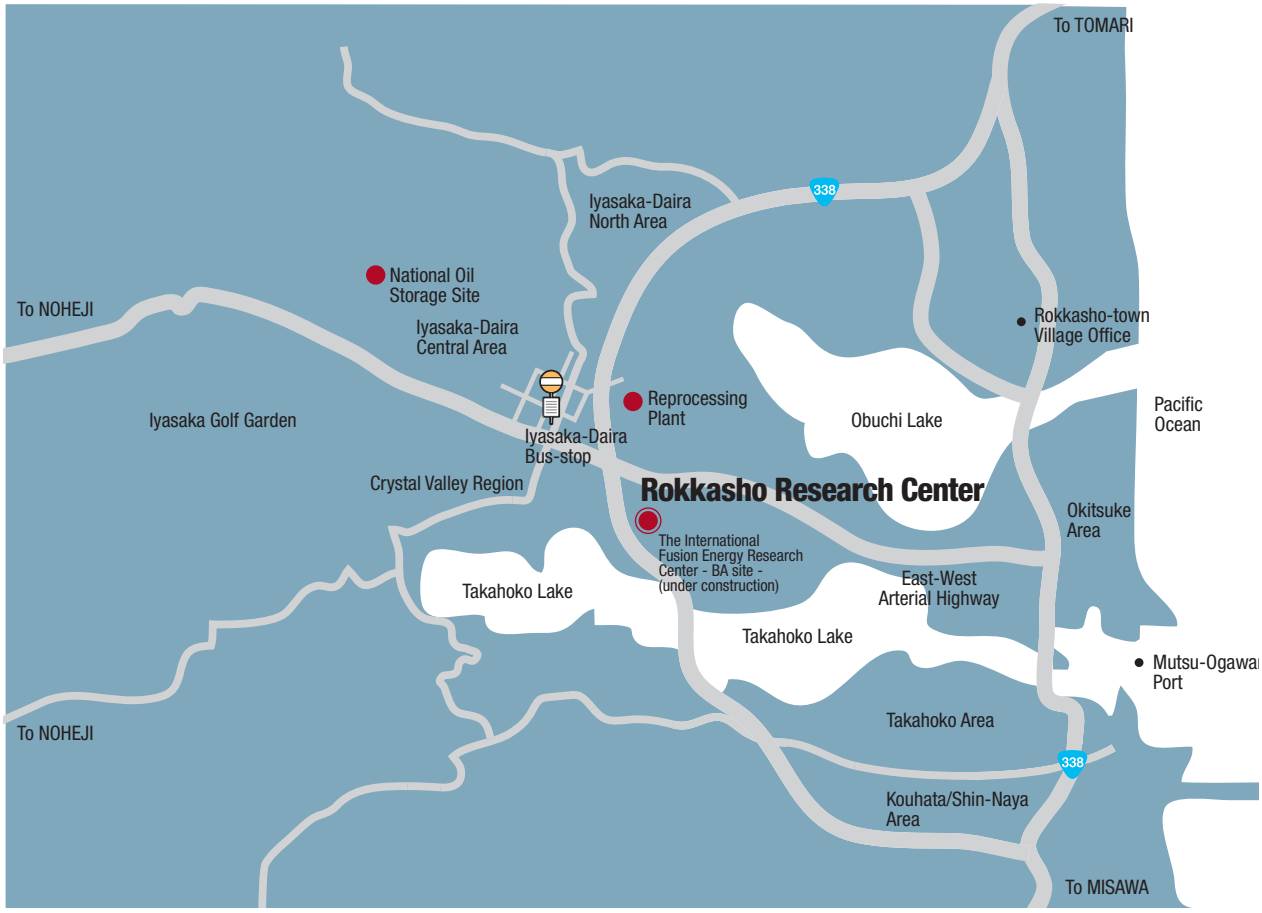

☐ACCESS

When you use the public transportation facility

◇from Tokyo

Tokyo – (Tohoku-Shinkansen) – Hachinohe Sta. (630km)
about 3hr

Hachinohe Sta. – (JR Tohoku Limited Express) – Noheji (51km)
about 30min

Noheji – (Shimokita Koutsu Bus) – Iyasaka-Daira (10km)
about 40min

Iyasaka-Daira .....on foot..... Rokkasho Research Center (0.7km)
about 8min

◇from Misawa Airport

Misawa Airport – (Bus) – Misawa (2km)
about 13min

Misawa – (JR Tohoku Limited Express) – Noheji (30km)
about 20min

Noheji – (Shimokita Koutsu Bus) – Iyasaka-Daira (10km)
about 40min

Iyasaka-Daira .....on foot..... Rokkasho Research Center (0.7km)
about 8min

◇from Aomori Airport

Aomori Airport – (Bus) – Aomori (12km)
about 40min

Aomori – (JR Tohoku Limited Express) – Noheji (45km)
about 30min

Noheji – (Shimokita Koutsu Bus) – Iyasaka-Daira (10km)
about 40min

Iyasaka-Daira .....on foot..... Rokkasho Research Center (0.7km)
about 8min

National Institute for Fusion Science

Building Arrangement

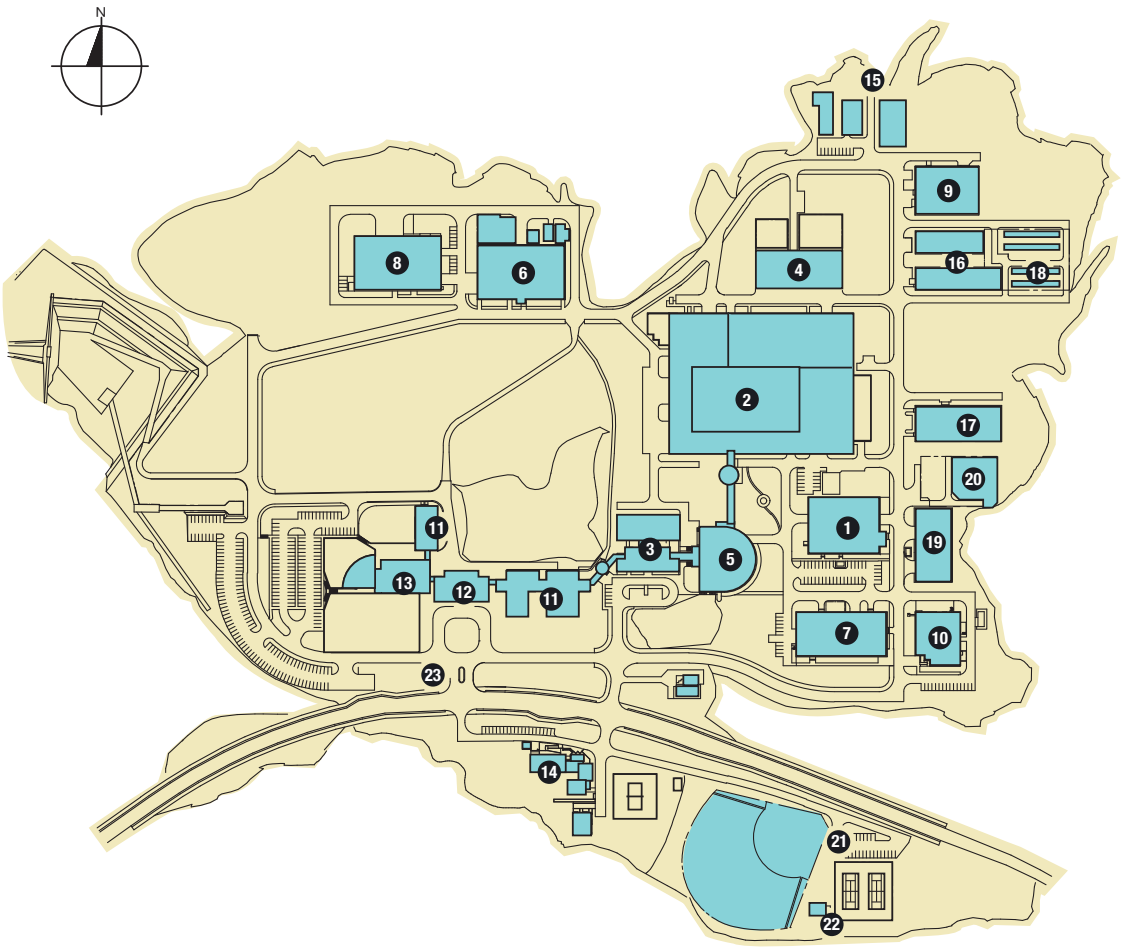

NIFS plot plan

1. Superconducting Magnet System Laboratory
2. Large Helical Device Building
3. Simulation Science Research Laboratory
4. Heating and Power Supply Building
5. LHD Control Building
6. Fusion Engineering Research Laboratory
7. Plasma Diagnostics Laboratories
8. R & D Laboratories
9. Motor-Generator Building
10. Central Workshops
11. Research Staff Building
12. Library Building
13. Administration Building
14. Helicon Club (Guest Housing)
15. High-Voltage Transformer Station
16. Cooling Water Pump Building
17. Helium Compressor Building
18. Cooling Tower
19. Equipments Room
20. Helium Tank Yard
21. Recreation Facilities
22. Club House
23. Guard Office